NAGOYA UNIVERSITY

Effect of applied load, sliding distance, mating materials and nano-particles on tribological properties of diamond-like carbon coatings in the base oil lubrication condition

Xiang Li

A thesis submitted in partial fulfillment for the degree of Doctor of Engineering

in the DEPARTMENT OF MECHANICAL SCIENCE AND ENGINEERING GRADUATE SCHOOL OF ENGINEERING

January 2018

Contents

Abstract

Diamond-Like Carbon (DLC) coatings have been widely used as protective surface film to mechanical components due to their excellent tribological performance under various mild sliding contact conditions. For automobile engine industry, urgent demands have been focused on the wear and seizure resistance of DLC coatings under high contact pressure conditions under oil lubrication conditions.

Firstly, this thesis investigated the seizure resistance of amorphous hydrogenated carbon (a-C:H) and hydrogen-free tetrahedral amorphous carbon (ta-C) under oil boundary lubrication condition and the effects of load and sliding distance on the wear and friction behavior of each coating were tested in poly-alpha-olefin base oil. The coated and non-coated SUJ2 steel cylindrical specimens were slid with their central axes parallel to the sliding direction against a rotating steel counterface. Both DLC coatings resist seizure much better than the non-coated specimens. Under a relatively low applied load, ta-C shows much lower specific wear rate than the a-C:H. When the load is raised above a critical value, the specific wear rate of ta-C increases rapidly and became 3 - 5 times higher than that of a-C:H. While in the case of a-C:H, the specific wear rate decreases significantly when the load exceeds a critical value and maintains that lower wear rate even the load increases. By contrast, ta-C shows a rapid increase in specific wear rate as sliding distance increases. While the specific wear rate of a-C:H decreases slightly and shows much lower specific wear rate than ta-C. Based on the results of Raman Spectroscopy, Atomic Force Microscope and Scanning Electron Microscopy, it is concluded that ta-C and a-C:H coatings are influenced by different

sets of wear mechanisms when it slid under boundary lubrication conditions in pure base oil.

Then a comparative study on the wear behavior of a-C:H and ta-C when they rubbed against various selected mating materials is conducted to find out the optimal tribopair which could prolong the lifespan of DLC coating in high contact pressure conditions. In this thesis, a-C:H and ta-C coating were slid against various mating materials under boundary lubrication condition in base oil to clarify the wear mechanisms of a-C:H and ta-C coating. It is expected that such findings could be used as a guideline to select the optimal combinations of DLC/mating material. Tribological tests were performed in a cylinder-on-disc tribotester, Field Emission Scanning Electron Microscopy (FESEM) and Raman Spectroscopy were used for the characterization of worn surface of ta-C and a-C:H coatings. The results show that the specific wear rate of ta-C coating increases along with the increase of the hardness and roughness of mating material, while the specific wear rate of a-C:H coating increases together with an increment in the I_D/I_G ratio. It is concluded that for ta-C coating, local stress concentration-induced microfracture is the main wear mechanism in relative high wear condition, along with minor graphitization-induced wear which prevails in low wear condition. On the other hand, a-C:H coating shows that simultaneous generation and the removal of the graphitized layer on the contact surface is the predominant wear mechanism.

Moreover, under high sliding contact pressure condition, the effect of various nanoparticles with distinct size on the wear of ta-C and a-C:H under oil boundary lubrication condition was clarified. When the friction components are exposed to some

severe operation circumstances where containing large amounts of foreign particles, such as dust or grains of sand, the friction and wear could be enhanced by introducing foreign particles. However, such particles may inversely behave as protective additives to reduce the friction and wear of the whole tribo-system due to the unique mechanical or chemical properties of those foreign particles. Based on the obtained results, we proposed a potential replacement of the current chemical-based lubrication additives with a novel environmental friendly ZrO_2 nanoparticle to further improve the wear resistance of ta-C coating in base oil boundary lubrication conditions. The results show that by adding ZrO_2 nanoparticles, the wear of ta-C coating could be reduced about 40% compared to non-additive base oil condition.

Chapter 1

Introduction

1.1 Significance of automobile tribology

Tribology is the interdisciplinary science and technology of interacting surfaces in relative motion and associated subjects and practices [1]. A considerable amount of energy is consumed to overcome friction, especially in the transportation, industrial, and power-generation sectors and major economic losses are also due to wear of products and components and their replacement [2]. Jost concluded that studies conducted in several industrial countries indicate that 1.0 to 1.4 % of the gross national product can be saved by introducing better tribological practices [3]. Therefore, it still requires vast and continuous investment in research of tribology in the future.

Recent UK government Transport Statistics reveals that up to 2015, there were 36.5 million licensed vehicles, 61% petrol-fueled and 38% diesel with a very small hybrid-powered and electricity-powered group [4]. The conventional internal combustion (IC) engine still accounts for the vast majority of power units used in fossil-fuel-driven vehicles, and whilst it will remain to be dominant and primary power units in the decades. Even IC engine is remarkably reliable and versatile, it does have enormous negative influences on environment and ecology due to emission of toxic particulate, nitrous oxide and hydrocarbon emissions and to the greenhouse effect via carbon dioxide emissions [5]. Meantime, major components of the engine, namely, the piston assembly, the valve train and the journal bearings, would account for considerable

energy dissipation due to inevitable friction in relative motion. Especially, when the engine experiences start-up or stall stage, such frictional components would suffer from lubrication failure and therefore causes high friction and severe wear. Concerning energy consumption within the engine as shown in Fig. 1.1, friction loss is the major portion (48%) of the energy consumption developed in an engine [6]. The other portions are the acceleration resistance (35%) and the cruising resistance (17%). In the case of passenger car, the friction-induced energy loss by engine components accounts for 11.5% of total fuel energy (Fig. 1.2) [7]. While for heavy duty vehicles, the friction-induced energy loss by engine components accounts for 7.3% of total fuel energy (Fig. 1.3) [8].

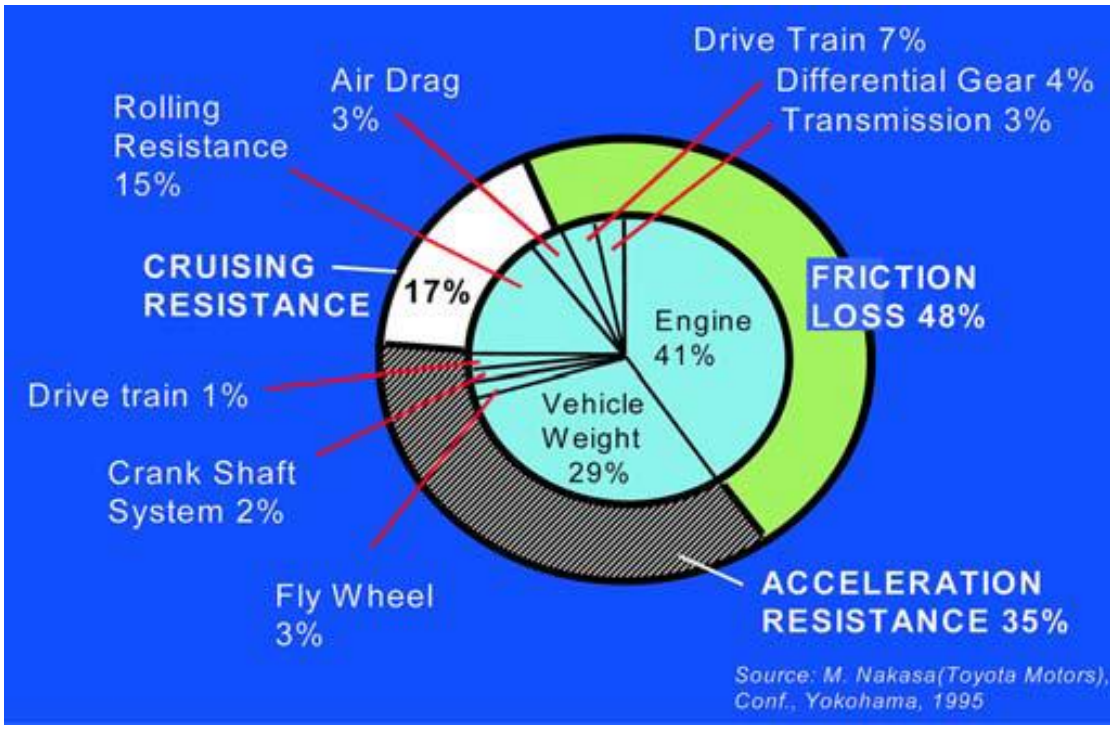

Figure 1.1 Energy consumption developed in an engine [6].

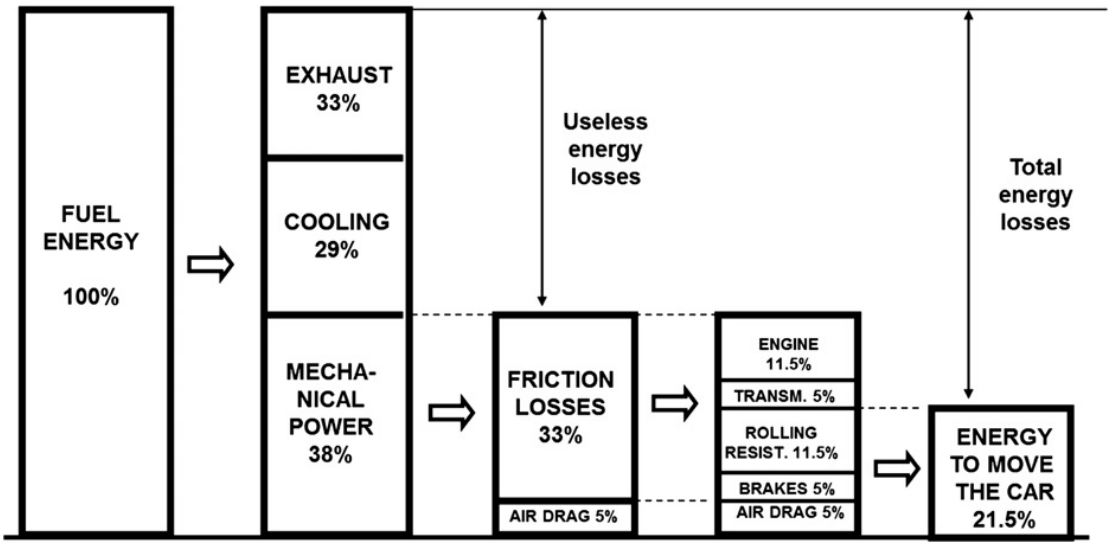

Figure 1.2 Breakdown of passenger car energy consumption [7].

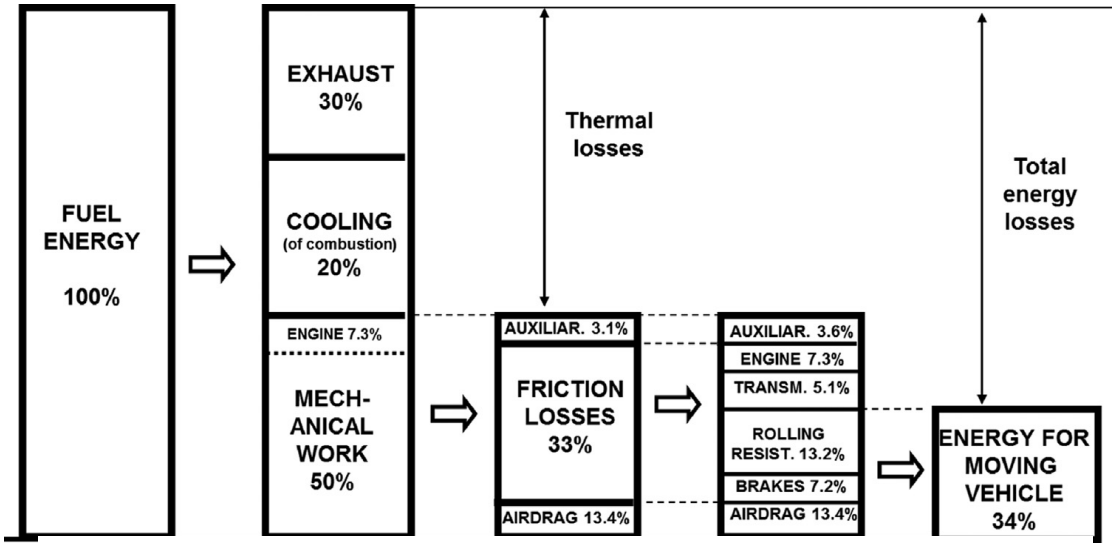

Figure 1.3 Breakdown of average energy consumption in heavy duty [8].

Therefore, it is essential to improve the tribological performance of automobile IC engine for environmental and economic concerns. From the viewpoint of the tribologist, improvements in the tribological performance of engines can generate the following benefits [9]:

- Reduced fuel consumption,
- Increased engine power output,

- Reduced oil consumption,
- A reduction in harmful exhaust emissions,
- Improved durability, reliability and engine life,
- Reduced maintenance requirements and longer
- Reduced maintenance requirements and longer service intervals.

Understanding of tribological principles is essential for the successful design of machine elements. As tribology study mainly focus on interacting surfaces, proper surface engineering approaches are desirable in many cases to improve the tribological performance of a tribosystem and lower the cost by using low-cost substrate material [10]. And, such surface engineering approaches can be broadly divided into four categories: (1) Microstructural modification treatments [11-13]; (2) thermochemical diffusion treatments [14-16]; (3) surface topography modification treatments [17-19]; (4) surface coating treatments [20-23]. Among above techniques, Diamond-Like Carbon (DLC) coating has been widely accepted as a versatile protective coating material in automobile engine industry due to its high hardness, chemical inertness, low friction and superior wear resistance under dry or lubricated contacts [24-26].

1.2 Application of DLC coatings in automobile industry

In the recent decades, with the development of the coating deposition technologies, the scope of application of DLC coating has been extended from initial small-scale surface thin-film deposition used in microelectronics and magnetic hard disk, to large-scale surface thick-film deposition for automobile engine components. Especially, such

DLC coating can be deposited on the surface of key frictional automobile components, such as piston cylinder liner, valve lifter and cam follower which is shown as Fig. 1.4. However, most of those applications are characterized by low contact pressure. While in the case of high contact conditions, it is strongly expected that the DLC coating could show excellent tribological performance among other materials. For example, in the case of engine bearings, the contact pressure is higher than that of the above-mentioned components in Fig. 1.4, and the applied load keeps changing while the vehicle is in operation. In such cases, severe wear could occur on the contact interface and leads to seizure of the sliding surfaces where the friction force increases rapidly. Seizure refers to severe adhesion between directly contacted surfaces which are in relative motion and can be triggered at any sliding velocity but high contact pressure [27]. Based on these industrial needs, DLC coating is considered to be a promising tribological material which can avoid the severe wear and maintain the low friction property under the high contact conditions, such as engine bearings.

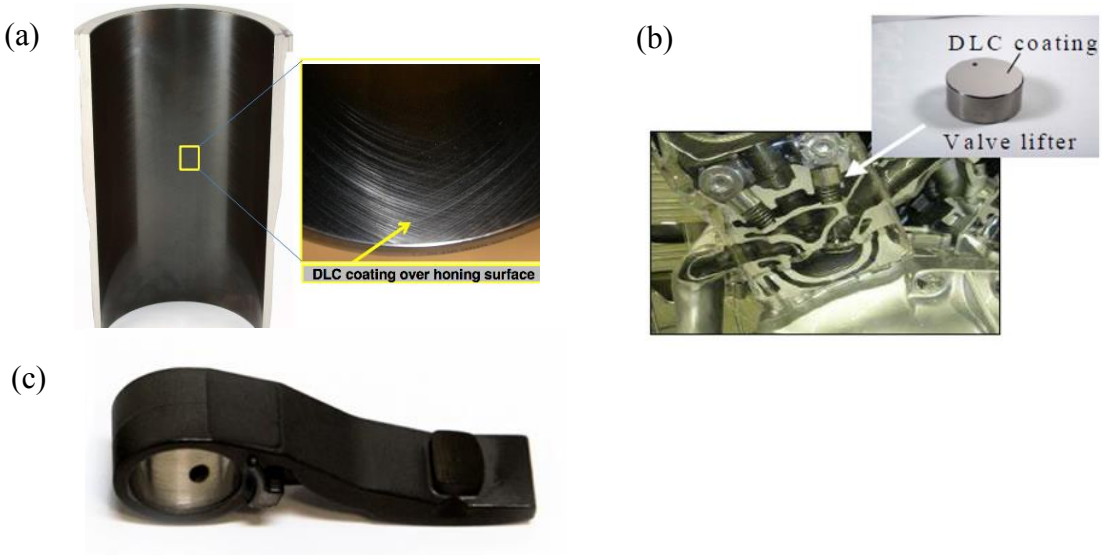

Figure 1.4 Application of DLC coating in (a) cylinder liner, (b) valve lifter, (c) cam follower.

Friction and wear are described as a function of a tribo-system and they are not constant property of materials and can differ depending on the working environment (velocity, load, temperature, humidity and etc.), operating conditions (dry contact, lubrication, additives and etc.), material properties and surface characterization of counter surfaces [28,29]. Therefore, application-orientated tribological research must take into the consideration of practical applications of certain objective component. In automobile industry, since engine bearing suffers from variable high contact pressure in boundary lubrication conditions, which is a typical applications of severe sliding contact conditions. Hence in this thesis, we take the engine bearing as application models to clarify the effect of various parameters on the tribological properties of DLC coatings. And we believe the achievements based on this application could be conducive to apply DLC coating for other severe contact conditions.

Nowadays, the automobile industry is experiencing an innovation period in which the conceptions of light weight design and zero emission are highlighted. Therefore, downsizing of gasoline engine is considered to be one of the solutions [30,31]. However, it is expected that such downsized engine still achieves the torque curve of a modern, large-capacity naturally-aspirated engine. In this situation, the engine bearing will suffer from higher contact pressure and trigger the occurrence of seizure to cause high friction and severe wear or even damage of the engine bearing. Therefore, DLC coating is expected to be effective to improve the tribological performance of engine bearing under oil boundary lubrication condition, as shown in Fig. 1.5.

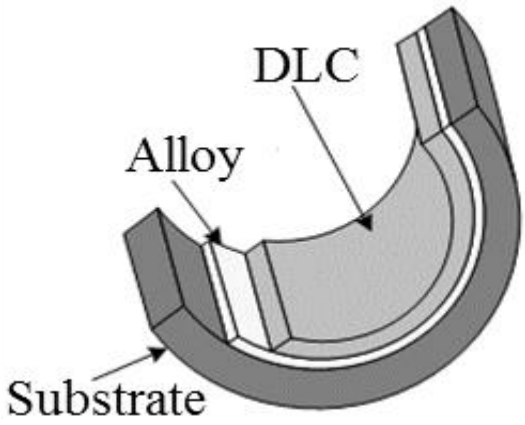

Figure 1.5 Schematic of engine main bearing coated with DLC on the inner surface.

To apply DLC coating on engine main bearing, it is necessary to investigate the friction and wear performance of those DLC coatings by taking into consideration of practical operation condition (Fig. 1.6).

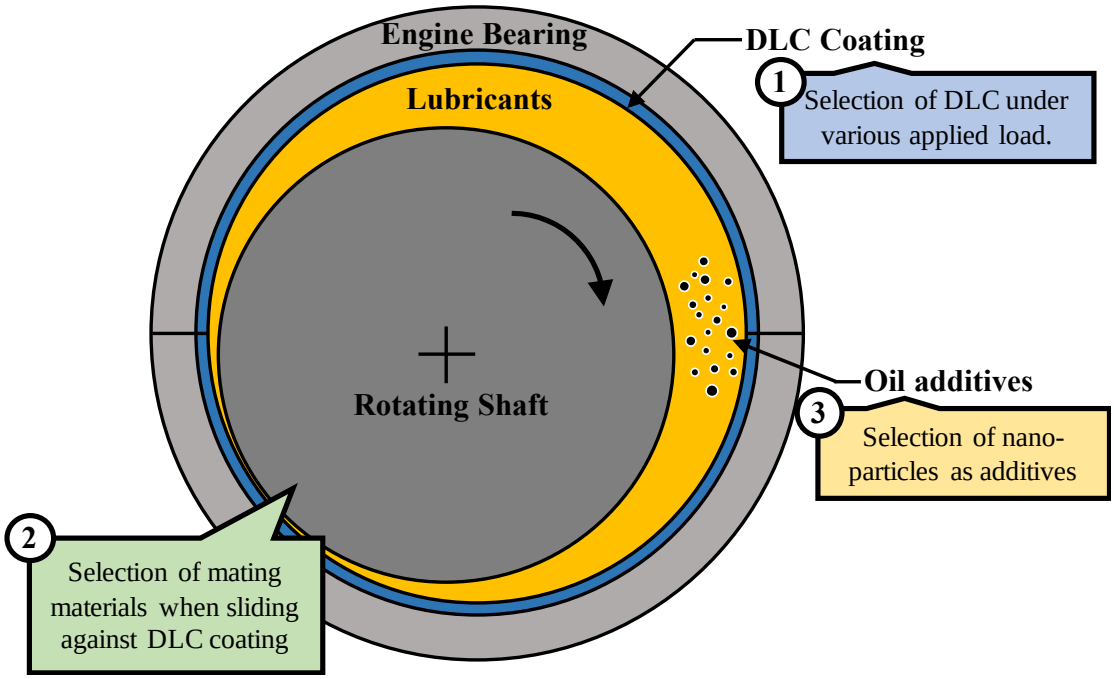

Figure 1.6 Specific operation condition of engine main bearing.

Firstly, it is well known that during the operation of engine, the normal load applied on the engine bearing is not constant but variable, therefore the seizure resistance of those DLC coating under different applied load is needed to be confirmed at the first

stage, and the effect of applied load on the friction and wear behavior of those DLC coatings is also needed to be clarified to find out what kind of DLC coating is optimal as the main bearing coating material. In addition, the comparison of wear and friction mechanism between different DLC coatings is worthy of being clarified.

Secondly, when DLC-coated engine bearing sliding against journal/shaft, the selection of journal/shaft material and its' surface characteristics has a significant effect on the wear and friction of counter DLC coating under boundary lubrication condition. Until now, the study about the effect of mating material properties, such as hardness and roughness, on the tribological performance of various DLC coating has not been proposed yet. By understanding that, it can provide guidelines for the design of engine bearing and journal/shaft to reduce the wear and friction.

Thirdly, in order to improve the tribological performance of DLC coatings under oil boundary lubrication condition, usage of oil additives is indispensable solutions. Presently, even several prevailing commercial oil additives, such as MoDTC, ZnDTP, have been widely used in boundary lubrication conditions. It has also aroused intensive public concerns since those conventional oil additives contain sulfur and phosphorus which are known to be poisonous to the environment. It is essential to replace the conventional oil additives with novel green additives which could be compatible with DLC coatings to improve the tribological performance of the whole tribo-system. Recently some studies proposed that the introduction of some nanoparticles could reduce the wear and friction to some degree under oil boundary lubrication condition as conventional oil additives but without environmental concerns [32,33], however the

study about the effect of such novel green additives on the friction and wear properties of ta-C and a-C:H is still insufficient.

Therefore, this thesis systematically focuses on the effect of applied load, sliding distance, counter material and nano-particle additives on the tribological properties of two prevailing DLC coatings, which are ta-C (tetrahedral amorphous carbon) coating and a-C:H (hydrogenated amorphous carbon) coating, under base oil boundary lubrication.

1.3 Tribology theory in lubrication condition

1.3.1 Regimes of fluid film lubrication

Lubricants plays a key role in reducing the friction between moving parts and protecting the contact surfaces from being worn. Therefore, studies of lubricants which are applicable to various complicated work condition have made tremendous contributions to modern machinery industry. Broadly, lubricants can be divided into two categories: solid lubricant and fluid lubricant. Solid lubricants have inherent self-lubricating capability such as graphite, molybdenum disulfide, PTFE etc. The low-friction mechanism of those solid lubricants is mainly attributed to a layered structure on the molecular level with weak bonding between layers. Such layers can slide relative to each other with minimal adhesion force, thus giving them their low friction properties. These solid lubricants can be deliberately applied to moving surface directly which suffering from extreme contact pressures or elevated temperature when liquid lubricants are hardly possible to survive. For the fluid lubricant, it can be liquid or

gaseous that generate a thin fluid film which could separate two sliding surfaces to reduce friction and wear. According to classical lubrication theory, depending on the lubricant viscosity, velocity and normal load, four types of fluid film lubrication can be defined: hydrodynamic lubrication, elastohydrodynamic lubrication, mixed lubrication, boundary lubrication. The variation of friction coefficient and transition between lubrication regimes can be graphically illustrated by use of Striberck curve (Fig. 1.7) [34]. The horizontal axis shows a dimensionless parameter (Λ) that is a function of minimum film thickness and roughness of mating surfaces (Eq.1.1). The left vertical axis is friction coefficient, while the right vertical axis is film thickness generated between two relative-moving surfaces. When $\Lambda<1$, the lubrication regime is boundary lubrication; when $1<\Lambda<3$, the lubrication regime is mixed lubrication; when $\Lambda>3$, the lubrication regime is elastohydrodynamic/hydrodynamic lubrication [34].

$$\Lambda = \frac{h_{min}}{\sqrt{{R_{q,a}}^2+{R_{q,b}}^2}} \tag{1.1}$$

Where h_{min} is the minimum film thickness, $R_{q,a}$ is the surface roughness of mating surface a, $R_{q,b}$ is the surface roughness of mating surface b.

Boundary lubrication is that condition in which the solid surfaces are so close together that surface interaction between monomolecular or multimolecular films of lubricants (liquids or gases) and the solid asperities dominate the contact. In the absence of boundary lubricants, friction may become very high (>1). Mixed lubrication is a transition between the elastohydrodynamic/hydrodynamic and boundary lubrication regimes and there may be both solid contacts and a portion of the bearing surface remains supported by a partial hydrodynamic film. Hydrodynamic lubrication, also

known as thick-film lubrication, is that condition in which a thin layer of fluid is pulled through because of viscous entrainment and is then compressed between the bearing surfaces, creating a hydrodynamic pressure to support the load without any external pumping agency. Hydrodynamic lubrication is referred to as the ideal lubricated contact condition because the thick fluid film can prevent the direct solid contact, and meanwhile low shear stress of fluid film may result in low friction (0.01 - 0.001), depending on the viscosity-temperature characteristic of liquid lubricants and work condition.

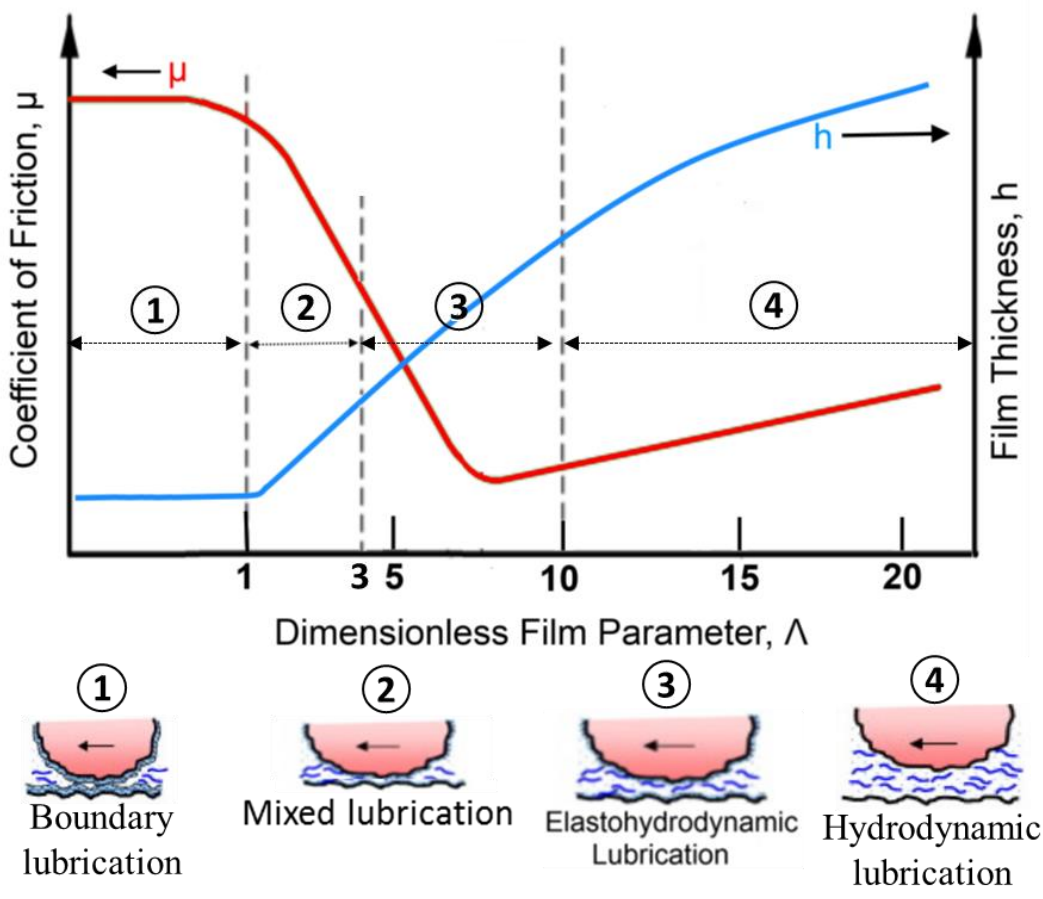

Figure 1.7 Stribeck Curve and Lubrication Regimes [30].

1.3.2 Friction and wear in boundary lubrication

Friction is the resistance to motion during sliding or rolling that is experienced when one solid body moves tangentially over another with which it is in contact [1]. And friction is not a material property but a system response. According to the classical friction model presented by Bowden and Tabor, friction energy is mainly to overcome adhesion between asperities and deformation of contacting surfaces during relative motion [Eq.1.2] [35]. In which, F_i is total intrinsic frictional force, F_a is the force needed to shear adhered junctions and F_d is the force needed to supply the energy of deformation.

$$F_i = F_a + F_d \tag{1.2}$$

In boundary condition, surface interaction is substantially solid contact with a small portion of lubrication film. Therefore, the friction is mainly attributed to the mechanical interaction of asperities of the contacting surfaces and viscosity of lubrication film. The adhesion friction force in boundary lubrication is defined as [Eq.1.3] [35] as follows:

$$F_a = A_r[\alpha\tau_a + (1-\alpha)\tau_l] \tag{1.3a}$$

and

$$\tau_l = \frac{\eta_l V}{h} \tag{1.3b}$$

where A_r is the real contact area between the two surfaces, α is the fraction of unlubricated area; τ_a and τ_l are the average shear strengths of the dry contact and of the lubricant film respectively; η_l is the dynamic viscosity of the lubricants; V is the relative sliding velocity; and h is the liquid film thickness.

Wear is defined as the removal of material from two surfaces under the mechanical

action of the two surfaces rubbing together, meanwhile take into account substrate deformation, surface damage, or chemical corrosion [36]. Wear is highly complex phenomenon because the very nature of the wear process is transient and cumulative process. In addition, wear is a system function, which depends on the system, including the materials, surface roughness, lubricants, environments, operation conditions, temperature [37]. Under hydrodynamic or mixed lubrication regimes, wear can be significantly reduced due to the presence of fluid film which separate the contact surface. However, under the boundary lubrication regime, most of lubricating film is squeezed out between the solid surfaces, and solid-to-solid contact occurs. Since the sufficient fluid film formation is not possible, the applied load is primarily supported by numerous asperities on contacting surfaces and the plastic shearing occurs originally within contact asperities. Especially, with severe operating condition in boundary lubrication regime, such as high load, elevated temperature, effect of lubrication starvation becomes more remarkable to result in high friction and severe wear, even accompanied by seizure and failure of contact surfaces. Thus, in order to improve the tribological performance under boundary lubrication condition, special surface modification or lubricants modification techniques are applied, such as surface coating, surface strengthen treatment, surface texturing and oil additives. Among those techniques, oil lubricants have been widely accepted as a vital complement in most commercial base engine oil.

Lubricants are blended with approximately 10% of additives package to enhance their lubricating capabilities under boundary lubrication and mixed lubrication regimes

[38]. Oil additives are chemical compounds that improve the lubricant performance of base oil and particularly effective under boundary lubrication. There are three possible types of additive action [39]: (1) Chemical reaction of the additives with the mating surfaces and lubrication by reaction products; (2) Decomposition of the additives on the surface and lubrication by decomposition products; (3) Adsorption on the surface and lubrication by adsorbed films. With introducing those oil additives, boundary layer is formed on the mating surface to serve as protective layer as shown in Fig. 1.8.

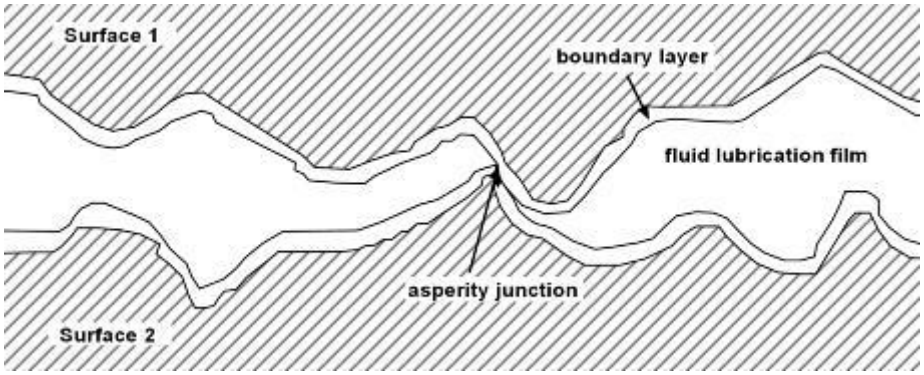

Figure 1.8 Boundary layer formed on the mating surfaces [35].

Surface coating is another desirable surface modification solution to improve the mechanical and tribological performance of sliding components. In the recent decades, hard DLC coating has become more and more prevailing in engine industry to reduce the friction and wear under boundary lubrication condition. Even though some researchers suggested that friction and wear of DLC coating could be further reduced by certain conventional oil additives if optimal combination of DLC and oil additives is utilized, it would be better we can abandon the use of those environmental unfriendly oil additives and use only DLC or simultaneously with combination of other novel green additives for engine components.

1.4 Diamond-Like Carbon coatings

Diamond-Like Carbon (DLC) is a name attributed to a variety of amorphous carbon materials, some containing up to about 50 at. % hydrogen (a-C:H), other containing less than 1% hydrogen (ta-C) [40]. DLC is originally produced by ion beam deposition method from a carbon arc source by Aisenberg and Chabot [41] and Spencer et al. [42]. With the continuous improvement and innovation of deposition methods, DLC coating can be produced by a wide range of methods, such as ion beam deposition (IBD) [43], plasma enhanced chemical vapor deposition (PECVD) [44], magnetron sputtering [45], ion plating [49], microwave voltage coupled plasma deposition (MVP) [50] and pulsed laser deposition [51], which make it possible to deposit DLC coating on objects with high rate and low energy consumption. Except the two mainstream DLC coating, ta-C and a-C:H, other element-doped DLC coatings, such as carbon nitride coatings (CNx) [49], silicon-doped diamond-like carbon (Si-DLC) [50], metal-doped diamond-like carbon [48], have also been synthesized to fulfill some special operation conditions. However, due to the widely usage of ta-C and a-C:H in industry, our research mainly focuses on these two DLC coatings.

Both ta-C and a-C:H are metastable materials, which have been accepted as a solid lubricant to be used widely in many areas as protective coating due to their promising mechanical and tribological properties such as high hardness, chemical inertness, low coefficient of friction and high wear resistance [52]. Figure 1.9 shows the typical ternary phase diagram of various DLC coatings with different sp2, sp3 and hydrogen contents.

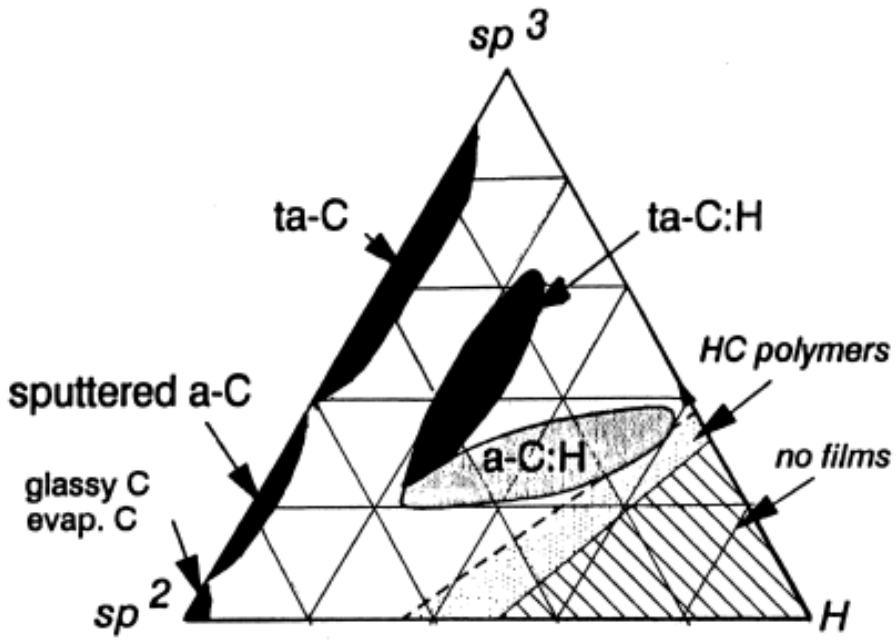

Figure 1.9 Phase diagram of diamond-like carbon materials [36].

The diverse types of DLC coatings have shown unique tribological properties depending on coating methods, dopant elements, temperature, working conditions, surrounding environment, lubricants and substrate materials [53-57]. Generally, ta-C coating shows high friction and wear in dry or vacuum condition but shows low friction and wear in humidity condition or additives-containing base oil boundary lubrication condition [23,58]. In comparison, a-C:H can show low friction and wear even in dry or vacuum condition but shows relative higher friction and wear in the water and/or oxygen containing environments due to strengthened bonding at the sliding interface by oxidation of a-C:H films [59].

Under the oil boundary lubrication regime without oil additives, tribological properties of ta-C and a-C:H are less concerned due to the most of the widely used commercial lubricant oil contain additives. For the viewpoint of green tribology [60], tribological properties of ta-C and a-C:H under the oil boundary lubrication with green

additives or without any additives is worth further studying.

1.5 Purpose of this study

In this thesis, to clarify the tribological performance of DLC coatings in high contact pressure application, the effect of applied load, sliding distance, counter materials and nano-particles on the friction and wear behaviors of ta-C and a-C:H coatings under boundary lubrication condition were investigated. The main exact objectives of this study are as follows:

1. To clarify the seizure mechanism of a-C:H and ta-C coatings in base oil lubrication under high contact condition on the basis of the effect of applied load and sliding distance on the tribological properties of a-C:H and ta-C coatings. Wear mechanisms of ta-C and a-C:H coatings were also proposed.
2. To clarify the effect of mating materials on wear properties of a-C:H and ta-C in base oil lubrication. In this research, we investigated the effect of hardness and roughness of mating material on the wear performance of ta-C and a-C:H and found out the key factors which dominate the wear of ta-C and a-C:H respectively.
3. To clarify the effect of nano-size particles on the wear properties of ta-C coating in oil boundary lubrication condition. In this research, we used ZrO_2 and CeO_2 with different hardness and size to study how these particles affected the wear of ta-C coating and the corresponding mechanism was also presented.

1.6 Outline of Dissertation

This dissertation presents the latest tribology research in the field of oil boundary lubrication of two prevailing DLC coatings, which are ta-C and a-C:H respectively. This first chapter begins with a description of significance of automobile tribology and industrial needs of DLC coatings. Then this chapter presents a brief introduction of lubrication theory with regard to the three lubrication regimes of Stribeck curve; hydrodynamic lubrication, mixed lubrication and boundary lubrication. The chapter also reviews briefly the DLC coatings and its application in oil boundary lubrication. The organization of dissertation is presented graphically in Fig. 1.10.

Chapter 2 firstly confirms the seizure resistance of DLC coating when sliding against S55C steel disk by taking uncoated SUJ2 roller as a reference. Then the effect of the applied load and sliding distance on the wear of ta-C and a-C:H is comparatively investigated after cylinder-on-disk friction tests. To clarify the wear mechanism of ta-C and a-C:H respectively, various surface analysis methods were applied on the worn area of tested DLC surfaces. Based on surface analysis, different wear mechanisms of ta-C and a-C:H under base oil boundary lubrication condition are proposed in detail.

Chapter 3 clarify the effect of mating material on the wear of ta-C and a-C:H coatings under base oil boundary lubrication condition. Six types of mating material: TiC, Cr, Ni, steel, Cu and Al, with different hardness and another three types of steel disk with variant roughness are prepared to investigate the effect of roughness and hardness on wear behavior of ta-C and a-C:H respectively. The hypothesis of wear mechanism of these two DLC coatings proposed in chapter 2 is verified and the key

factors that dominates the wear of each DLC coating are identified eventually.

Chapter 4 elucidates the effect of nano-particle as oil additives on the wear properties of ta-C coating in oil boundary lubrication condition. We present the effect of CeO_2 and ZrO_2 nano-particles on the wear rate of ta-C coating. Further we propose that the ZrO_2 nanoparticles can serve as an anti-wear oil additive to reduce the wear of ta-C coating. By the means of surface analysis methods, we clarify the anti-wear mechanism of nanoparticles additives.

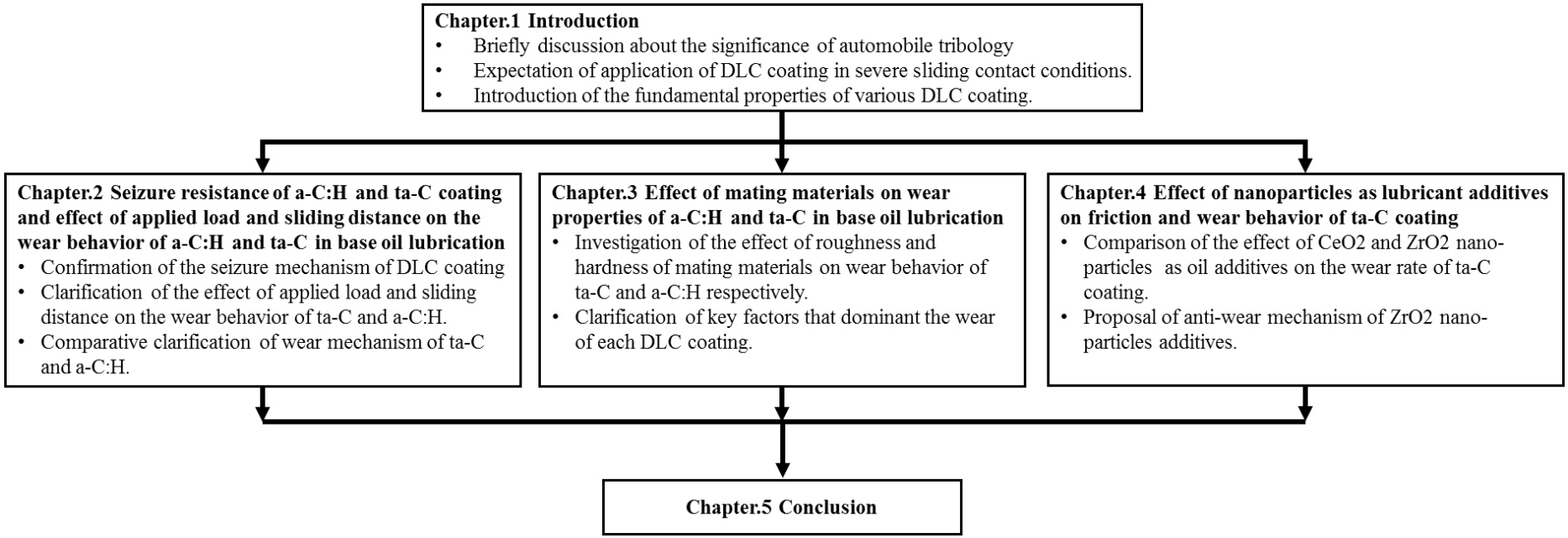

Figure 1.10 Organization of dissertation.

Chapter 2

Seizure resistance of a-C:H and ta-C coating and effect of applied load and sliding distance on the wear behavior of a-C:H and ta-C in base oil lubrication

2.1 Introduction

In the engine industry, nearly 30% energy loss was further caused by bearing components [61], whereby boundary lubrications are inevitable in the processes of start and stop, or under rigorous working conditions between working parts. In these cases, severe wear [62] and even seizure [63] of contact surfaces is prone to occur and therefore give rise to a negative effect on extra energy dissipation or life-span of such sliding components. Thus, tribological properties of such sliding components starve for further enhancement by surface approaches, and among which surface coating technology has been widely utilized as a desirable solution [26].

Diamond-like carbon (DLC) coating has been characterized as low friction, high wear resistance and remarkable mechanical properties, thus can be applied to the critical engine components as a protective coating to reduce the friction and wear effectively, even under the boundary lubrication condition [52], wherein direct contact of both mating surfaces are predominant. In this case, highly reliable and robust DLC coating for mating surface of engine bearings were in urgent need currently. Distinct DLC

coatings show discrepant wear and friction behaviors under identical environment [52]. Presently, two main types of DLC, which are hydrogenated amorphous carbon (a-C:H) and tetrahedral amorphous carbon (ta-C), has been widely utilized in automotive engine industry. These two types of coating generally offer low friction and high wear resistance, but they also have some dissimilarities in friction and wear properties due to their different hydrogen content and microstructure [58]. Basically, a-C:H coating gives ultra-low friction in inert or vacuum environments whereas ta-C coating provides ultra-low friction and wear in the presence of oxygen, hydrogen or water molecules [64,65]. However, most previous research works were performed separately on either ta-C or a-C:H, an elaborate comparison of tribological behaviors between this two DLC coating materials under the oil boundary lubrication condition was still insufficient.

Seizure of contacting elements is a catastrophic failure of tribological systems in dry or boundary lubrication conditions [66]. Most seizure-related researches have been concentrated on metal or alloy materials, seizure resistance of DLC coatings on steel has been rarely investigated. Apart from the fatal failure of seizure, regular wear of DLC coatings when sliding against steel are still needed to be inhibited or alleviated. Up to now, considerable studies have been focusing on the wear properties of various DLC coatings under oil boundary lubrication [28,67-59], among which, most of them were related to the effect of oil additives and category of lubricating oil on tribological performance of DLC coatings. Basically, by using oil additives, the chemical reaction induced the formation of various corresponding tribolayer that protect the contact surface from being worn out to a certain extent, however, the utilization of such

phosphorus and sulfur-containing oil additives easily brought in environmental problems due to the hazardous emissions and sludge obtained during purification [70]. Some studies even showed that wear of different DLC coatings (pure and doped) was independent of introducing additive or not in combination with biodegradable oils [71]. Hence intensive study on the tribological behavior of environmentally preferable DLC coatings in additive-free lubricants is imperative.

The primary goal of this chapter is to find out which DLC coating is preferable for engine main bearing, wherein high load capacity, stability and long lifespan are of the essence. Therefore, seizure resistance of a-C:H and ta-C coatings on steel were confirmed preferentially in pure poly-alpha-olefin (PAO4) boundary lubrication condition by the means of cylinder-on-disk friction test under stepwise increased applied load. Moreover, friction and wear behavior of both DLC coatings were investigated in the same lubrication conditions with various load and sliding distance. In the end, friction and wear mechanism of each DLC coatings was elucidated by the means of optical and scanning electron microscope, atomic force microscope and Raman spectroscopy.

2.2 Experimental details

2.2.1 Material characterization and lubricants

The cylinder pin and disk were made from high carbon chrome steel (SUJ2) and carbon steel (S55C, 0.56 - 0.58 at. % of carbon concentration) respectively. Two commercially available categories of DLC coatings, which is hydrogenated amorphous

carbon (a-C:H) and tetrahedral amorphous carbon (ta-C), were supplied by Nippon ITF Inc. They were deposited on the curved surface of cylinder pins, wherein a-C:H was deposited by PECVD (plasma enhanced chemical vapor deposition) methods and ta-C was deposited by ion plating method. And both DLC coatings were finishing polished subsequently to remove the droplets and particles which formed on the top surface during deposition process. Surface roughness, hardness and Young's modulus were measured by atomic force microscopy (SEIKO, Nanopics 1000) and Nanoindenter (NANOPICS 1000 Elionix ENT-1100a). Detailed properties of DLC coated pin and disc are listed in Table 2.1.

Table 2.1 Properties of disk and ta-C & a-C:H coated cylinder

Properties	**Disk**	**Cylinder**	
		ta-C	a-C:H
Dimension (mm)	ϕ22.5×4	ϕ5×5	ϕ5×5
Substrate	S55C	SUJ2	SUJ2
Coating method	-	Ion plating	PECVD
Thickness (μm)	-	0.8 ~ 1	3.7 ~ 4.1
Surface Roughness R_a (μm)	0.01± 0.005	0.024 ± 0.02	0.031 ± 0.04
Hardness (GPa)	3.5 ± 2	38 ± 2	12 ± 2
Hydrogen Content (at.%)	-	<1	25~30

The lubricant oil used in this research is synthetic poly alpha olefin (PAO4) which has a viscosity of 5.25 mm^2/s and a pressure-viscosity coefficient of 14.2 GPa^{-1} at 80 ℃.

2.2.2 Tribological experiments

In this study, both seizure tests and friction tests were performed using a unidirectional cylinder-on-disk tribotester under boundary lubrication condition (Fig.

2.1). For seizure tests, stepped-fixed load was applied vertically ranging from 10 N to 50 N, and increased stepwise by 10 N at a same time interval (corresponding to a maximum initial Hertzian contact pressure of 170 MPa, 240 MPa, 295 MPa, 340 MPa and 380 MPa respectively for each load step). And the uncoated (SUJ2) cylinders were used here as reference. Note here that time interval of each fixed loading stage for a-C:H/S55C and SUJ2/S55C was set as 30 min to insure than running-in could be passed away. And each test was repeated three times for confirm the reproducibility.

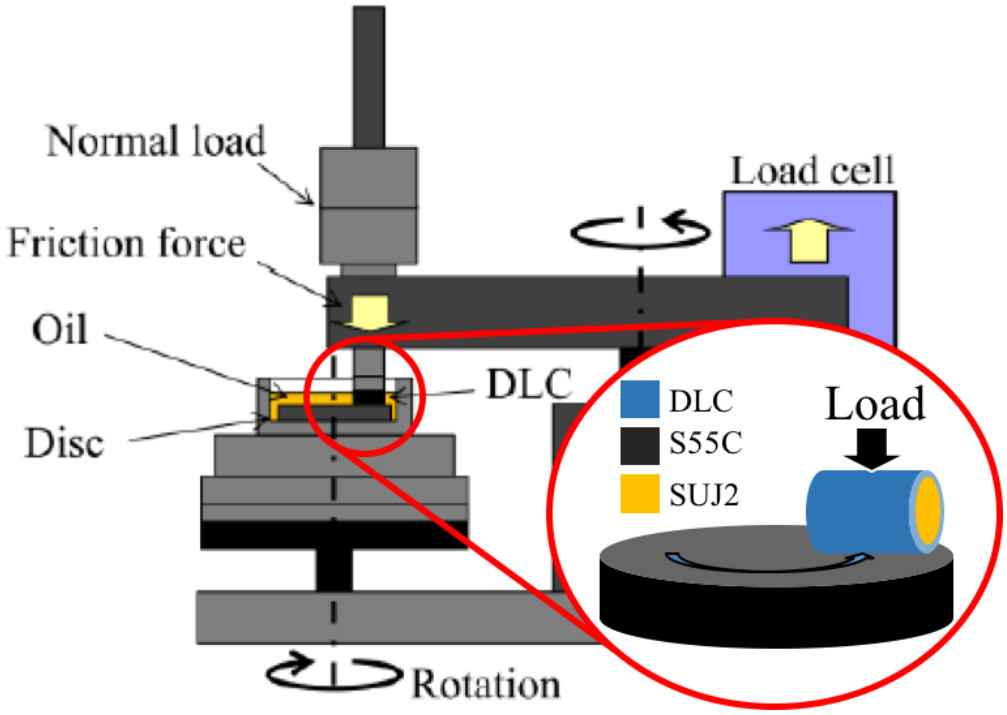

Figure 2.1 Schematic of reciprocating cylinder-on-disk tribotester

As for friction tests, the DLC-coated cylinder was loaded by 5 N, 10 N, 20 N and 30 N (corresponding to a maximum initial Hertzian contact pressure of 120 MPa, 170 MPa, 240 MPa and 295 MPa respectively), and rubbed against uncoated steel disk under pure sliding condition. Both cylinder and disk were immersed into the pure PAO4 oil and the temperature was kept at 80 ℃ constantly during the sliding test. The rotational

radius and speed were fixed at 6.65 mm and 100 rpm (0.065m/s) respectively. Test duration was set as 30 min, 60 min, 90 min and 120 min and the corresponding sliding distance were calculated approximately as 125 m, 250 m, 375 m and 500 m respectively. The friction coefficient was simultaneously recorded by load cell unit. Wear volume of DLC coatings on the cylinder was roughly calculated by measuring the width of rectangular-shape wear scar with optical microscope. Before and after the friction tests, all samples were cleaned with benzene and acetone successively in an ultrasonic bath to remove oil species and contaminants. In addition, all the tests were repeated three times for reproducibility.

The minimum film thickness (h_{min}) for rectangular conjunctions and dimensionless lambda ratio (Λ) were calculated using Eqs. (2.1) and (2.2), respectively, by Hamrock and Dowson [72].

$$h_{min}=1.806(w'_z)^{-0.128}(\eta_0\tilde{u})^{0.694}\xi^{0.568}R_x^{0.434} \quad (2.1)$$

$$\Lambda = \frac{h_{min}}{\sqrt{R_{q,a}{}^2+R_{q,b}{}^2}} \quad (2.2)$$

where w'_z is the normal load per unit width, η_0 is the absolute viscosity at the pressure of 0 Pa and the temperature of 80 ℃, $\tilde{u}$ is mean surface velocity in sliding direction, ξ is pressure-viscosity coefficient, Rx is effective radius of cylinder, $R_{q,a}$ is the surface roughness of cylinder and $R_{q,b}$ is the surface roughness of disc. The calculated lambda ratio at initial contact condition is 0.23 and 0.3 for a-C:H/steel and ta-C/steel tribosystem respectively, which both are less than unity, thus operating lubrication regime is boundary lubrication.

2.2.3 Surface analysis

Worn surfaces of cylinder and disk were studied by using optical microscopy, Raman spectroscopy (NRS-1000 Laser, Jasco Inc., Japan), field-emission scanning electron microscope (JEOL, JSM-7000FK) and atomic force microscopy (Nanopics 1000, SEIKO). Raman spectroscopy measurements with 532 nm Ne laser radiation were carried out to characterize structural information of DLC coatings.

2.3 Results and Discussion

2.3.1 Seizure resistance of a-C:H and ta-C

Seizure tests were conducted by applying stepped-fixed load, and occurrence of seizure is noticed in terms of large mass flow on the disc, sharply increased friction coefficient, and abnormal vibration and noise from the pin-on-disc assembly.

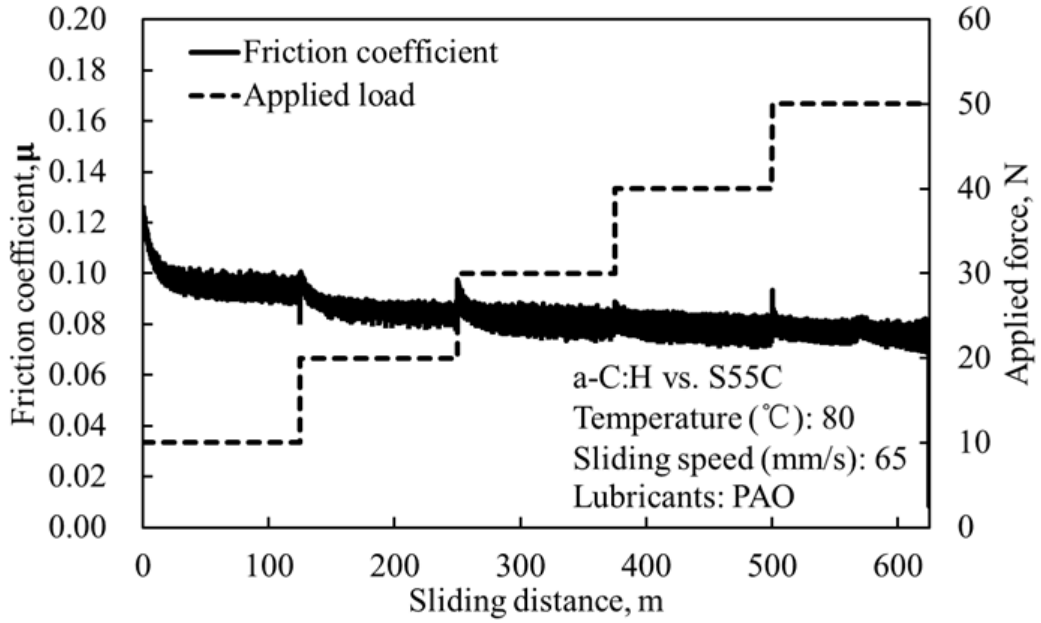

(a) a-C:H against S55C

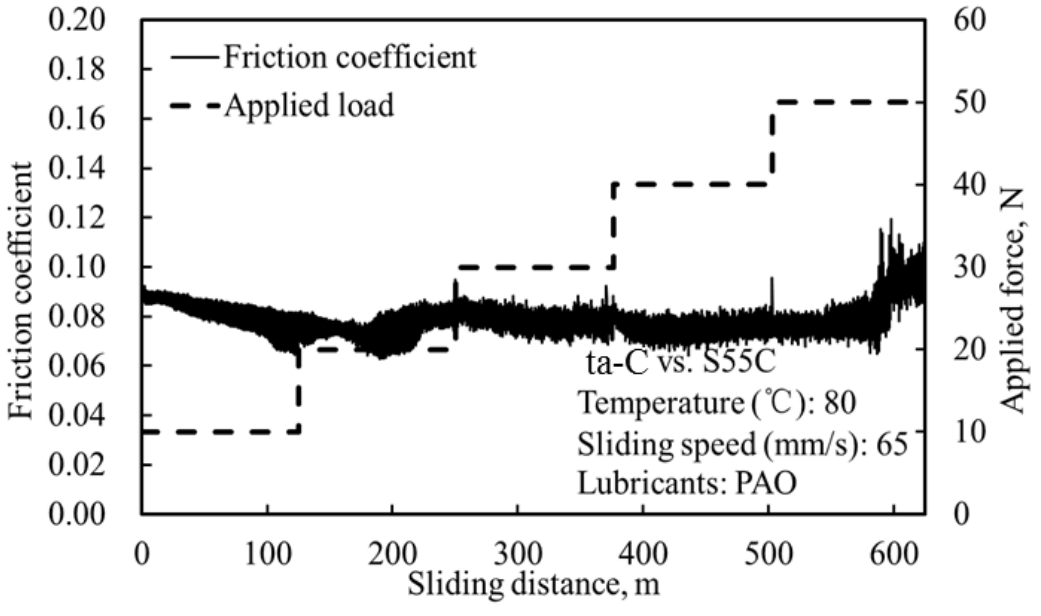

(b) ta-C against S55C

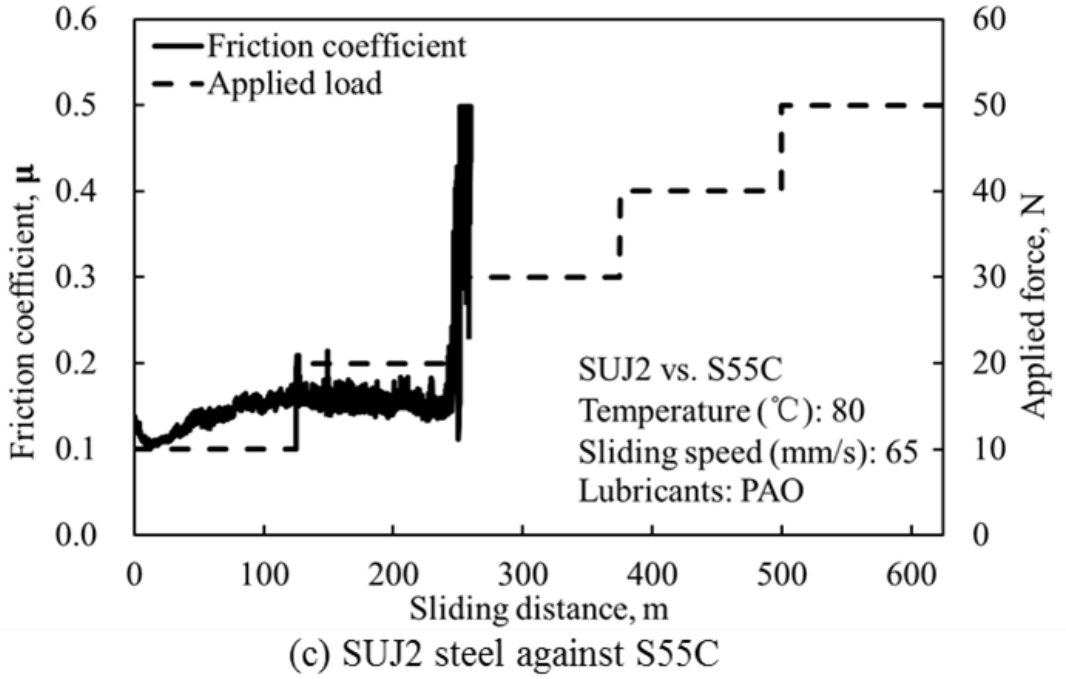

(c) SUJ2 steel against S55C

Figure 2.2 Representative friction coefficients as sliding distance and stepped-fixed load between (a) a-C:H cylinder and S55C steel; (b) ta-C cylinder and S55C steel; (c) SUJ2 cylinder and S55C steel

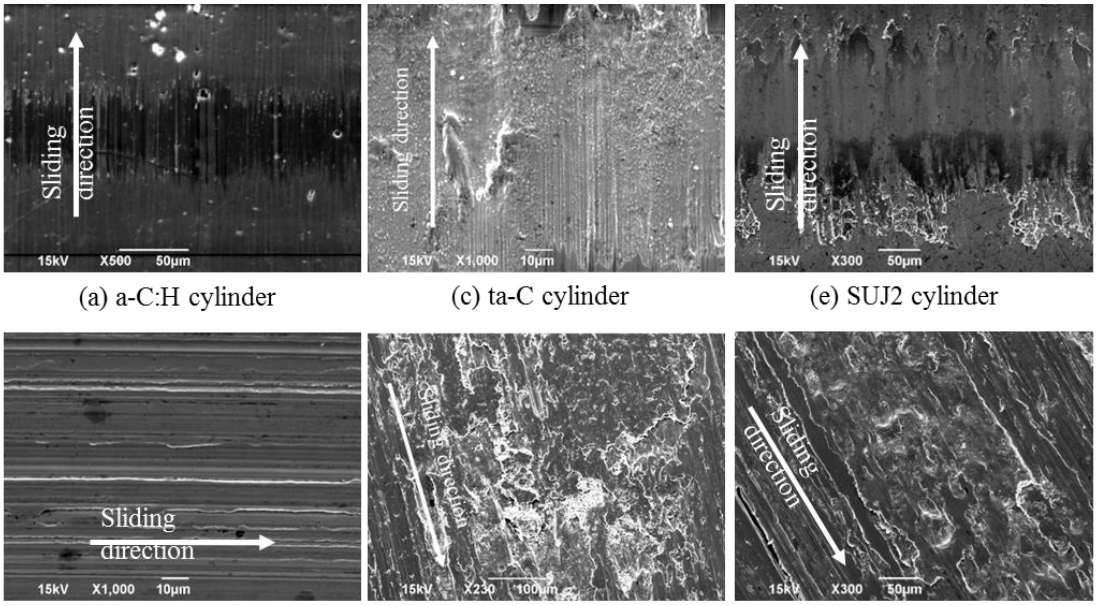

(a) a-C:H cylinder (c) ta-C cylinder (e) SUJ2 cylinder

(b) S55C disk against a-C:H (d) S55C disk against ta-C (f) S55C disk against SUJ2

Figure 2.3 SEM images of wear scar on (a-b) a-C:H coated cylinder and counterpart S55C disk (c-d) ta-C coated cylinder and counterpart S55C disk (e-f) uncoated SUJ2 cylinder and counterpart S55C disk after seizure test.

Figure 2.2(a) shows the friction coefficient as a function of sliding distance and applied load for a-C:H/steel tribosystem under boundary lubrication condition. As this figure shows, friction coefficient decreases gradually with increase in applied load and sliding distance. In addition, initially rapidly decreases friction coefficient indicates that a-C:H/steel tribosystem experienced a running-in period, and familiar phenomenon comes out in the next two fixed-load stages.

Figure 2.2 (b) depicts the friction coefficient as a function of sliding distance and applied load for ta-C/steel tribosystem under boundary lubrication condition. It is observed that friction coefficient doesn't change significantly with increasing stepped-fixed load until the last 25 m, however abruptly increase remarkably and becomes unstable.

Figure 2.2 (c) represents the friction coefficient as a function of sliding distance and applied load for uncoated SUJ2/steel tribosystem under boundary lubrication condition. It is evident that friction coefficient increases slight and remains stable around 0.15 until applied load is 20 N. However, when applied load is more than 20 N, friction coefficient increased at a sudden, accompanying with hoarse noise and vibration. Therefore, test was suspended immediately then.

FE-SEM images of wear scar on the a-C:H coated cylinder and S55C disk are shown as Fig. 2.3(a) and Fig. 2.3(b) respectively, relatively dark wear scar could be observed in the middle of the curve surface of a-C:H coating and no adhesive materials could be detected inside and outside the wear scar. On the counterpart side of S55C disk, only obvious scratch grooves along the sliding direction could be found. Figures 2.3 (c) and

(d) indicates the wear scar on the ta-C coated cylinder and S55C disk respectively, partial spalling of ta-C coating could be observed on the cylinder side (Fig. 2.3(c)), amounts of flake shape deformation are detected on the disk surface. Wear scar of uncoated SUJ2 cylinder is shown in Fig. 2.3 (e), it is evidently that a mass of adhesive matters is detected nearby round the wear scar. Moreover, other than plowing grooves, large scale plastic deformation is observed on the counterpart S55C disk in Fig. 2.3 (f).

It is reasonable to deduce from Fig. 2.2 and Fig. 2.3 that seizure does not occur in the case of a-C:H/steel tribopair when applied load is up to 50 N since neither large-scale adhesion nor abnormal condition, such as vibration, noise or high and unstable friction coefficient are detected during the whole experiment. For ta-C/S55C tribopair, it shows adequate seizure resistance when friction coefficient remains relative stable, when high load is applied, hard and brittle ta-C is easy to suffer from brittle fracture and spalling, meanwhile friction coefficient increases abruptly and becomes unstable, it is assumed to result in mild seizure in the ending seizure test, which can also be proved by adhesive flake like deformation as shown in Fig. 2.3(d). For SUJ2/S55C tribopair, seizure arises when applied load is increased up to 30 N, characterized by a surge of friction coefficient, heretofore friction coefficient remains roughly stable around 0.15. Besides, scaled plastic flow (Fig. 2.3(f)) on the disk could also back up the occurrence of seizure in steel/steel tribopair.

Seizure is essentially attributed to intense micro-welding located in the interfaces. It is intrinsically dominated by nature of mating materials themselves and extrinsically triggered by applied stress rather than relative velocities [73]. In our research, both ta-

C and a-C:H can provide seizure resistance only if such coating are not spalled or peeled off from the substrate. However, ta-C coating appears to be undesirable to be used as anti-seizure coatings due to their poor load capacity.

2.3.2 Friction results

Friction tests were performed for DLC/steel tribopair in pure PAO4 oil to differentiate the tribological performance between ta-C and a-C:H coatings.

Figures 2.4(a) and (b) show representative friction coefficient of ta-C and a-C:H under PAO4 boundary lubrication condition at applied load of 5 N,10 N, 20 N and 30 N respectively and sliding distance of 250 m. Average values of steady-state friction coefficient of both ta-C and a-C:H coatings under the applied load of 5 N, 10 N, 20 N and 30 N respectively are summarized as Fig. 2.5. The steady-state friction coefficients for each data point are calculated by taking the average friction coefficient of last 500 cycles of each test. Briefly, friction coefficient of both ta-C/steel and a-C:H/steel tribopairs generally lie between 0.055 and 0.12. Generally, ta-C/steel tribopair exhibits lower friction coefficient than a-C:H/steel tribopair. It is also found that friction coefficient generally decreases with increase in applied load for both DLC coatings.

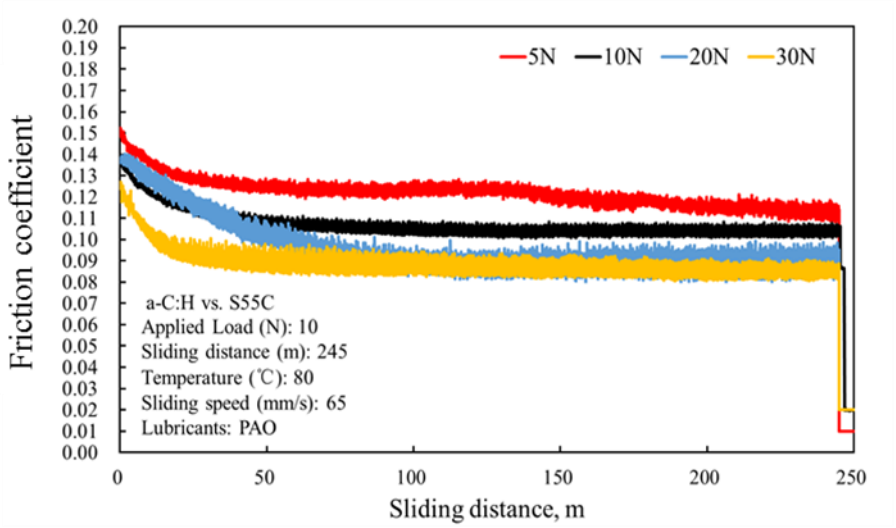

(a) a-C:H against S55C disk

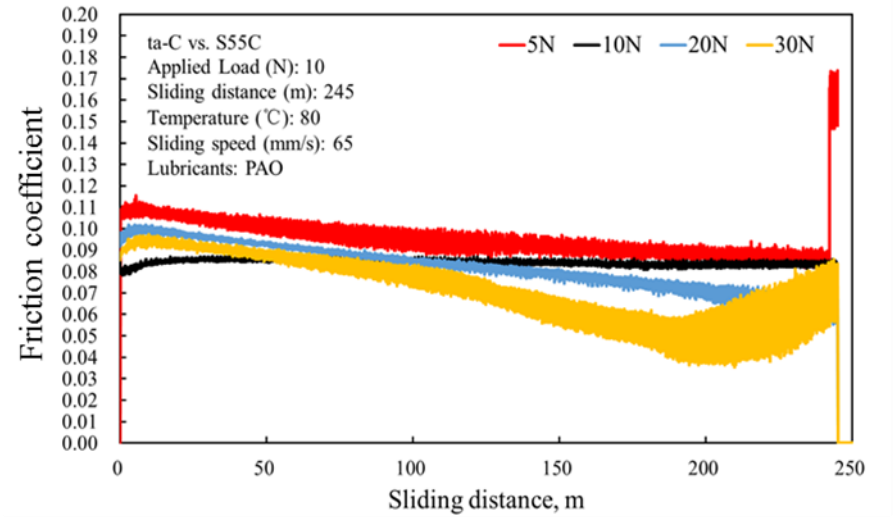

(b) ta-C against S55C disk

Figure 2.4 Representative friction coefficients as sliding distance between (a) a-C:H against S55C disk and (b) ta-C against S55C disk under 5 N, 10 N, 20 N and 30 N respectively.

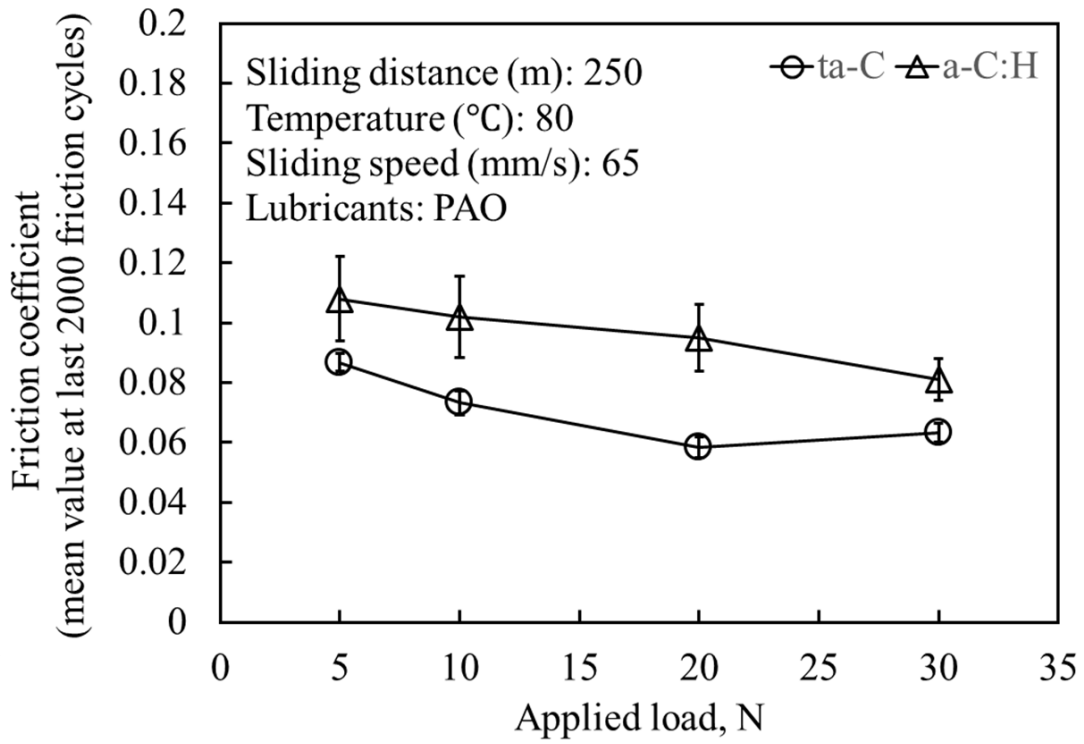

Figure 2.5 Comparison of steady-state friction coefficient of ta-C/steel and a-C:H/steel contacts under 5 N, 10 N, 20 N and 30 N respectively.

2.3.3 Effect of applied load on the wear of DLC coatings

To differentiate the wear behavior between ta-C and a-C:H coatings and to investigate the corresponding wear mechanism taking into consideration of the dependence of applied load and sliding distance, specific wear rate was calculated after each friction test.

Figure 2.6 displays the dependence of specific wear rate of ta-C and a-C:H on the diverse applied load, which is set as 5 N, 10 N, 20 N and 30 N respectively. The specific wear rate of ta-C is quite few ($\approx 3.5\times10^{-9}$ mm^3/mN) under 5 N applied load. By comparison, this value is almost 4 times lower than that of a-C:H (approximately 13.6×10^{-9} mm^3/mN) under the same condition. However, when applied load exceeds 5 N and reach 10 N, the specific wear rate of ta-C increased significantly by 5 times

(nearly 18.2×10^{-9} mm^3/mN), in contrast, specific wear rate of a-C:H decrease with increase in applied load. As applied load keeping adding up to 20 N, ta-C/steel exhibits severer wear than prior cases. Eventually, ta-C is worn out at load of 30 N due to its limited thickness (1 μm), hence the wear volume couldn't be calculated precisely at this data point. As shown in Fig. 2.7(a), partial spalling is observed inside the wear scar of ta-C coated cylinders those are loaded at 10 N, 20 N and 30 N respectively, except in the case of 5 N where evident spalling or other fracture could be rarely identified. However, there is no partial spalling spot could be detected at any applied load for a-C:H coating (Fig. 2.7(b)).

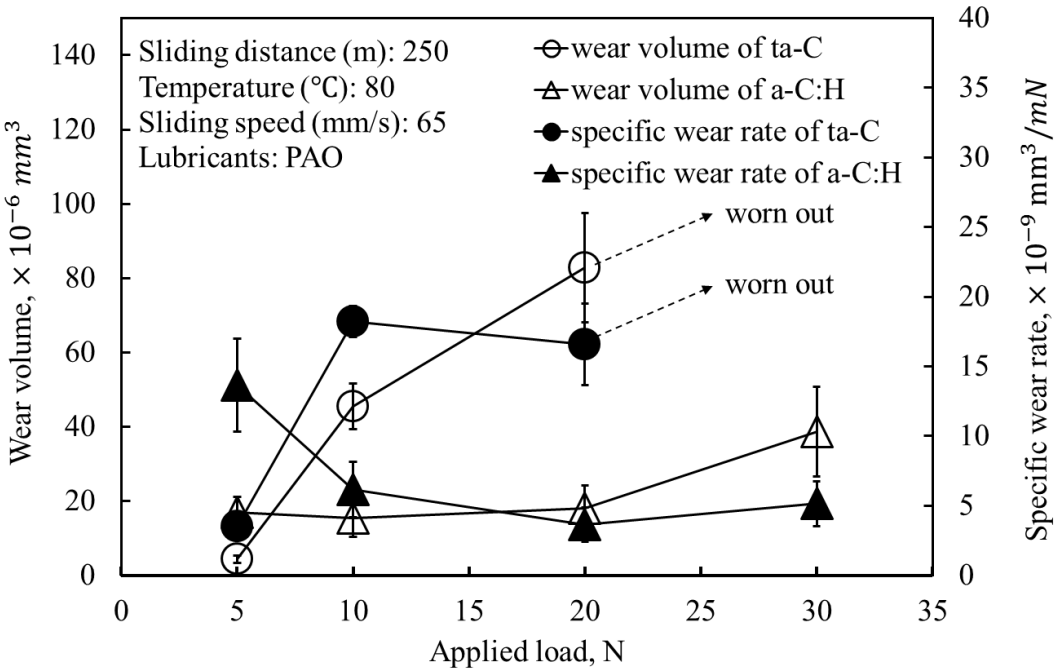

Figure 2.6 Wear volume loss and specific wear rate of ta-C and a-C:H under different applied load.

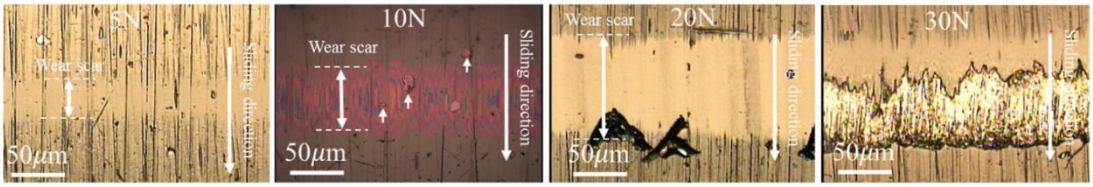

(a) ta-C

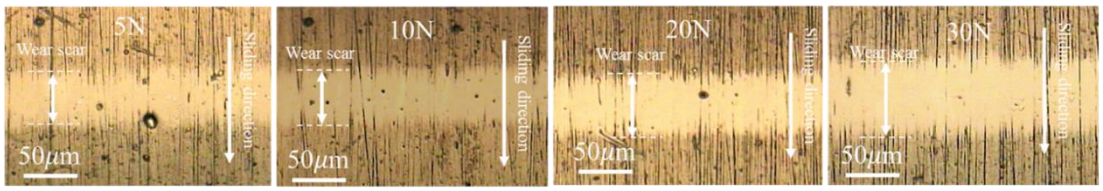

(b) a-C:H

Figure 2.7 Optical microscope images inside wear scar of (a) ta-C and (b) a-C:H at different applied load.

2.3.4 Effect of sliding distance on the wear of DLC coatings

Furthermore, dependence of wear characteristics of both DLC coatings on the sliding distance is also studied and summarized. Figure 2.8(a) shows the calculated data of specific wear rate for both ta-C and a-C:H coatings rubbed through different sliding distance. As for a-C:H, specific wear rate keeps decreasing slightly with the sliding distance up to 500 m, and during entire period, specific wear rate is retained below 10×10^{-9} mm^3/mN. Nevertheless, ta-C shows unusual different wear behavior, specific wear rate of ta-C raises up drastically step by step and finally wear out when the sliding distance is prolonged to 500 m. Figure 2.9(a) shows the optical microscopy images of ta-C worn surfaces tested against steel disc at various sliding distance. As it is seen in Fig. 2.9(a), no obvious spalling occurred inside the wear scar at the sliding distance of 125 m. However, as the sliding distance is extended to 250 m, small partial spalling areas emerge either inside or nearby the border of wear scar. The spalling areas expand to larger scale at sliding distance of 375 m and spread to the whole wear scar at the

sliding distance of 500 m. Figure 2.9(b) shows the wear scar on a-C:H cylinder at various sliding distance and no obvious partial spalling can be identified inside the wear scar throughout all the sliding distance.

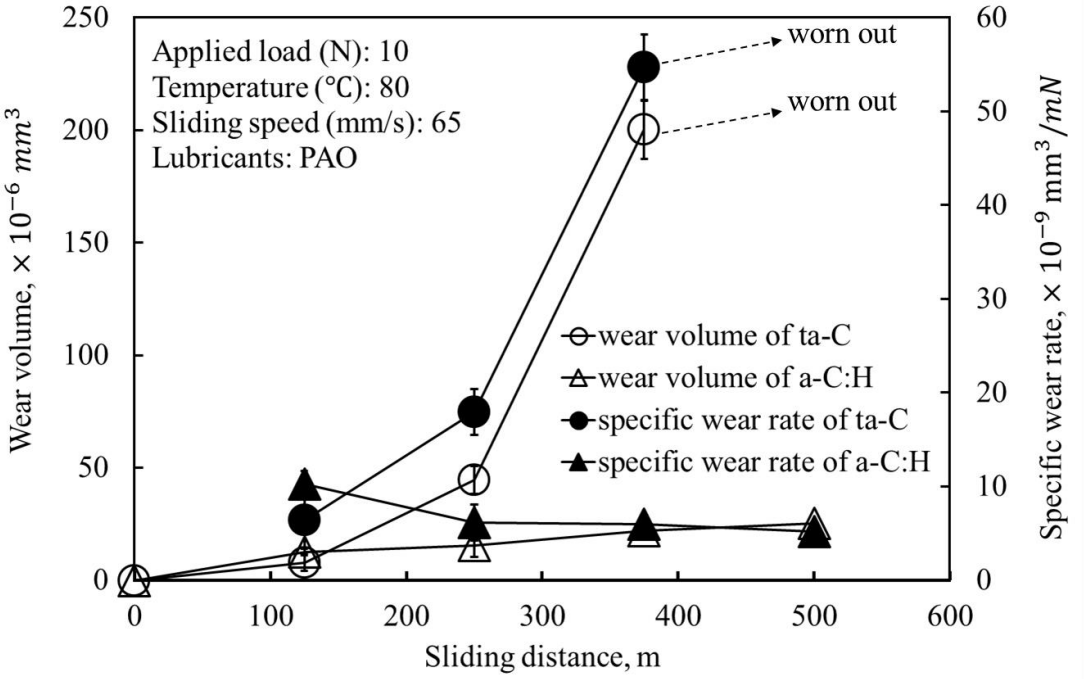

Figure 2.8 Wear volume loss and specific wear rate of ta-C and a-C:H under different sliding distance.

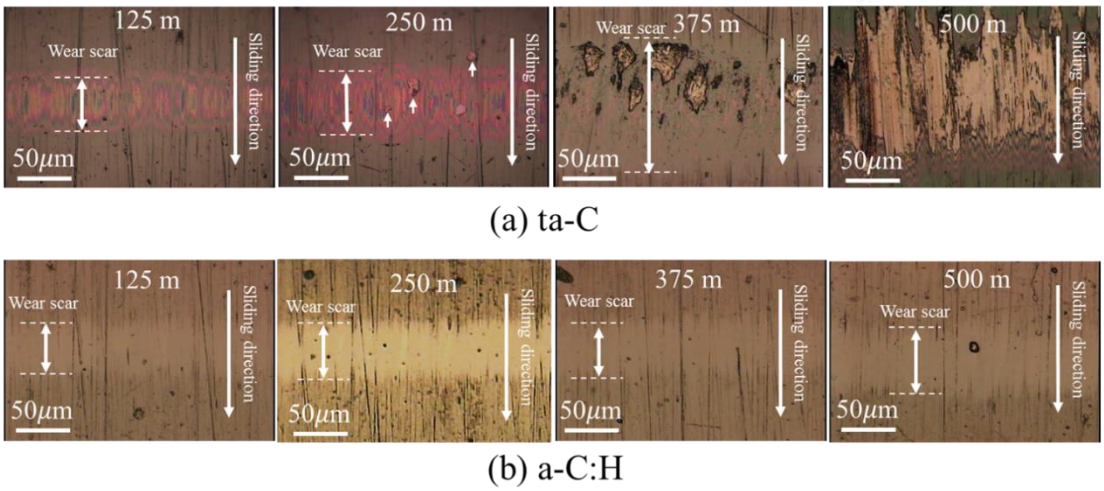

Figure 2.9 Optical microscope images inside wear scar of (a) ta-C and (b) a-C:H at different sliding distance.

2.3.5 Surface analysis with Raman spectroscopy and AFM

To clarify the wear mechanism of each DLC coating under base oil boundary lubrication condition, surface analysis on the wear scar with Raman spectroscopy and AFM is conducted.

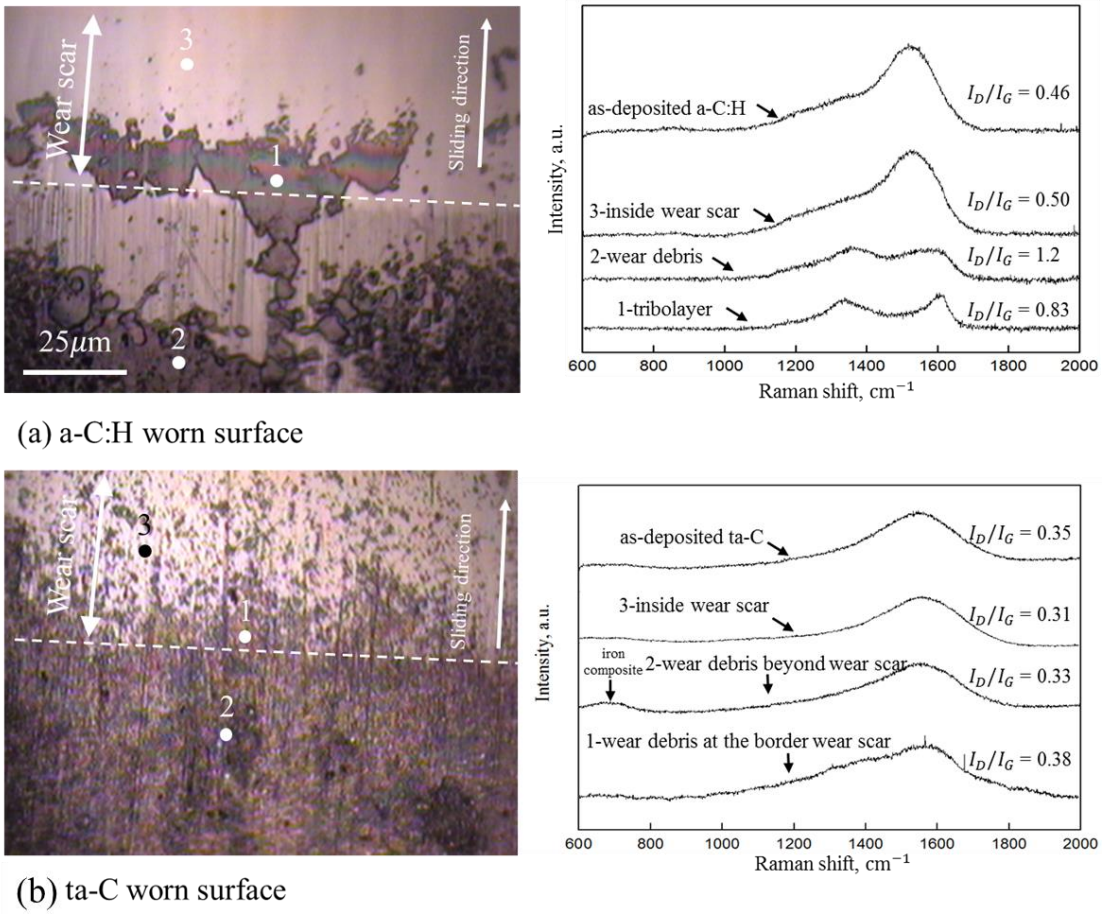

Figure 2.10 Optical microscope images of transfer layer on the wear scar of (a) a-C:H and (b) ta-C at applied load of 10N and sliding distance of 250m

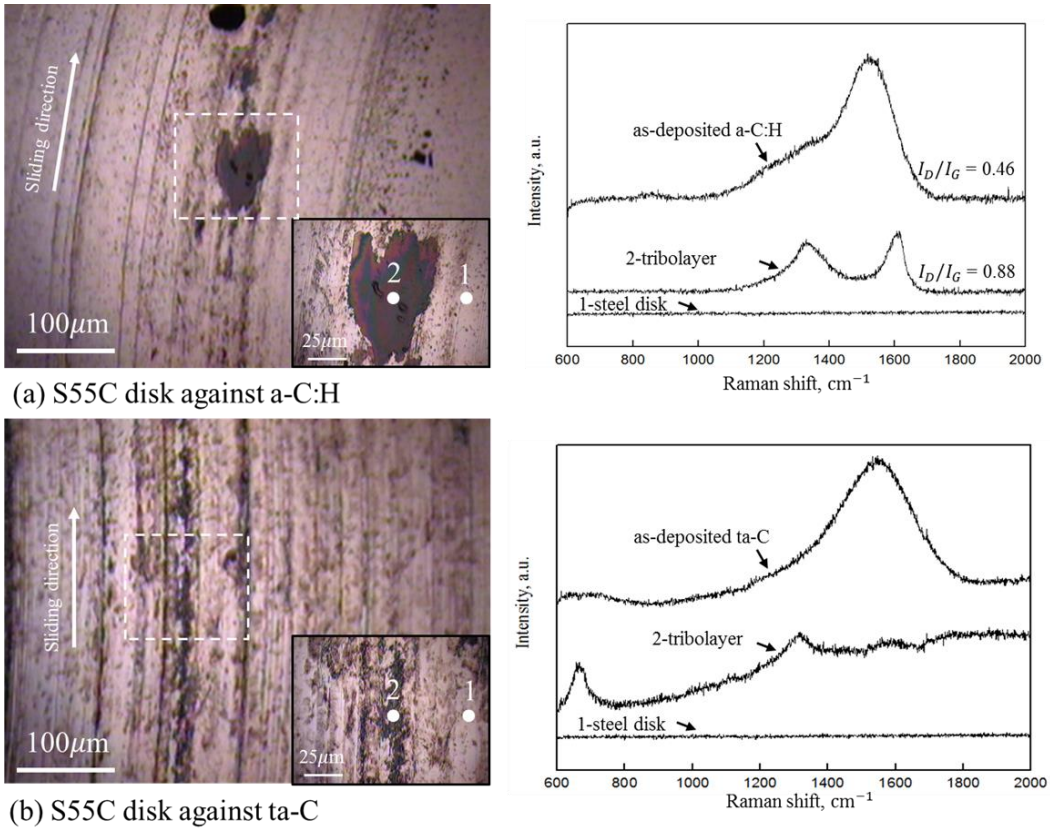

Figure 2.11 Optical microscope images of transfer layer on the disk which rubbed against (a) a-C:H and (b) ta-C at applied load of 10N and sliding distance of 250m

Raman spectroscopy measurements were taken to identify graphitization inside and nearby the wear scar on both DLC surfaces which were tested at the applied load of 10 N and sliding distance of 250 m. It's worth mentioning here that both DLC coated cylinders were just rinsed in benzene and acetone without ultrasonic bath after rubbing to preserve the adherent tribolayer nearby the wear scar. Graphitization can be interpreted from an increase in the intensity ratio (I_D/I_G) indicated by the maximum disordered D-peak (I_D) intensity and the maximum graphite G-peak (I_G) intensity in the Raman spectra [73]. Figure 2.10(a) shows the optical microscopy images of tribolayer near the border of the wear scar of a-C:H coating and its Raman spectra obtained on different areas. In comparison with as-deposited a-C:H coating, Raman spectrum of

tribolayer shows D peak more evidently and significant increase in I_D/I_G (from 0.46 to 0.83). Meanwhile, the Raman spectrum of a-C:H inside the wear scar without coverage of tribolayers is also detected and it shows marginal difference from the as-deposited a-C:H coating and only slight increase in I_D/I_G could be confirmed (from 0.46 to 0.50). Besides, tribolayers are also detected beyond the wear scar, Raman spectrum indicates that those tribolayers suffer from further graphitization than those around the border of the wear scar. In the case of ta-C worn surface, evident tribolayer cannot be observed inside or nearby the wear scar as it is shown in Fig. 2.10(b). Raman spectra of different areas where located inside, on the border and beyond the wear scar respectively are measured to ascertain the graphitization of ta-C after rubbing against steel disk. The change in the Raman spectra of those areas is too slight to decide whether this change may originate from graphitization of topmost surface. And the Raman spectrum of the dark areas where are beyond the wear scar shows peak at Raman shift of 700 cm^{-1}, it may result from the generation of iron composites during rubbing process [74]. Figure 2.11 shows the optical images of wear scar on disk which rubbed against a-C:H (Fig. 2.11(a)) and ta-C (Fig. 2.11(b)). According to the Raman spectra of dark tribolayer, it is clearly that graphitized carbon layer is formed and transfer from mating a-C:H coating to steel disk. However, for the disk which rubbed against ta-C coating, only iron oxides can be detected inside the wear track as confirmed by Raman spectra [74].

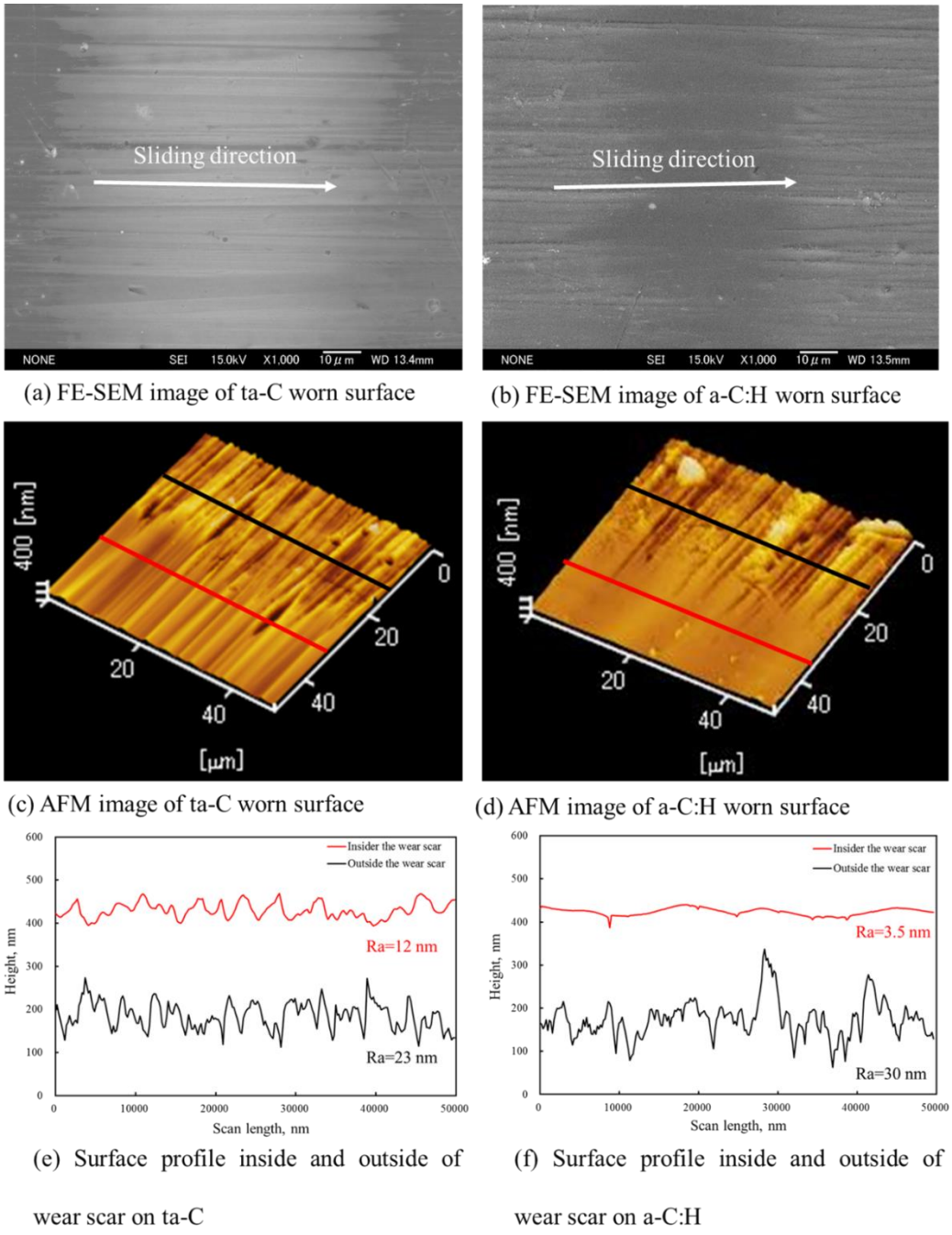

(a) FE-SEM image of ta-C worn surface

(b) FE-SEM image of a-C:H worn surface

(c) AFM image of ta-C worn surface

(d) AFM image of a-C:H worn surface

(e) Surface profile inside and outside of wear scar on ta-C

(f) Surface profile inside and outside of wear scar on a-C:H

Figure 2.12 Representative FE-SEM images of wear scar on (a)ta-C and (b) a-C:H and surface topography located near the border of wear scar for (c) ta-C and (d) a-C:H by AFM, and corresponding surface profile inside and outside the wear scar of (r) ta-C and (f) a-C:H.

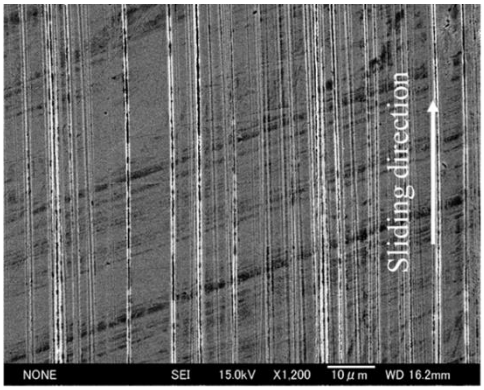

(a) FE-SEM images of wear scar on S55C disk which rubbed against ta-C

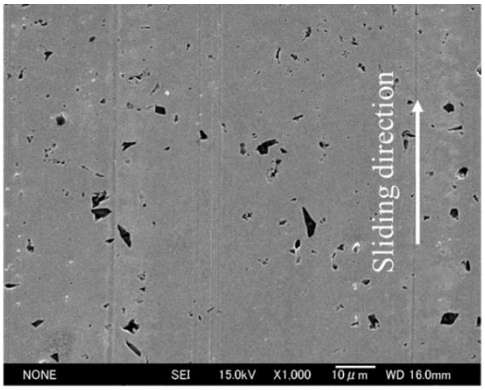

(b) FE-SEM images of wear scar on S55C disk which rubbed against a-C:H

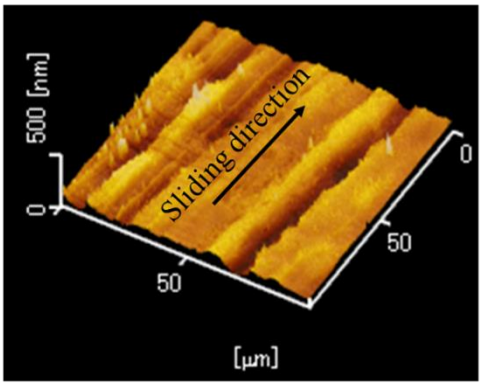

(c) AFM images of wear scar on S55C disk which rubbed against a-C:H

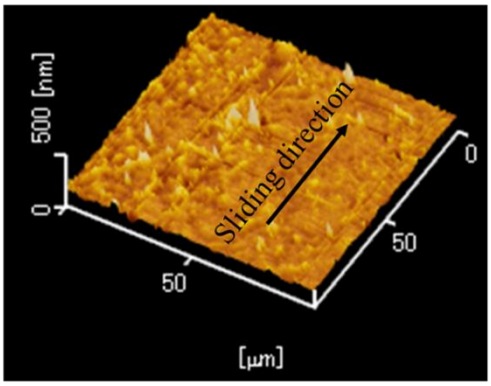

(d) AFM images of wear scar on S55C disk which rubbed against ta-C

Figure 2.13 Representative FE-SEM images of wear scar on disk which rubbed against (a) ta-C and (b) a-C:H; and (c)-(d) AFM images of each wear scar.

Figures 2.12 (a)-(b) exhibits the representative FE-SEM images of both ta-C and a-C:H after rubbing 250 m at applied load of 10 N. It can be clearly seen that scratch grooves are found in the central wear region of ta-C. However, in the case of a-C:H, original groove-patterns are hardly seen in the central wear region, except for certain deep-like ones. Surface topography located near the border of wear scar for both ta-C and a-C:H by the means of AFM are obtained as shown in Figures 2.12 (c)-(d). It can be clearly seen that wear scar of ta-C is rather rougher than that of a-C:H, and the corresponding surface profile of each DLC coating surface inside and outside the wear scar are measured as Figures 2.12 (e)-(f). It appears that a-C:H is more smoothened

after rubbing than ta-C. It may owe to two distinct wear mechanisms for each DLC coating which will be discussed later. In addition, FE-SEM and AFM analysis shows that scratch lines parallel to the sliding direction are generated after rubbing against ta-C coating, whereas relative smoother worn surface is formed when rubbing against a-C:H coating (Fig. 2.13).

2.3.6 Friction mechanism of ta-C and a-C:H coatings

Generally, two fundamental theories are widely accepted to explain the low friction mechanism of DLC. First, friction-induced graphitization of DLC has been widely considered as the one of the main cause of low friction due to graphite-like lamellar structure which easily shear between each plane [75,76]. However, in our research, graphitization of a-C:H coating is observed either on the border of wear scar or beyond the wear scar as Fig. 2.10(a) whereas no sign of graphitization could be detected nearby the wear scar of ta-C as Fig. 2.10(b), it may be due to graphitization of ta-C is much harder to be triggered than a-C:H under lubricated conditions [58]. According to the friction-induced graphitization mechanism, friction coefficient of a-C:H should be lower than ta-C with the lubricity effect of graphitized layer. However, figure 2.5 represents the contrary results, where ta-C coating exhibits lower friction coefficient than a-C:H coating in steady state under all the applied load. It indicates that graphitization mechanism is inadequate to explain the low friction phenomenon of DLC in base oil boundary lubrication condition. As a matter of fact, although abundant of researchers observed graphitization of DLC coatings, it remains an open question that

whether such graphitized sp^2-rich layer can mimic the low friction behavior of graphite due to its intrinsic lamellar structure [77]. And, it was proposed that such graphitized layer is more likely equilibrium between disordering and ordering processes under mechanical stimulus [78]. Similarly, Sanchez-Lopez et al. [79] also stated that evidence of extended graphite layer formation was not observed by transmission electron microscope (TEM) observation.

Another theory account for low friction mechanism of DLC is attributed to passivation of dangling bond by water and/or oxygen molecules [80], hydroxyl (-OH) [81] and hydrogen [82]. By comparing ta-C and a-C:H coating, polar carbon dangling bond of ta-C coating is significantly more than a-C:H since majority of intrinsic dangling bonds inside a-C:H are passivated by hydrogen atom during deposition process. In addition, all the friction tests were conducted in the pure base oil which is just a hydrocarbon with no polarity, hence it is hardly impossible for ta-C to be passivated by any polar species with in the oil. Therefore, friction coefficient of ta-C should be higher than that of a-C:H, however, figure 2.5 shows the contrast results. Even if thermos-oxidation could slightly occur within the rubbing contact surface, where high flash temperature and stress concentration may facilitate the degradation of PAO with inevitably dissolved oxygen or water molecule from ambient environment to generate certain polar species to passivate the ta-C surface during rubbing, a-C:H is also passivated during deposition process by hydrogen atoms, it is rather arbitrarily to assert which passivation effect is more predominant to lead to low friction.

In conclusion, it appears that neither of these two fundamental low friction theories of DLC could explain lower friction coefficient of ta-C than that of a-C:H under base oil boundary lubrication condition. As can be seen in Fig. 2.7(a) and Fig. 2.9(a), partial spalling of ta-C could be found inside or nearby the wear scar when applied load is higher than 10N and/or sliding distance is more than 250 m. In contrast, no evident spalling could be traced around the wear scar of a-C:H in all test conditions. It is reasonable to deduce that partial spalling of ta-C is owed to its relative low fracture toughness and residual stress remained from deposition especially under high load condition, and it is logical to deduce that such spalled ta-C fragments are easily to be trapped between rubbing interface as free third-body abrasives or embedded into soft mating steel surface. As can be seen in Fig. 2.12(a), relative rougher wear scar of ta-C is believed to be abraded by trapped hard ta-C fragments which originally spalled from ta-C coating itself. However, for a-C:H, the wear scar appears to be smoothened during rubbing and lead to larger real contact area between a-C:H and steel surface (Fig. 2.12(b)).

From the above, we believed that such trapped ta-C fragments can separate the rubbing contact surface to some extent and resulted in reduction of real contact area. As a result, friction coefficient of ta-C decrease to a lower value in comparison with that of a-C:H wherein relative intimate contact leads to larger real contact area and thus higher friction coefficient. In addition, friction of ta-C/steel tribopair is assumed to be caused by ploughing effect of spalled ta-C fragments against ta-C coating itself. For a-C:H/steel tribopair, friction force may result from adhesive force between topmost

graphitized layer and mating steel surface at larger real contact area than the case of ta-C/steel tribopair. Therefore, ta-C/steel tribopair showed lower friction coefficient than a-C:H/steel tribopair.

2.3.7 Comparison of wear mechanism between ta-C and a-C:H

Generally, it has been commonly accepted that hard materials wear less than softer materials under mild experimental conditions. Nevertheless, in severe conditions, hard material with low fracture toughness readily suffers from fracture when applied load/stress exceed certain critical value. And such fracture mechanisms-induced wear may cause the rate of material removal to be about ten times that for abrasive wear [83]. And it has long been considered that microfracture is important in the wear of both diamond and DLC coating, and usually lead to thickness-through crack or spalling ultimately [84].

Our research works shows that under relative low load of 5 N, ta-C coating showed better wear resistance than a-C:H coating (Fig. 2.6). However, when the load increased from 10 N to 30 N, the wear volume of ta-C increased rapidly until worn out at applied load of 30 N, whilst a-C:H shows much weaker load dependence on its wear volume. Meanwhile, it is noted that significant increase in wear of ta-C is accompanied by the occurrence of extending partial spalling as shown in Fig. 2.7(a) and Fig. 2.9(a). For a-C:H coating, on the contrary, no partial spalling could be found inside/around wear scar of a-C:H under various applied load. Therefore, it is reasonable to state that spalling of

ta-C strongly dependent on the applied load whereby 10 N is sufficient to trigger the partial spalling which likely initiated by micro-fracture or spalling primarily at the protuberant areas contact with stress concentration. K.A.M Aboua et al. states that ta-C topmost surface could be weakened by carbon diffusion from ta-C to mating steel and suffers from micro-brittle fracture [85], and in our study, higher load perhaps favors the carbon diffusion.

Furthermore, it can be deduced from Fig. 2.9(a) that such spalling of ta-C may causes rapid increase in wear volume of ta-C at sliding distance between 125 m and 250 m. It may be due to a fraction of spalled ta-C fragments is readily to embedded into much softer steel disk to abrade against ta-C coating in reverse, stripy scratch grooves on ta-C worn surface could support this deduction (Fig. 2.12). With the spalled ta-C fragments accumulating between the rubbing interface, ta-C coating is assumed to experience ongoing violent wear and expanding spalling as shown in Fig. 2.9(a). Therefore, such mutual promoted effects of spalling and abrasion gives rise to tremendous wear of ta-C under high load and long sliding distance. H. Abdullah Tasdemir et al. [70] proposed that in pure PAO boundary lubrication condition, ta-C/steel tribopair is attributed to be mechanical abrasive wear associated with chemical wear (graphitization). In our research, graphitization isn't detected inside the wear scar of ta-C as shown in Fig. 2.10(b), mechanical abrasive wear combining with partial spalling appears to be predominant wear mechanism of ta-C coatings, and partial spalling is believed to promote the mechanical abrasive wear to a large degree.

As for a-C:H, applied load and sliding distance appeared to imperceptibly affect the wear volume loss of a-C:H. Raman analysis (Fig. 2.10(a)) shows that those graphitized layers could only be traced either on the fringe of or beyond the wear scar. It indicates that the generation of graphitized layer is simultaneously accompanied by the removal and then ejected to the fringe of wear scar, finally adheres to mating surface and adjacent regions outside the wear scar. As a result, we propose that the principal wear mechanism of a-C:H coatings under base oil boundary lubrication conditions is graphitization combining with adhesive wear, whereby a-C:H is worn off by the way of persistently removal of the graphitized a-C:H and disperse into lubricant oil or adhere to mating steel as shown in Fig. 2.11(a).

Therefore, we propose that ta-C coating possess better wear resistance than a-C:H coating only in mild load condition, where micro-fracture in protruding areas is main wear mechanism of ta-C. When applied load is high enough to trigger the partial spalling of hard brittle ta-C coating, wear of ta-C could be tremendously enhanced and result in large-scale spalling or delamination eventually. In addition, internal residual stress of ta-C coating due to relative large thickness and lack of buffer effect of interlayer could also contributes to the spalling of ta-C in such severe condition.

2.4 Conclusion

The purpose of this chapter is to compare the seizure and wear resistance of ta-C coating with that of a-C:H coating for possible use in base oil boundary lubrication

condition. Based on friction and wear results, Raman spectroscopy analyses, and wear track observations, the following insights and conclusions are obtained:

(1) Seizure does not occur in the case of a-C:H/steel tribopair during the whole step-loading process. However, for ta-C/S55C tribopair, seizure does not occur until partial spalling of ta-C coatings is triggered by high load of 50 N (380 MPa) and it results in mild seizure. For SUJ2/S55C tribopair, severe seizure arises when applied load is increased up to 30 N (295 MPa).

(2) Generally, the friction coefficient at frictional steady state for ta-C/steel tribopair is lower than that of a-C:H/steel tribopair under various applied load, even though graphitized layer is only formed in the case of a-C:H/steel tribopair. We propose that spalled ta-C fragments may be easily trapped between the rubbing interface to reduce the real contact area between two surfaces and thus lead to lower friction. However, for a-C:H, adhesion force between graphitized topmost layer and mating steel surface at a much larger real contact area may contribute to relative higher friction.

(3) Wear of ta-C/steel strongly depends on the applied load and sliding distance, while wear of a-C:H/steel does not show great dependence on the applied load and sliding distance. Wear mechanism of ta-C is suggested to begin with brittle micro-fracture in the protruding parts and followed by partial spalling as an evolution of micro-fracture. And such spalled ta-C fragments serve as abrasive particles to result in much more tremendous wear of ta-C coating. In comparison, wear mechanism of

a-C:H is mainly attribute to graphitization on the topmost surface accompanying by persistently removal of such weakened transformed layer.

Chapter 3

Effect of mating materials on wear properties of a-C:H and ta-C in base oil lubrication

3.1 Introduction

With the raising of public environmental consciousness and concerns about sustainable energy future, the modern automobile industry is tending to commit larger capital expenditures in reducing energy loss. It was estimated that approximately up to 30% of the fuel energy loss inside the engine is attributed to friction between bearing components under oil boundary lubrication conditions [61]. Meanwhile, anti-wear performance is also highly pursued in order to prolong the lifespan of such bearing components. Therefore, it is urgent to minimize the friction and wear of engine bearings-included tribosystem to reduce the energy consumption.

Surface coating technology has been the focus of attention of the automobile industry during the recent decades [7]. Diamond-like carbon (DLC) coatings could be used as a surface functional material to achieve the low friction between coating and mating material due to its remarkable mechanical and tribological performance, such as high hardness, low friction and high wear resistance [26,52]. Among which, tetrahedral amorphous carbon (ta-C) and amorphous hydrogenated carbon (a-C:H) coating are most commonly used DLC coatings which are usually synthesized by physical vapor

deposition (PVD) and chemical vapor deposition (CVD) respectively. In recent years, these hard carbonaceous coatings have been widely applied to the engine bearing components which work under oil boundary lubrications [86,87]. Since then, studies mainly concentrated on the effect of various oil additives on the friction and wear properties of DLC-mating tribopairs [23,28,88,89]. Although these oil additives could enhance the wear resistance of certain type of DLC coating and reduce the friction coefficient to a certain extent by formation of protective tribofilm with low shear strength, the utilization of such phosphorus and sulfur-containing oil additives easily brought in environmental problems due to the hazardous emissions and sludge obtained during purification [70]. Therefore, it is more desirable that the use of these additives could be displaced by appropriate DLC/mating material combination under the pure base oil boundary lubrication condition.

Friction and wear are not constant property of material and can differ depending on the operating condition, working environment (humidity, lubrication, additives, temperature), material properties and counter surfaces [90-94]. In terms of DLC coating working under oil boundary lubrication condition, it is reported that combination of lubricant formulation and the mating material is a crucial factor for the use of DLC in lubricated conditions [28]. However, very little emphasis has been put on the combination of mating materials and above-mentioned two types of widely used DLC coating (ta-C and a-C:H) [95], especially under oil boundary lubrication condition without commercial additives.

In this chapter, comparative study on wear behavior of ta-C and a-C:H coating when sliding against various mating materials under pure base oil boundary lubrication condition is conducted to investigate which DLC coating/mating materials combination is optimal with low friction and high wear resistance. Hardness of mating material is considered to be a key factor which affects the wear behavior of counter DLC coating. Therefore, three types of industrial coating materials (TiC, Cr and Ni) and three types of industrial bulk materials (steel, Al and Cu) are purposely selected as mating materials which are of diverse hardness (from 2.4 GPa to 14.7 GPa) and similar surface roughness. Furthermore, we also aim to elucidate different wear mechanism of ta-C and a-C:H coating under pure base oil boundary lubrication condition.

3.2 Experimental details

3.2.1 DLC coatings and counter materials

Two commercially available categories of DLC coatings, which are hydrogenated amorphous carbon (a-C:H) and tetrahedral amorphous carbon (ta-C), were supplied by Nippon ITF Inc. They were deposited on the curved surface of cylinder pins, measuring 5 mm in diameter and 5 mm in length. And a-C:H was deposited by PECVD (plasma enhanced chemical vapor deposition) methods and ta-C was deposited by ion plating method. And both DLC coating were finishing polished subsequently to remove the droplets and particles which formed on the top surface during the deposition process. The detailed properties of DLC coated cylinder are listed in Table 3.1.

Basically, six kinds of materials were used as counterpart disk plate, measuring 22.5 mm in diameter and 4 mm in thickness, to slide against with DLC coated cylinders. Among which, TiC, Cr and Ni were coated in steel plate with the thickness of 1 μm, the rest of three counterparts were all made by bulk S55C steel, Cu and Al respectively. Detailed properties are shown in Table.3.2. In addition, to investigate the effect of surface roughness on wear behavior of each ta-C coating, S55C steel were deliberately ground by several specific types of abrasive papers to prepare various surface roughness.

Table 3.1 Properties of ta-C & a-C:H coated cylinder

Substrate Material	SUJ2	
Coating Material	ta-C	a-C:H
Deposition method	Ion plating	PECVD
Hardness *H*, GPa	38±2	12±2
Young's Modulus (GPa)	435 ± 50	105 ± 20
Surface roughness R_a, nm	24	31
Film thickness *t*, μm	1.0	4.0

Table 3.2 Properties of mating materials

Material	Hardness *H*, GPa	Young's Modulus, GPa	Surface roughness R_a, nm
TiC	14.7	439± 17	11
Cr	12.4	285±12	10
Ni	6.6	213±16	14
S55C-1	4.4	201±13	5.8
S55C-2			23
S55C-3			85
S55C-4			309
Cu	2.7	128±10	14
Al	2.4	73±4	32

3.2.2 Tribological experiments

In this study, tests were performed using a unidirectional cylinder-on-disk tribotester under the boundary lubrication condition (Fig. 3.1). The DLC-coated cylinder was loaded by 5 N (corresponding to a maximum initial Hertzian contact pressure of 80 MPa) and rubbed against six types of disks under pure sliding conditions. Both the cylinder and the disk were immersed into the pure PAO4 oil, which has a viscosity of 5.25 mm^2/s and pressure-viscosity coefficient of 14.2 GPa^{-1} at 80 ℃, where the temperature was kept at 80 ℃ constantly during the sliding test. The rotational radius and speed were fixed at 6.65 mm and 100 rpm (0.065m/s) respectively. Test duration was set as 60 min and the corresponding sliding distance was calculated approximately as 250 m. The friction coefficient was simultaneously recorded by load cell unit. Wear volume of DLC coatings on the cylinder was roughly calculated by measuring the width of rectangular-shape wear track with optical microscope. Before and after the friction tests, all samples were cleansed with benzene and acetone successively in an ultrasonic bath to remove oil species and contaminants.

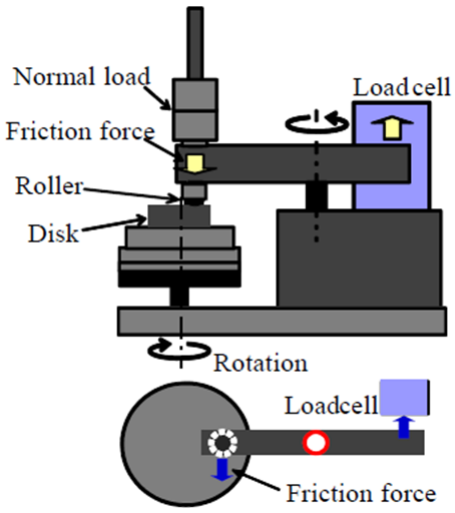

Figure 3.1 Schematic of reciprocating cylinder-on-disk tribotester

The minimum film thickness (h_{min}) for rectangular conjunctions and dimensionless lambda ratio (Λ) were calculated using Eqs. (3.1) and (3.2), respectively, by Hamrock and Dowson [72].

$$h_{min}=1.806(w'_z)^{-0.128}(\eta_0\tilde{u})^{0.694}\xi^{0.568}R_x^{0.434} \quad (3.1)$$

$$\Lambda = \frac{h_{min}}{\sqrt{R_{q,a}^2+R_{q,b}^2}} \quad (3.2)$$

where w'_z is the normal load per unit width, η_0 is the absolute viscosity at the pressure of 0 Pa and the temperature of 80 ℃, $\tilde{u}$ is mean surface velocity in sliding direction, ξ is pressure-viscosity coefficient, R_x is effective radius of cylinder, $R_{q,a}$ is the surface roughness of cylinder and $R_{q,b}$ is the surface roughness of disc. The calculated lambda ratio at initial contact condition is 0.23 and 0.3 for a-C:H/steel and ta-C/steel tribosystem respectively, which both are less than unity, it means that operating lubrication regime is boundary lubrication.

3.2.3 Surface analysis

Surface roughness, hardness and Young modulus were measured by atomic force microscopy (SEIKO, Nanopics 1000) and Nanoindenter (NANOPICS 1000 Elionix ENT-1100a). Raman spectroscopy (NRS-1000 Laser, Jasco Inc., Japan) measurements with 532 nm Ne laser radiation were carried out to characterize structural information of DLC coatings. Field-emission scanning electron microscope (FE-SEM, JEOL, JSM-7000FK) was used to image the DLC and S55C steel surface.

3.3 Results and Discussion

3.3.1 Wear results

Figure 3.2 displays the effect of the counter materials on the wear of hydrogen free ta-C DLC and hydrogenated a-C:H DLC respectively when tested in non-additive PAO oil. Hydrogen free ta-C coating suffers from the severest wear when rubbing against TiC coated plate and ta-C coating is partially worn out after a 160 m sliding distance. The lowest wear rate of ta-C coated cylinder is provided by ta-C/steel tribopair and ta-C/Cu tribopair. In the case of hydrogenated a-C:H coating, the highest wear rate is observed when rubbing against nickel while the lowest wear rate of a-C:H coating is detected for a-C:H/TiC and a-C:H/steel. As it is seen in Fig. 3.2, except the case of DLC/TiC tribopair, wear rate of a-C:H is generally higher than that of ta-C for the other tribopairs. And only for DLC/steel contact, ta-C and a-C:H coating exhibit similar wear rate with each other.

Figure 3.3 presents the steady state friction coefficients as a function of different counter materials rubbing against both DLC coated cylinders. And the fluctuation of steady-state friction coefficient is marked as the error bar in Fig. 3.3. Generally, the friction coefficient ranges from 0.08±0.04 for all tribopairs. In the case of ta-C/TiC combination, the friction coefficient reaches a low level of 0.043 but increases up to 0.11 level after partial wear out of ta-C and runs into an unsteady state which is shown as the bigger error bar. For the DLC/TiC, DLC/Ni and DLC/Al combination, ta-C coating could provide lower friction coefficient than a-C:H coating in steady state.

Whereas, for DLC/Cr, DLC/steel and DLC/Cu combinations, a-C:H coating gives lower friction coefficient than ta-C.

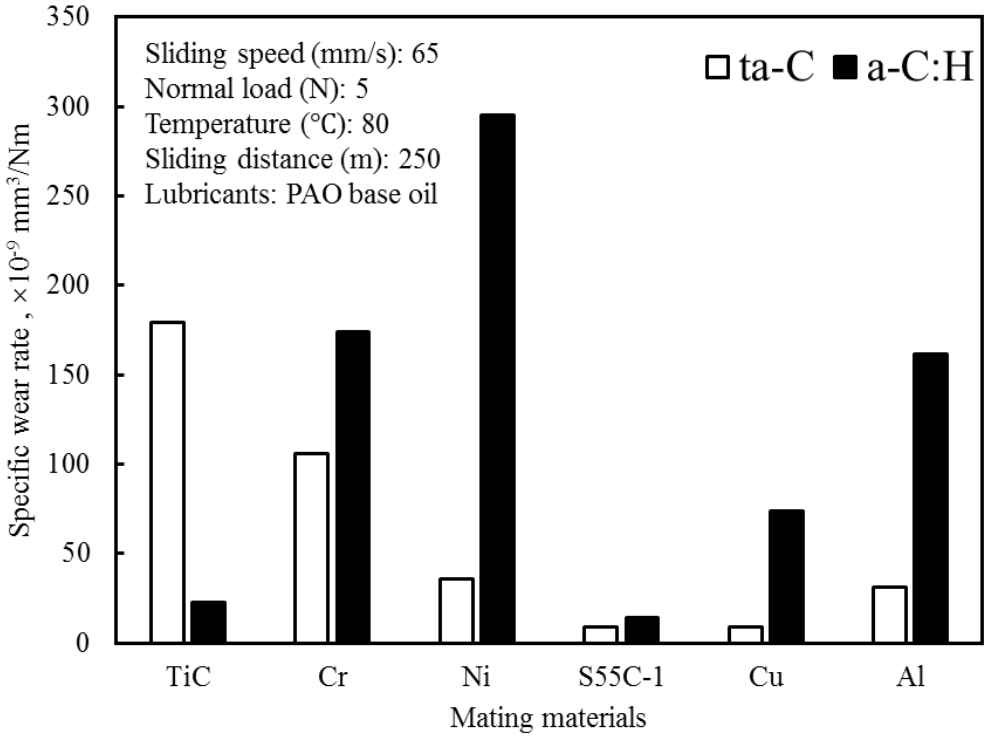

Figure 3.2 Specific wear rate of ta-C and a-C:H coating when rubbing against various mating materials

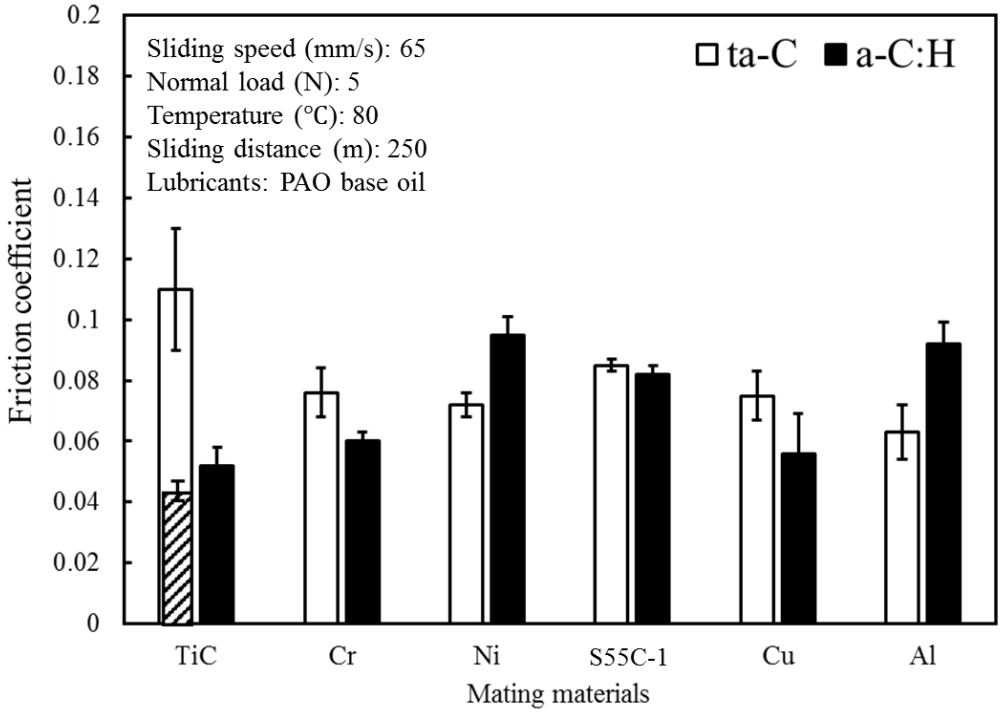

Figure 3.3 Steady-state friction coefficient of ta-C and a-C:H coating when rubbing against various mating materials.

SEM observation was conducted on wear track of ta-C and a-C:H coating. Figures 3.4 (a)-(f) reveals the surface appearance of ta-C coating inside the wear track after rubbed against TiC, Cr, Ni, steel, Cu and Al respectively. It is worth noting that obvious abrasive scratches are generated inside the wear track of ta-C coating after rubbing against TiC, Cr, Ni and Al (Figures 3.4 (a)-(c) and (f)). However, only in the case of ta-C/steel and ta-C/Cu tribopairs, the wear tracks appear to be relatively smoothened (Figures 3.4 (d)-(e)). For the wear track on the a-C:H coating, rather smoother wear tracks were generated on the rubbed surface for all tribopairs (Figures 3.5 (a)-(f)) and the wear track is obviously smoother in comparison with the as-deposited surface.

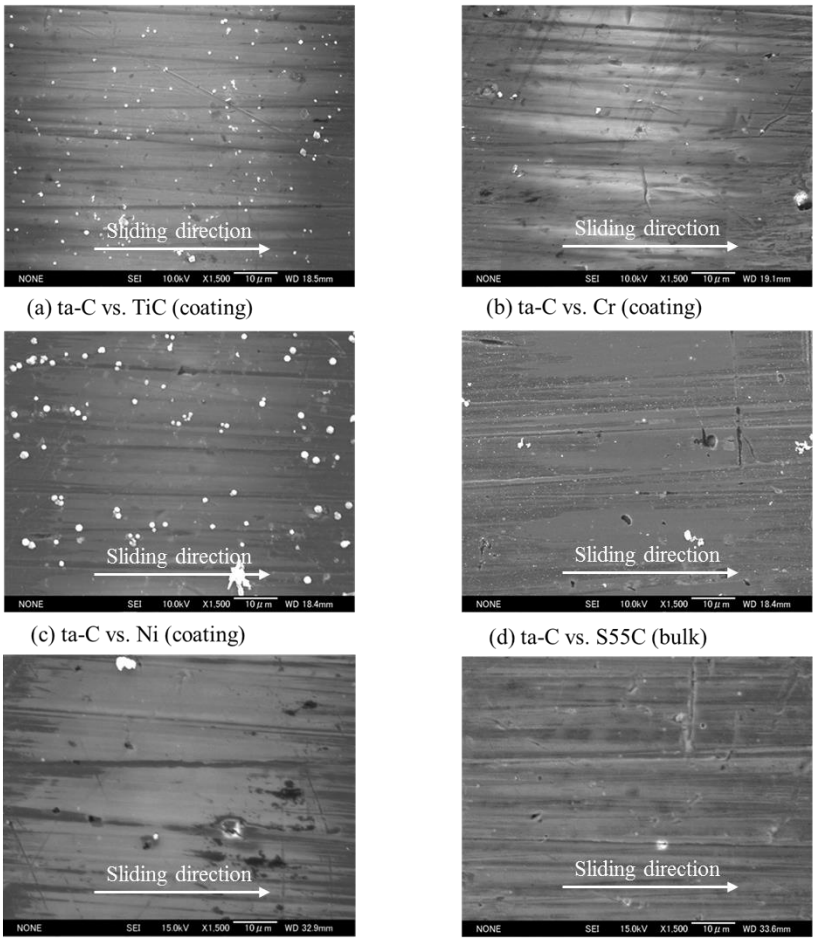

Figure 3.4 FE-SEM images of wear scar on ta-C coating when rubbing against various mating materials.

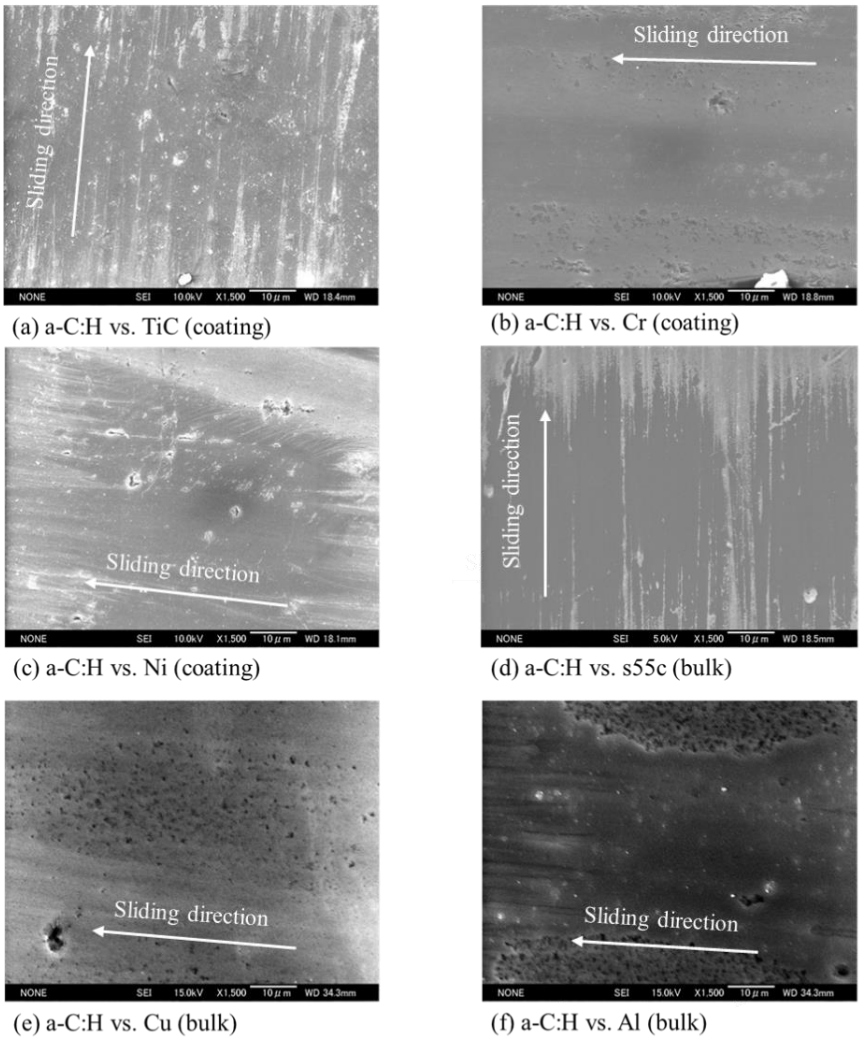

Figure 3.5 FE-SEM images of wear scar on a-C:H coating when rubbing against various mating materials.

3.3.2 Wear behavior depending on the hardness and roughness of mating materials

Tribological characteristics of tribosystem are described as a function of numerous factors [96]. In this study, the effect of hardness of various mating materials on the wear of both DLC coatings is investigated to illustrate the distinction at wear behavior between ta-C and a-C:H coating when sliding against various mating materials with a variation in hardness. Figure 3.6 presents the specific wear rate of ta-C coating as a function of the hardness of mating materials. As can be seen in Fig. 3.6, the specific wear rate of ta-C soars with the increase in hardness of the mating surface. Nevertheless, in terms of a-C:H coating, there is no apparent dependence of specific wear rate on the hardness of sorts of mating surfaces could be identified as it is seen in Fig. 3.7.

The variation in specific wear rate of the ta-C coating with various mating surface roughness (S55C-1, S55C-2, S55C-3, S55C-4) is shown in Fig. 3.8. It should be noted that the surface roughness was measured after friction test. The surge in specific wear rate of ta-C occurs when the surface roughness of mating surface increases from 0.015 to 0.023 μm, and become nearly invariant when the roughness of mating materials reaches 0.1 μm.

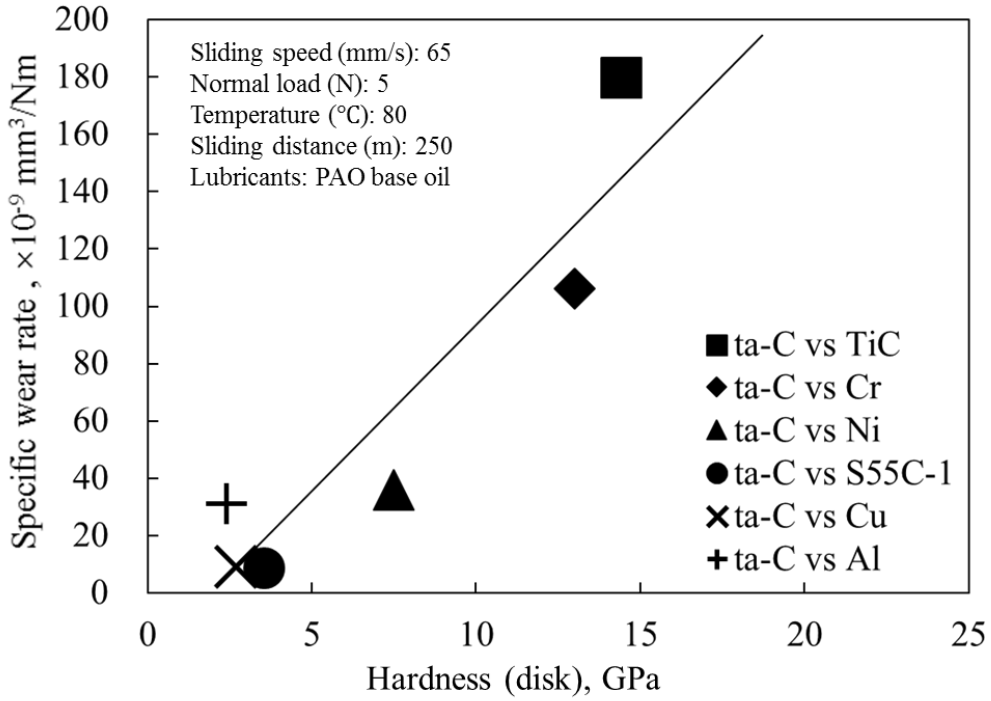

Figure 3.6 Variation of specific wear rate of ta-C coating as a function of hardness of mating materials

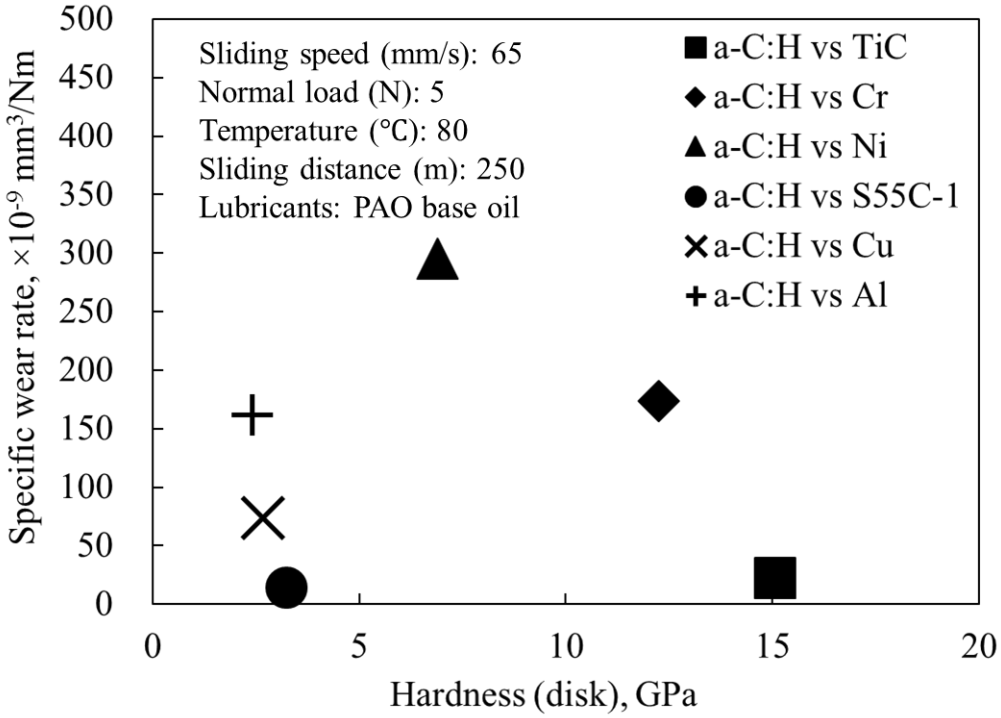

Figure 3.7 Variation of specific wear rate of a-C:H coating as a function of hardness of mating materials

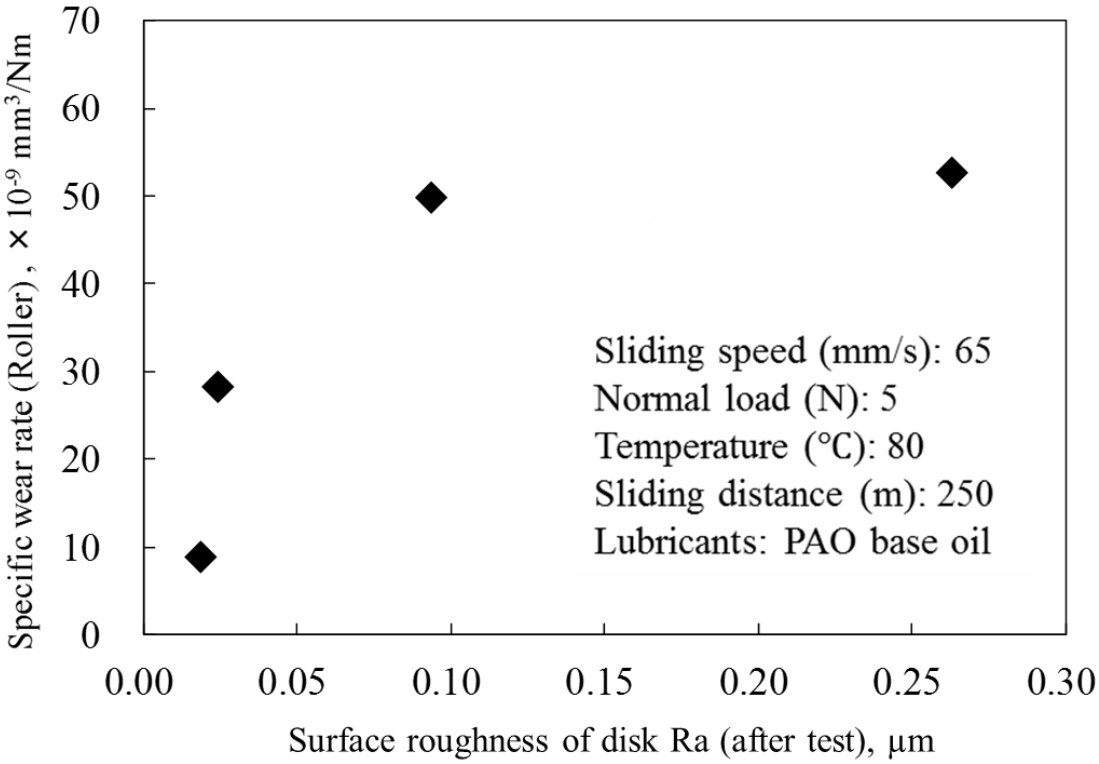

Figure 3.8 Variation of specific wear rate of ta-C coating as a function of roughness of steel material (S55C-1)

3.3.3 Surface analysis with Raman spectroscopy measurement

Due to the amorphous structural of DLC coatings, tribo-induced graphitization is readily to be detected on the topmost contact sliding surface in oil boundary lubrication with various additives [29,69,97,98]. Formation of such graphitization layer has always been considered as the primary factor to lead in low friction [76] and low wear rate as well [75]. Raman spectroscopy measurements were conducted on both DLC surfaces inside and outside the wear track to identify graphitization on the sliding interface. Graphitization can be characterized by an increase in the intensity ratio (I_D/I_G) of the maximum disordered D-peak (I_D) intensity to the maximum graphite G- peak (I_G) intensity in the Raman spectra [73]. Figure 3.9 compares the calculated I_D/I_G ratio of ta-C inside and outside of the wear track. It shows that either increase or decrease in I_D/I_G ratio occurred inside the wear track in comparison with those outside the wear track for various mating materials. And in both cases, the variation is too slight to confirm the occurrence of graphitization for ta-C wear track. In terms of a-C:H, I_D/I_G ratio of a-C:H inside the wear track is generally higher compared to those outside the wear track, especially when rubbing against Cr, S55C steel, Cu and Al, the I_D/I_G ratio inside the wear track increased by up to than 15% (Fig. 3.10). It indicates that graphitization occurred when a-C:H coating sliding against above mating materials. Figure 3.11 shows representative Raman spectra of ta-C and a-C:H coating measured inside and outside the wear scar respectively, after rubbing against nickel coated disk.

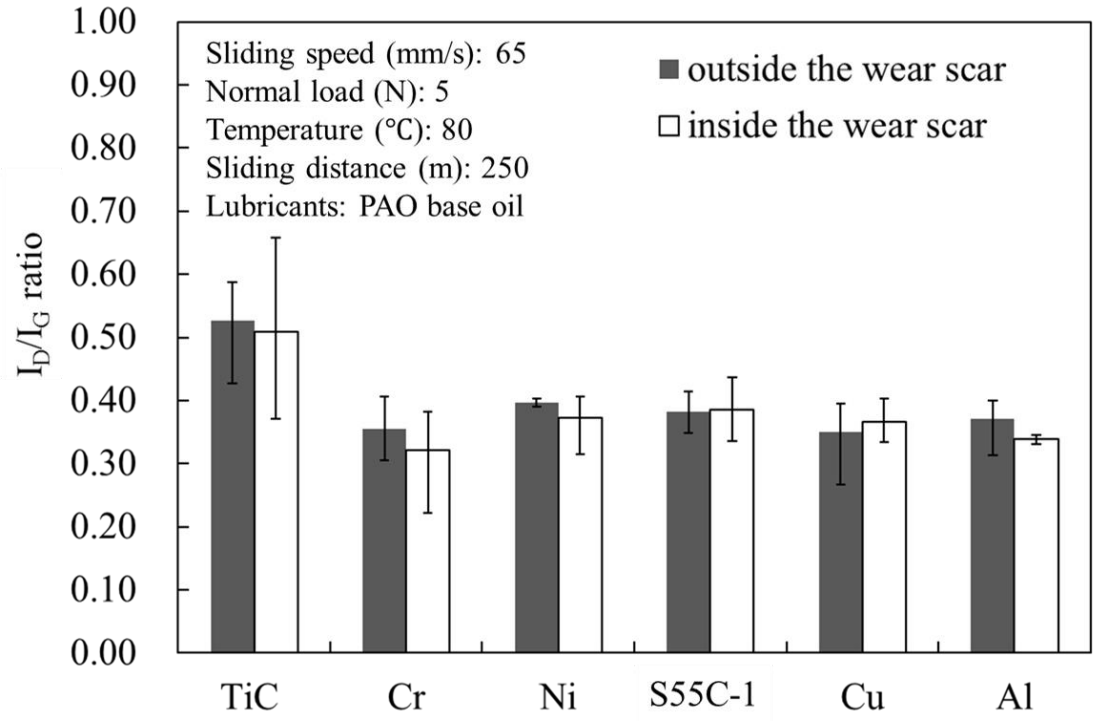

Figure 3.9 Variation of I_D/I_G ratio inside and outside the wear scar of ta-C coating when rubbing against various mating materials

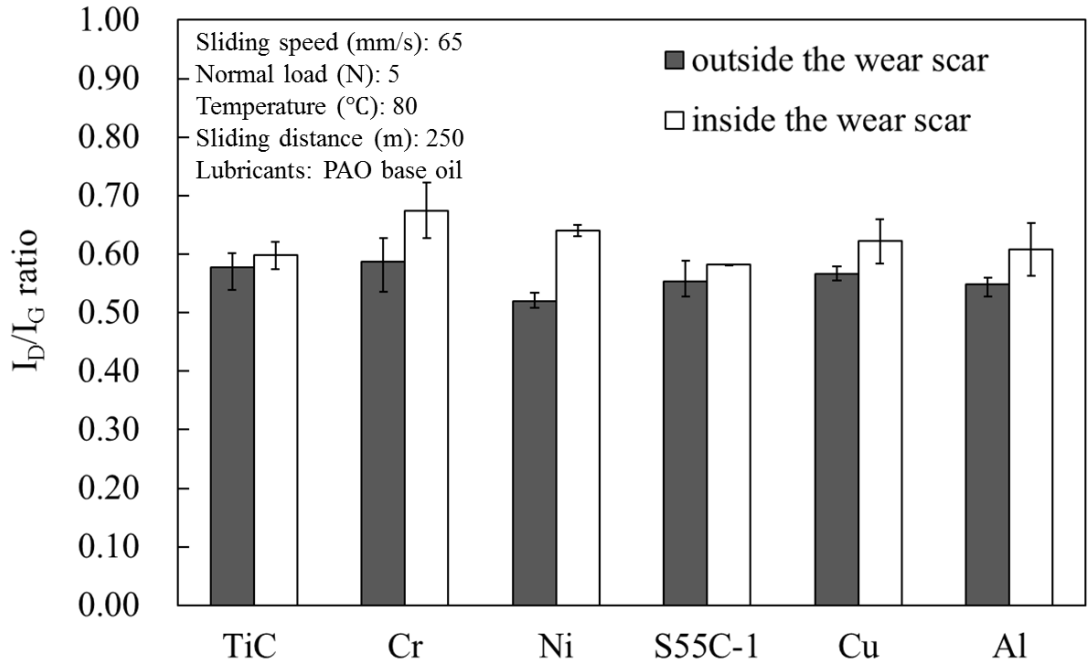

Figure 3.10 Variation of I_D/I_G ratio inside and outside the wear scar of a-C:H coating when rubbing against various mating materials

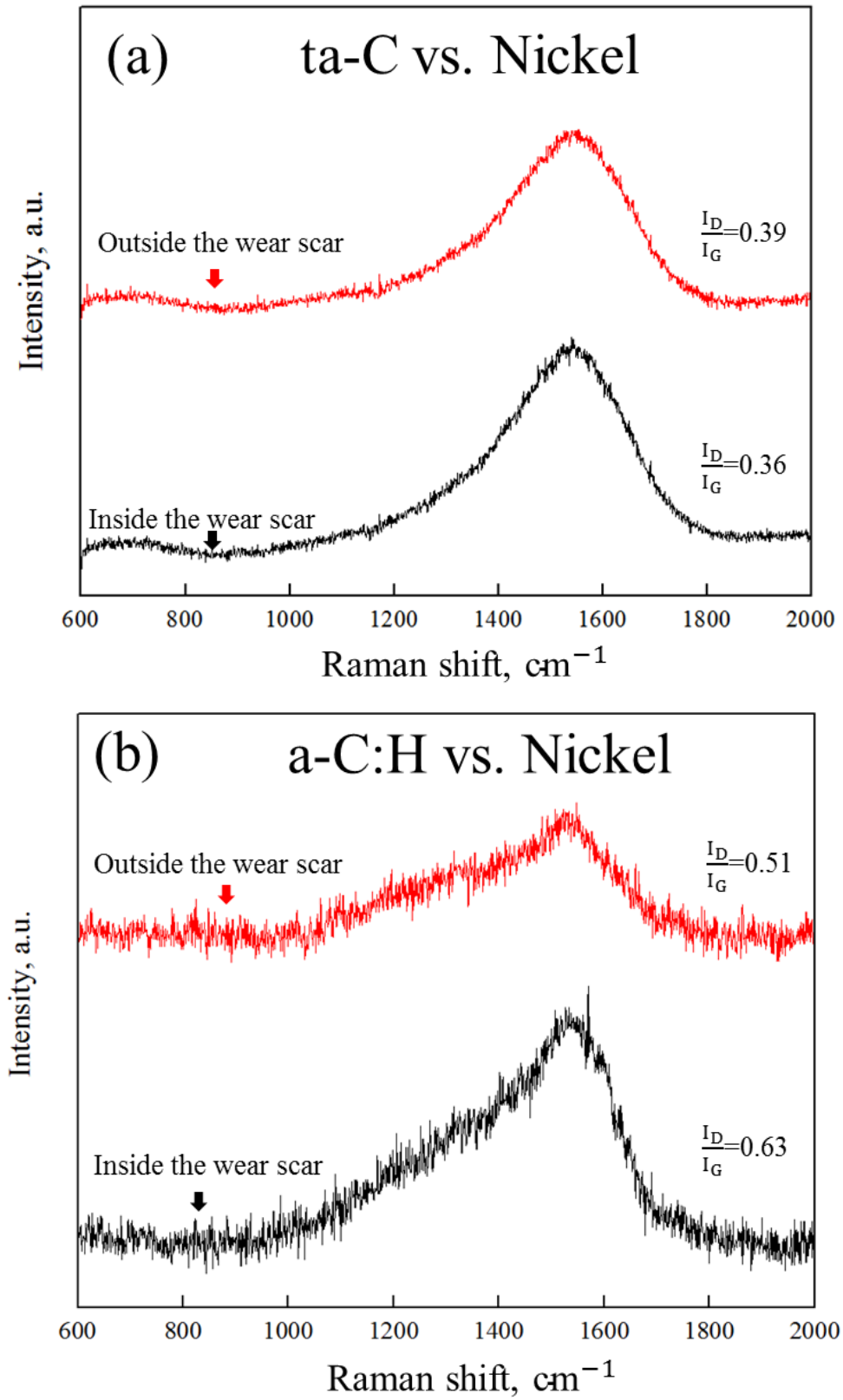

Figure 3.11 Representative Raman spectra of (a) ta-C and (b) a-C:H when sliding against nickel-coated disk.

The variations in specific wear rate as a function of I_D/I_G ratio increment rate for ta-C coating after rubbing against various mating surface are displayed in Fig. 3.12. The I_D/I_G ratio increment rate was calculated by the Eq. (3.3) as follows:

$$I=\frac{(\frac{I_D}{I_G})_{in}-(\frac{I_D}{I_G})_{out}}{(\frac{I_D}{I_G})_{out}}\times 100 \quad (3.3)$$

where I is the I_D/I_G ratio increment rate, $(\frac{I_D}{I_G})_{in}$ is the I_D/I_G ratio measured inside the wear scar of DLC coating surface, $(\frac{I_D}{I_G})_{out}$ is the I_D/I_G ratio measured outside the wear scar of DLC coating surface.

There is no clear correlation between specific wear rate and I_D/I_G ratio increment rate could be discerned. However, a-C:H coating shows increasing trend in specific wear rate with increase in increment rate of I_D/I_G ratio (Fig. 3.13). It is evidently indicated that with graphitization enhanced, the wear of a-C:H coating becomes severer.

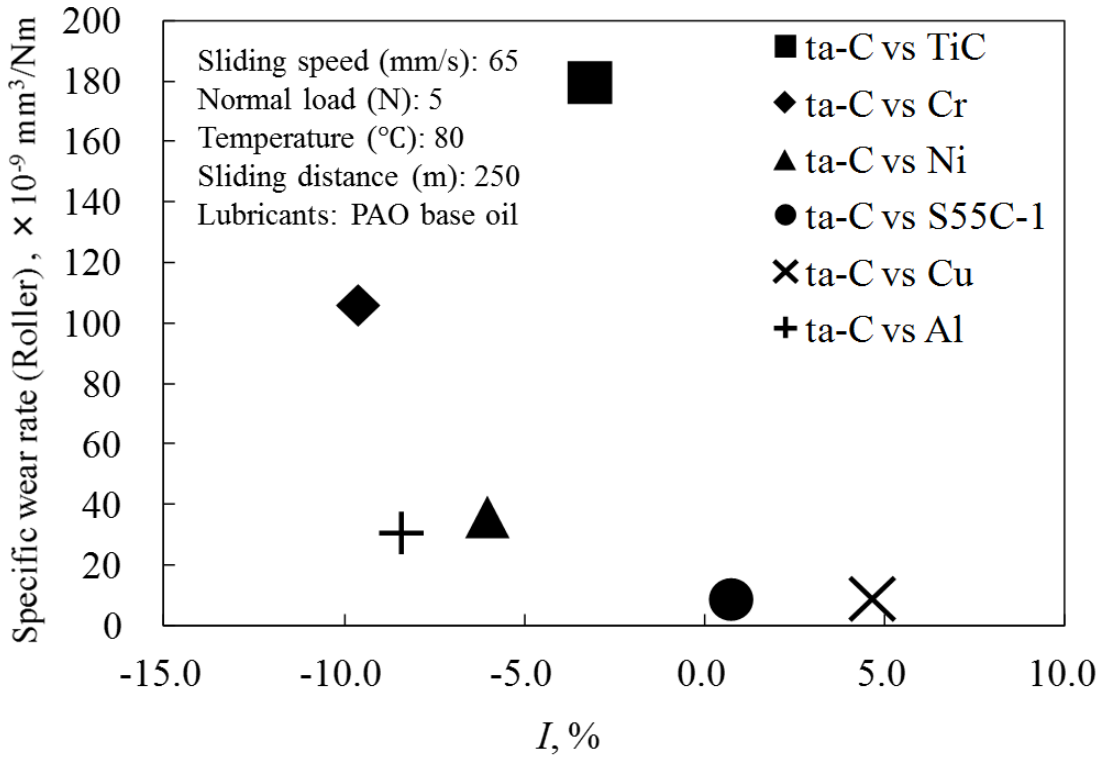

Figure 3.12 Variation of specific wear rate of ta-C coating as a function of increasing rate of I_D/I_G ratio.

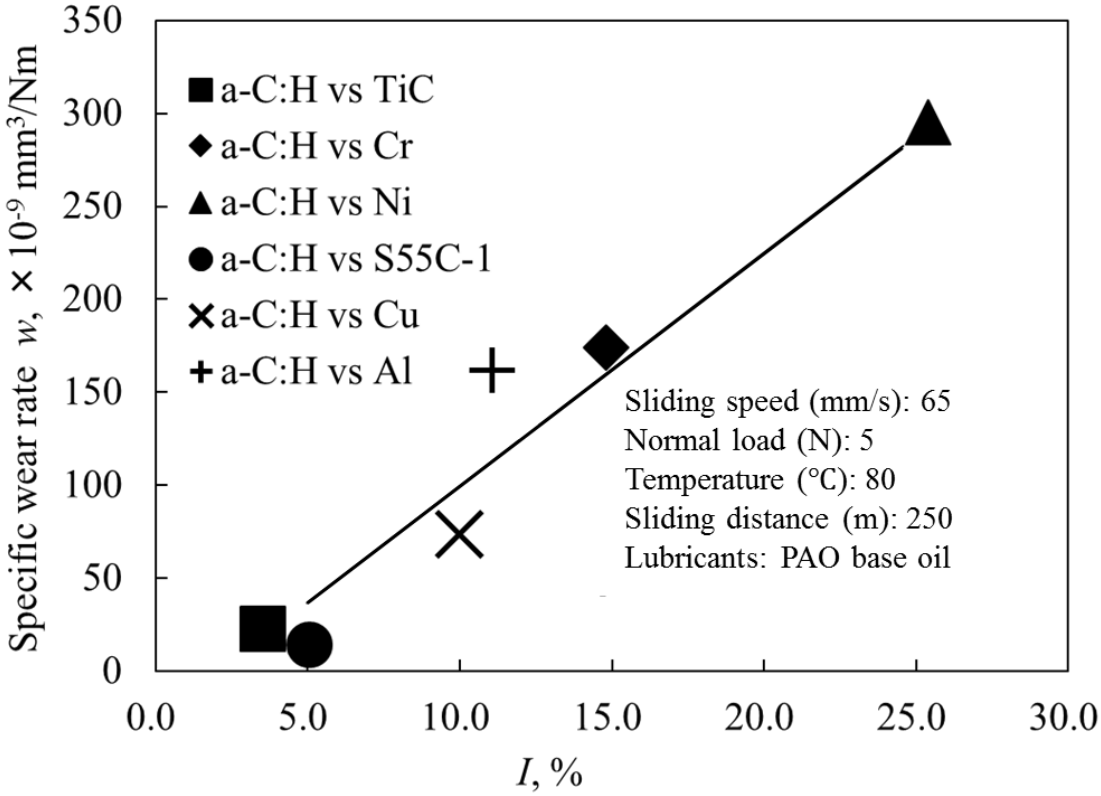

Figure 3.13 Variation of specific wear rate of a-C:H coating as a function of increasing rate of I_D/I_G ratio.

3.3.4 Wear mechanism of ta-C

The wear results in Fig. 3.2 reveal that in the case of ta-C/TiC, ta-C/Cr, ta-C/Ni and ta-C/Al tribopairs, ta-C coating shows relative high wear than the ta-C/steel and ta-C/Cu tribopairs. Moreover, when the ta-C coating exhibits low wear (rubbed against steel and Cu), the wear track of ta-C appears to be partially smoothened (Fig. 3.4 (d) and Fig. 3.4 (e)), while in the other cases, obvious scratch lines are generated along the sliding direction inside the wear track of ta-C coating. Therefore, we assume that wear mechanism of ta-C in the high wear condition and low wear condition are likely different.

According to the previous research, very hard coating usually shows no sign of scuffing or scratch lines, especially when the counterface material is much softer than the coating [99,100]. However, in the high wear condition, generation of these scratch lines on hard ta-C coating surface is confirmed in our research. It is probably due to the participation of some wear debris those are of similar or higher hardness in comparison with ta-C coating. It is known that wear debris produced during the sliding process are often caused by plowing effect of harder material against softer material where a softer material is easily removed to be turned into wear debris. In our experiment, it is not surprising that iron oxides (FeO, Fe_2O_3, Fe_3O_4) and iron carbides (Fe_3C) could be detected on the wear track of disk, however, all of these wear debris are much softer than the ta-C coating and the ta-C coating is hardly abraded by these soft wear debris. Therefore, the only particle that can serve as abrasive to scuff ta-C coating is assumed

to be ta-C debris, which very likely originates from the microfracture of ta-C occurs in the high-stress concentration areas during sliding process. Since for hard carbonaceous coating (such as DLC or high crystalline diamond coating), the intrinsic residual compressive stress due to deposition process is fatal to promote the microfracture of such thin coating, especially with stimulation of external stress. Meanwhile, it has long been considered that microfracture is important in the wear of both diamond and DLC coating [84]. And it was reported that such fracture mechanisms-induced wear may cause the rate of material removal to be about ten times that for abrasive wear [83]. Furthermore, the presence of scuffing suggests that the abrasive particles become significantly indented into the soft counterface disk [101]. Therefore, we propose that the trapped ta-C particles wear against ta-C coating in reverse to generate more fracture and ta-C debris and the mutual promotion effect between wear loss of ta-C and generation of microfracture-induced ta-C debris are proposed to be predominant wear mechanism of ta-C coating under oil boundary lubrication condition. Unfortunately, we couldn't detect the spalled ta-C particles on neither wear track of ta-C coating nor mating steel disk due to those minute particle size and subsequent cleansing procedure. Moreover, when counterface is rougher than mating ta-C coating surface, the roughness of counterface cause can generate local stress concentration which promotes fracture initiation to generate more ta-C abrasive particles [102,103]. Thus, it results in more wear loss of ta-C coating eventually (Fig. 3.8).

As the two lowest specific wear rates of ta-C are obtained when rubbing against two of the softest counter materials: Cu and steel, partial smoothing phenomenon of

wear track are confirmed. Thus, we deduce that microfracture of ta-C does not occur significantly to generate sufficient ta-C particles which cause the abrasive wear of ta-C in reverse. The reasons are given as following: when the counterface becomes softer, the indentation depth of ta-C asperities into counterface disk become higher and the real contact area becomes larger, which causes the local stress concentration to become lower to inhibit the microfracture and hence less wear loss of ta-C occurs which is in agree with the results showing in Fig. 3.6. It is noted that when the softest aluminum is used as counterface, the specific wear rate of ta-C is unexpectedly not the lowest among the whole six tribopairs. It may owe to the thin layer of alumina formed in the top surface of aluminum, whose hardness (mean value of 25 GPa) is much higher than aluminum, Cu and steel. Therefore, the real contact area is assumed to be smaller and the resulting higher local stress concentration probably induces microfracture of ta-C (as shown in Fig. 3.4(f)) and higher specific wear rate. In this low wear condition, we believe that the wear mechanism of ta-C from the top surface is caused by the removal of destabilized portions induced by graphitization occurs on the high-stress concentration areas. The removed graphitized wear debris is significantly softened [104] and cannot serve as abrasive particles to scuff ta-C coating. Previous studies have already stated that graphitization can occur on the diamond surface, which contains similar tetrahedral carbon structure as ta-C coating [105-107]. Even though we fail to confirm the graphitization on the top surface of ta-C by Raman spectroscopy, it is might due to the thickness of graphitization layer on ta-C surface is too thin to be detected by Raman spectroscopy measurement.

From above all, we believe that graphitization plays a key role only in low wear rate conditions; while in the high specific wear rate conditions, the microfracture on the contact areas of ta-C coating might be predominant in the wear process of ta-C coating.

3.3.5 Wear mechanism of a-C:H

In the case of a-C:H coating, the graphitization of topmost surface of a-C:H inside the wear track is confirmed by Raman Spectra as shown in Fig. 3.10. In comparison with ta-C coating, a-C:H is more vulnerable to suffer from graphitization due to its metastable amorphous structure [58]. And, from Fig. 3.13, it is found that the specific wear rate of a-C:H coating increases along with the growth rate of I_D/I_G ratio inside the wear track. Therefore, we believe that graphitization plays a key role in the wear loss of a-C:H. In other words, the a-C:H coating is consumed in a process of simultaneously formation and removal of graphitized layers. During the wear process of a-C:H coating, the original surface topography is smoothened by frictional sliding when rubbing against all sorts of mating materials (Figures 3.5(a)-(f)). It is assumed that at the initial running-in period of sliding contact, graphitization occurs around the asperities of a-C:H due to higher locally stress concentration. And these graphitized portions of the a-C:H coating are facile to be removed. As the topmost asperities are mostly removed, the surface of wear region of a-C:H coating becomes smoother gradually. As this smoothing phenomenon occurs, the stress distribution on the wear region become more even, hence the graphitization effect abates to some extent which inhibits the wear of

a-C:H after the running-in period. In conclusion, we believe that main wear mechanism of a-C:H coating is graphitization.

3.4 Conclusion

The purpose of this chapter is to compare the wear mechanism of ta-C with that of a-C:H when rubbing against various mating materials to find out which mating material is preferable for each DLC coating under base oil boundary lubrication condition. Three types of industrial coating materials (TiC, Cr and Ni) and three types of industrial bulk materials (steel, Al and Cu) were used as mating materials which are of similar surface roughness. Based on friction and wear properties, analyses, and wear track observations, the following insights and conclusions about the wear mechanisms in the two coatings were obtained:

(1) The ta-C coating could provide high wear resistance when rubbing against steel and Cu. While for a-C:H coating, high wear resistance is provided by rubbing against TiC and steel. And except the case of TiC, a-C:H coating generally shows higher specific wear rate than ta-C.

(2) Wear performance of ta-C coating shows a strong dependence on the hardness and roughness of mating material. The specific wear rate of ta-C increases as the hardness and roughness of mating material increases. And, in the low wear condition (less than 9.5×10^{-9} mm^3/Nm), main wear mechanism is assumed to be graphitization on the topmost of ta-C. However, in the high wear condition (more

than 30×10^{-9} mm^3/Nm), the microfracture on the contact areas of ta-C coating might be predominant in the wear process of ta-C coating due to local stress concentration.

(3) Wear performance of a-C:H coating shows a strong dependence on the increasing rate of I_D/I_G ratio inside the wear track of a-C:H. Specific wear rate of a-C:H coating increases as the increasing rate of I_D/I_G ratio increases. It apparently indicates that the main wear mechanism of a-C:H coating is graphitization.

Chapter 4

Effect of nanoparticles as lubricant additives on friction and wear behavior of tetrahedral amorphous carbon (ta-C) coating

4.1 Introduction

In automobile engine industry, boundary lubrication usually occurs under high load and low-speed condition in main bearing, cam and tappet interfaces, piston rings, etc., especially when the engine starts or stops suddenly. In boundary condition, surface interaction is substantially solid contact with a small portion of lubrication film. Therefore, the tribological performance in boundary lubrication condition principally depends on the contacting surface properties rather than the nature of the lubrication film. Accordingly, advisable surface engineering is expected to be a promising solution to reduce the friction and wear under boundary lubrication condition. Among various surface engineering technologies, Diamond-Like Carbon (DLC) coating is becoming prevailing in many industry fields as an effective solid lubricants due to its superior mechanical properties and low-friction and high wear resistance characteristics [25,49,86].

Additionally, oil additives, such as ZnDTP and MoDTC, have been long considered to be indispensable supplement in boundary lubrication condition to reduce the friction and wear of steel or ceramic materials [39,87,108]. In the past decades, researchers also

studied the efficiency of such conventional oil additives on DLC coating under oil boundary lubrication condition [69,109,110]. However, due to the high content of SAPS (sulfated ash, phosphorus and sulfur) in those commercial oil additives, widespread use of these additives results in harmful emissions and consequently arouse the environmental concerns. In order to gradually eliminate the usage of these high-SAPS additives, it is essential to explore a novel green oil additive candidate that can replace the current additives. Recently, it has been proposed that several nanoparticles can be used as oil additives to reduce the friction and wear for conventional metal/alloy material. Vijaykumar et al. [111] reported that addition of copper oxide nanoparticles could effectively improve the engine oil lubricating properties to result in low friction and wear of aluminum casting alloy in mixed lubrication regime. Ye et al. [112] presented that a tetrafluoro benzoic acid-modified TiO_2 nanoparticles exhibit good performance in wear and friction reduction of bearing steel. Abdullaha et al. [113] proposed that friction coefficient and wear were reduced significantly by dispersing several concentrations of hexagonal boron nitride nanoparticles in conventional diesel engine oil.

However, there are very few researches have focused on the effect of such nanoparticles additives on the tribological performance of DLC coating. Kalin et al. [32] reported that addition of MoS_2 nanotubes into base oil can reduce the friction of DLC coating by 50% under the boundary lubrication regime and proposed that such nano-material can be a potential replacement of the current chemical-based lubrication additives with novel, physical-based additive lubrication technology for DLC coatings.

However, in that research, author did not mention about the effect of MoS_2 nanotubes additives on the wear of DLC coating, and it is reasonable to deduce from the optical images of wear scar that addition of such nanotubes did not affect the wear of DLC coating significantly.

In this chapter, we investigate efficiency and effectiveness of two conventional abrasive particles: CeO_2 and ZrO_2 nanoparticles, on improving the tribological performance of ta-C coating under oil boundary lubrication condition. Although these two particles are usually used as abrasive particle to polish metal or alloy surface, whether they still work for much harder ta-C coating remains unknown. We successfully find that when CeO_2 nanoparticles are added into base oil, wear of ta-C coating is reduced significantly but relative higher friction coefficient was existed when it was compared to the pure oil lubrication. Meantime, we also confirm that when ZrO_2 nanoparticles are used as oil additives, friction of ta-C is reduced however wear of ta-C increased compared to the pure oil lubrication. It is strongly expected that these soft nanoparticles can show better tribological improvement if taking into consideration of their concentration and size in the near future. We are, for the first time, presenting the strong potential of these nanoparticles as novel environmental friendly oil additives for ta-C/steel contact condition.

4.2 Experimental details

4.2.1 Nanoparticles and lubricants

ZrO_2 nanoparticles with typical diameter around 500 nm (Fig. 4.1(a)) and CeO_2 nanoparticles with typical diameter around 300 nm (Fig. 4.1(b)) are dispersed into synthetic poly alpha olefin (PAO4) which has a viscosity of 5.25 mm^2/s and a pressure-viscosity coefficient of 14.2 GPa^{-1} at 80℃. Part of the experiments was performed using the base PAO oil without any additives, while the other part of the study was conducted by using PAO oil with 0.2 wt% ZrO_2 and CeO_2 nanoparticles respectively as additives. The suspension of the oil and nanoparticles was thoroughly mixed using ultrasonic (500 W, 50 Hz) for more than two hours and after which it was still kept in ultrasonic vibration until it was used in the experiment.

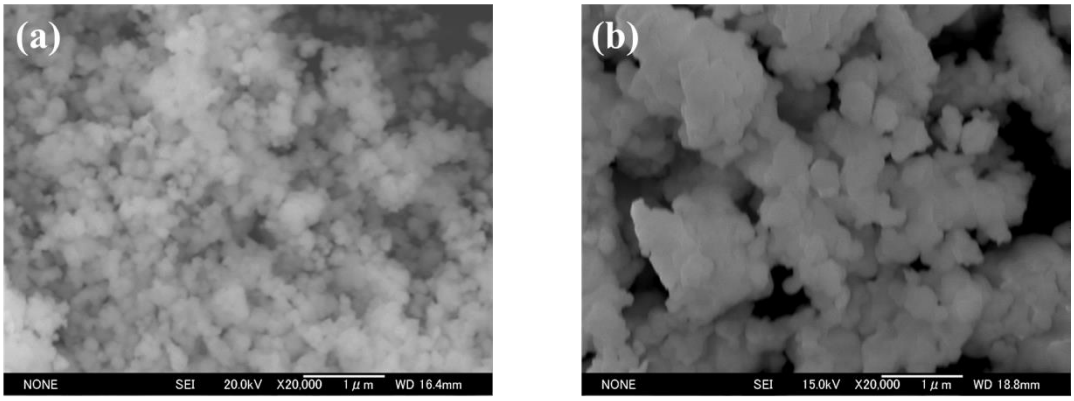

Figure 4.1 The FE-SEM images of (a) ZrO_2 particle and (b) CeO_2 particle.

4.2.2 DLC coatings and counter materials

The cylinder pin and disk were made from high carbon chrome steel (SUJ2) and carbon steel (S55C, 0.56 - 0.58 at. % of carbon concentration) respectively. The roller was 5 mm in diameter and 5 mm in length, while the disk was 22.5 mm in diameter and 4 mm in thickness. Tetrahedral amorphous carbon (ta-C), supplied by Nippon ITF Inc, were deposited on the curved surface of cylinder pins by ion plating deposition method. The characteristic of substrate and coating are shown in Table 4.1.

Table 4.1 Important characteristics of roller, coating and disk.

	Roller	Coating	Disk
Material	SUJ2	ta-C	S55C
Deposition method	-	Ion plating	-
Hardness H, GPa	8.5	38±2	4.4
Young's Modulus (GPa)	218±17	435 ± 50	201±13
Surface roughness R_a, nm	22	68	6
Film thickness t, μm	-	1	-

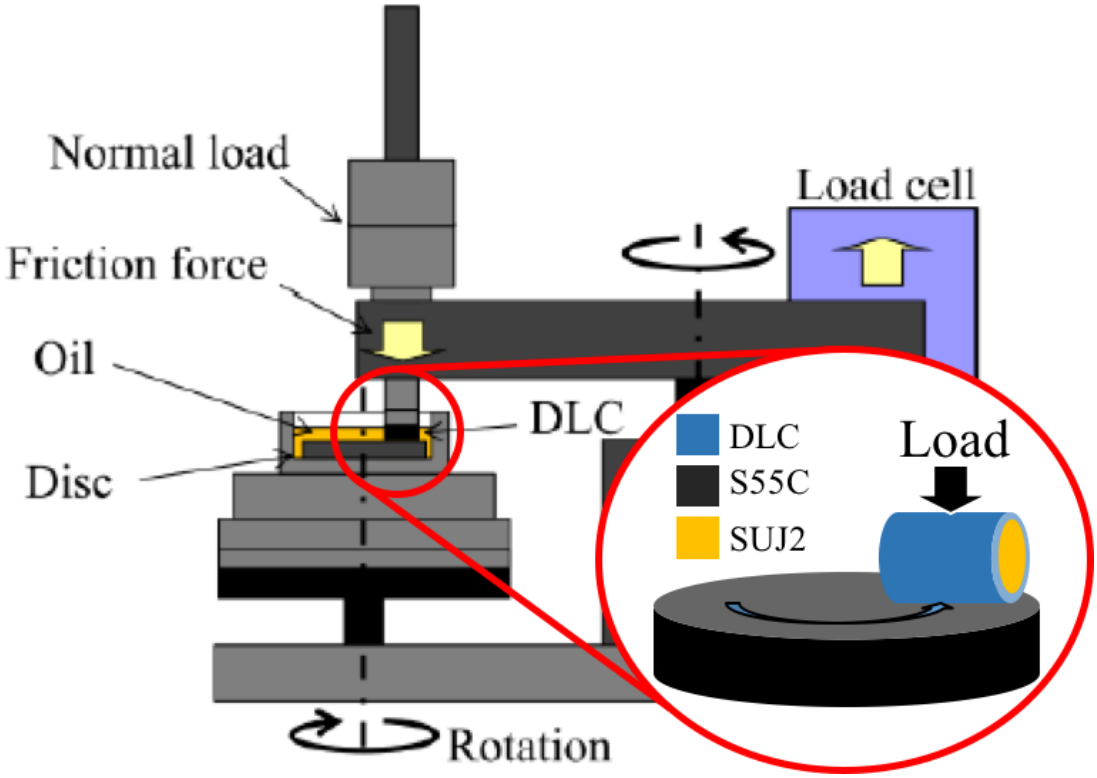

Figure 4.2 Schematic of reciprocating cylinder-on-disk tribotester

4.2.3 Tribological experiments

In this study, tests were performed using a rotating cylinder-on-disk tribotester under the boundary lubrication condition (Fig. 4.2). The DLC-coated cylinder was loaded by 10 N (corresponding to a maximum initial Hertzian contact pressure of 120 MPa), and rubbed against S55C disk. Both the cylinder and the disk were immersed into the pure PAO4 oil, where the temperature was kept at 80 ℃ constantly during the sliding test. The rotational radius and speed were fixed at 6.65 mm and 100 rpm (0.065m/s) respectively. Test duration was set as 60 min and the corresponding sliding distance was calculated approximately as 250 m. The friction coefficient was simultaneously recorded by load cell unit. Wear volume of DLC coatings on the cylinder was roughly calculated by measuring the width of rectangular-shape wear track with optical microscope. Before and after the friction tests, all samples were cleansed with benzene and acetone successively in an ultrasonic bath to remove oil species and contaminants.

The minimum film thickness (h_{min}) for rectangular conjunctions and dimensionless lambda ratio (Λ) were calculated using Eqs. (4.1) and (4.2), respectively, by Hamrock and Dowson [72].

$$h_{min}=1.806(w'_z)^{-0.128}(\eta_0\tilde{u})^{0.694}\,\xi^{-0.568}R_x^{0.434} \tag{4.1}$$

$$\Lambda = \frac{h_{min}}{\sqrt{R_{q,a}{}^2+R_{q,b}{}^2}} \tag{4.2}$$

where w'_z is the normal load per unit width, η_0 is the absolute viscosity at the pressure of 0 Pa and the temperature of 80 ℃, ũ is mean surface velocity in sliding direction, ξ

is pressure-viscosity coefficient, R_x is effective radius of cylinder, $R_{q,a}$ is the surface roughness of cylinder and $R_{q,b}$ is the surface roughness of disc. The calculated lambda ratio at initial contact condition is 0.6 for ta-C/steel tribosystem, which is less than unity, it means that operating lubrication regime is boundary lubrication. In addition, all the tests were repeated at least three times for reproducibility.

4.2.4 Surface analysis

Surface roughness and morphology were measured by non-contact, three-dimensional, scanning white light interferometry (Zygo Newview). Hardness and Young modulus were measured by Nanoindenter (NANOPICS 1000 Elionix ENT-1100a). Another scanning electron microscope (JEOL, JCM-5700NU) combined with an energy-dispersive X-ray detector (EDS) operated at an acceleration voltage of 10 keV to investigate the element on the wear scar on the disk. Prior to the investigation, all the worn surfaces were cleaned by repeatedly immersing into benzene and acetone bath.

4.3 Results

Figure 4.3 presents the friction coefficient of ta-C/steel contact lubricated by CeO_2 and ZrO_2 nanoparticles containing base oil. Firstly, the friction test of ta-C/S55C contacts without any additives was conducted as a reference. The PAO oil with ZrO_2 nanoparticles provides lowest friction coefficient of 0.5, which is significantly reduced by nearly 40% compared to the oil without additives. However, when CeO_2 is added into the PAO oil, the friction coefficient of ta-C/ steel contact increases up to 0.09, which is 10% higher than the pure PAO oil lubrication condition. In addition, it is noted

that only in the case when ZrO_2 nanoparticles are used as oil additive, ta-C/steel clearly exhibits running-in period in the beginning 1000 cycles, where friction coefficient decreases gradually from initial 0.082 to 0.05 and remains the same value until the end of the friction test.

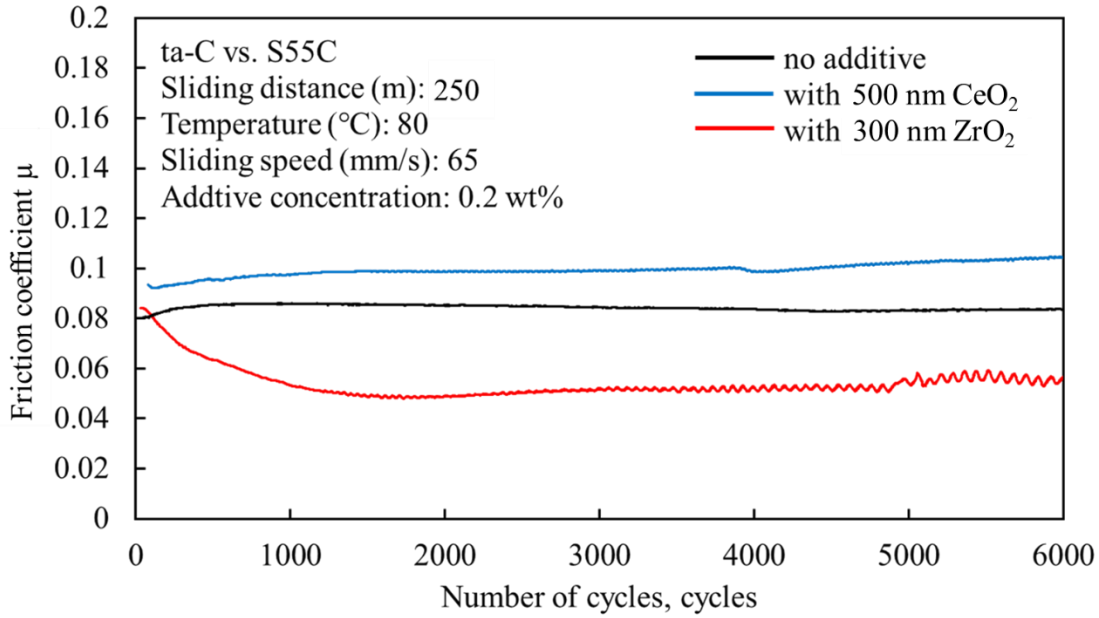

Figure 4.3 Friction coefficient versus sliding cycles for ta-C/steel contact with CeO_2 and ZrO_2 nanoparticles additives.

Figure 4.4 represents the specific wear rate of ta-C coating when lubricated with CeO_2 and ZrO_2 nanoparticles-containing PAO oil, and the specific wear rate of ta-C coating in pure base PAO oil is also calculated as a reference. The ta-C coating shows lowest specific wear rate of $4.2 \times 10^{-9}\ \mathrm{mm}^3/mN$ when CeO_2 nanoparticles are used as oil additives, which is a 77% reduction in comparison with non-additives PAO lubrication condition. However, in the case of ZrO_2 nanoparticle-containing oil lubrication condition, the ta-C coating exhibits higher specific wear rate of $26.2 \times 10^{-9}\ \mathrm{mm}^3/mN$ than non- additives PAO lubrication condition.

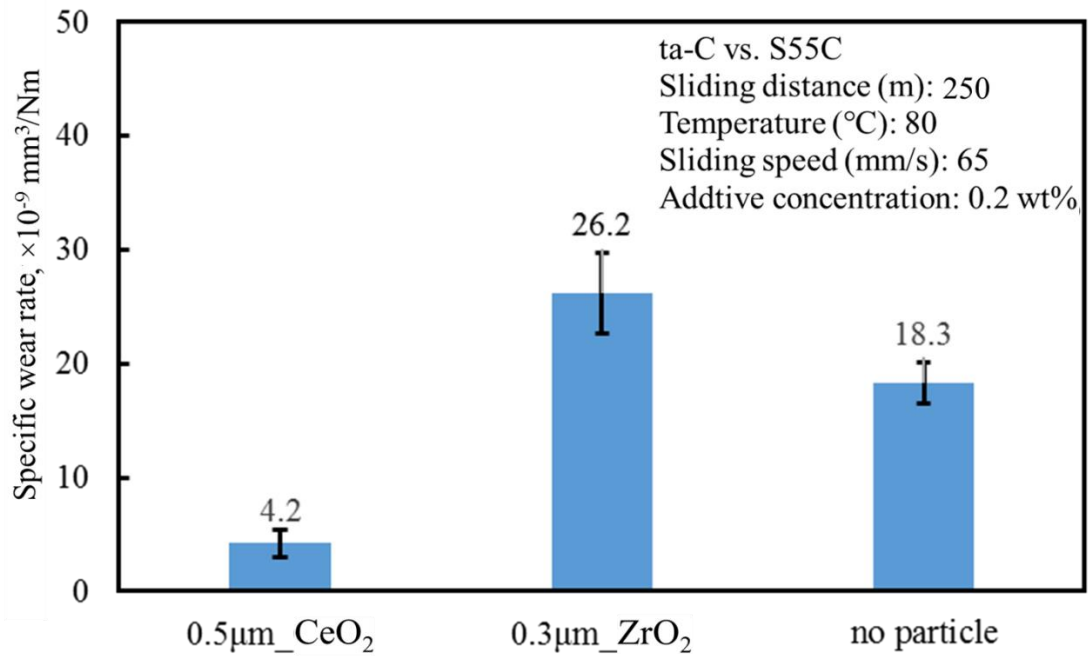

Figure 4.4 Specific wear rate of ta-C coating lubricated with CeO_2 and ZrO_2 nano-particle-containing PAO oil and pure base PAO oil.

Figure 4.5 shows the results of ex-situ optical micrographs of wear scar on the S55C disk which rubbed against ta-C in different additives included lubrication oil. As shown in Fig. 4.6(a), obvious scratch lines can be observed along the sliding direction and it is detected that inside of the wear scar is dotted with brown debris. For ZrO_2 nanoparticles-containing oil, discontinuous tribofilms are formed inside the wear scar on S55C disk and scratch lines are almost invisible (Fig. 4.6(b)). When tested in pure PAO oil, very few debris could be found inside the wear scar and only several shallow scratch lines are generated during the friction test.

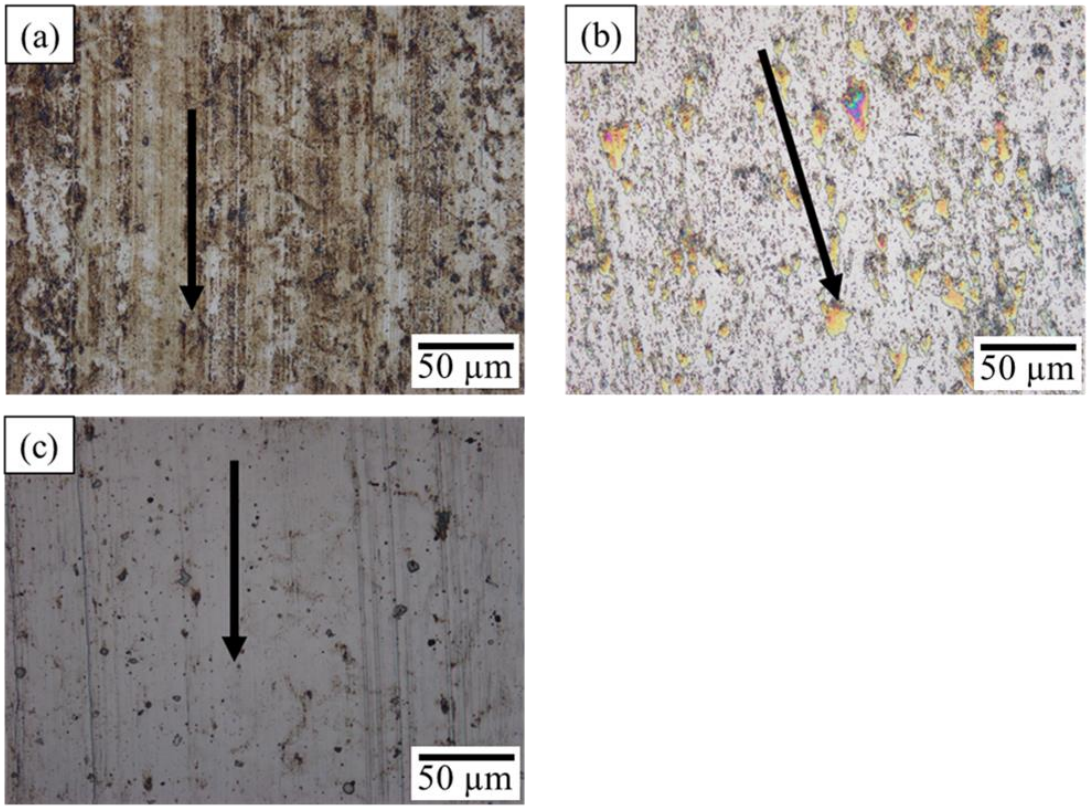

Figure 4.5 Ex-situ optical micrographs of the wear scar on S55C disk after friction test lubricated with (a) CeO_2 nanoparticles-containing oil, (b) ZrO_2 nanoparticles-containing and (c) non-additives oil. (The black arrows represent the sliding direction)

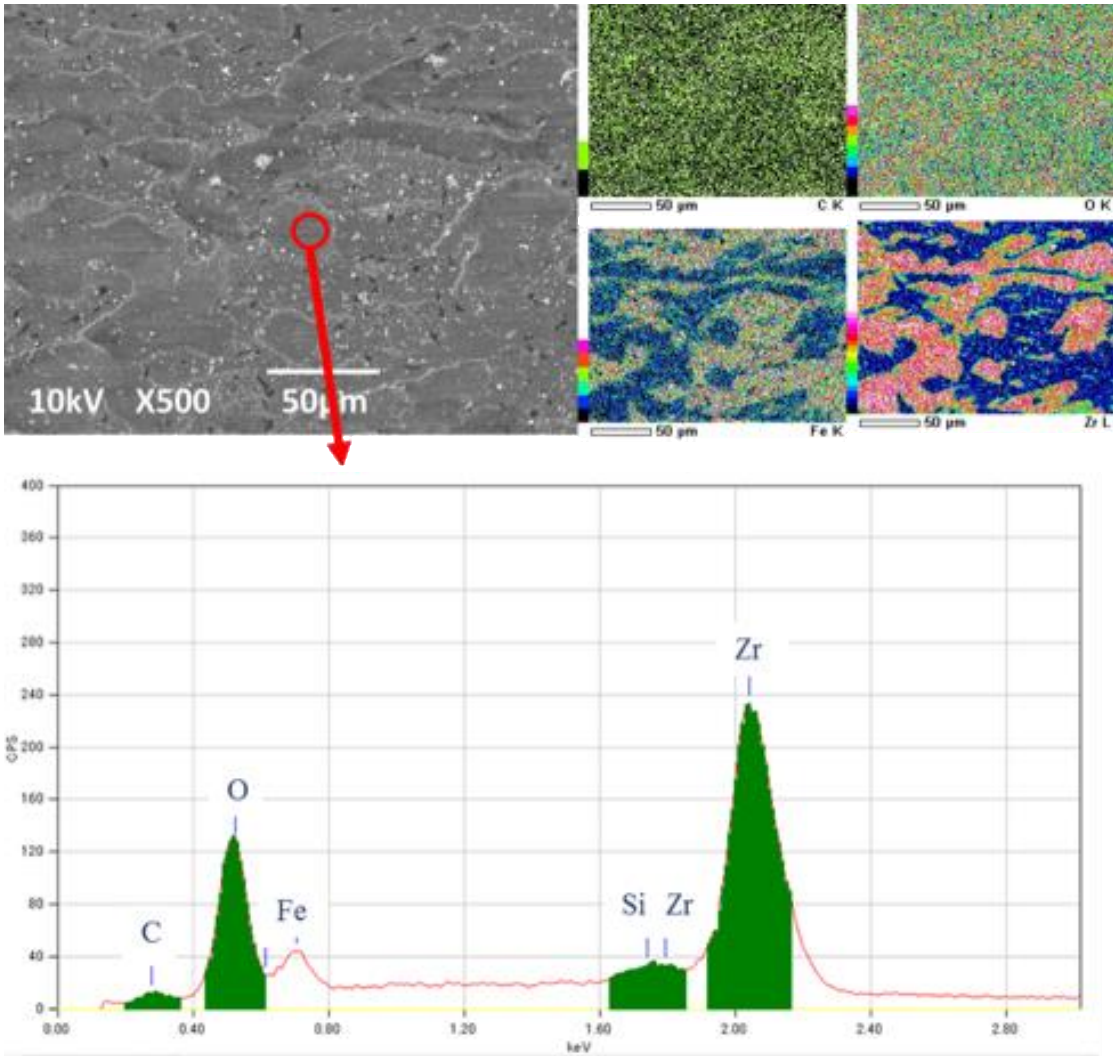

Figure 4.6 SEM micrographs of adhered tribofilm formed lubricated by ZrO_2 nanoparticles-containing oil. Panels (b) show EDS element mapping results and panel (c) shows element composition of corresponding location by EDS analysis.

Tribofilms formed by addition of ZrO_2 nanoparticles are further investigated by energy-dispersive X-ray spectroscopy (EDS) analyses, as shown in Fig. 4.6. Amounts of raised island-like tribofilm can be identified from the SEM micrographs in Fig. 4.6 (a). The corresponding EDS element mapping and the detailed element composition of one of these specified tribofilms are shown as Fig. 4.6 (b) and Fig. 4.6 (c) respectively, indicating that those raised tribofilms mainly consist of ZrO_2 and slight iron and iron oxides. Based on the appearance of these tribofilm layers obtained from optical

micrographs (Fig. 4.5 (b)) and SEM micrographs (Fig. 4.6 (a)), it is noted that these tribofilm layers are not just loose agglomeration of massive ZrO_2 nanoparticles. It seems like these ZrO_2 nanoparticles "melt" together to reform a bulk layer to adhere to the S55C disk during friction process. Figure 4.7 (a) presents the SEM micrographs of wear scar on disk lubricated by CeO_2 nanoparticles-containing oil and the element composition of the corresponding wear scar surface is revealed by EDS analysis, which is shown in Fig. 4.7 (b). It indicates that when lubricated with CeO_2 nanoparticles-containing oil, there are only iron oxides exist inside the wear scar after hand-operated cleaning procedures.

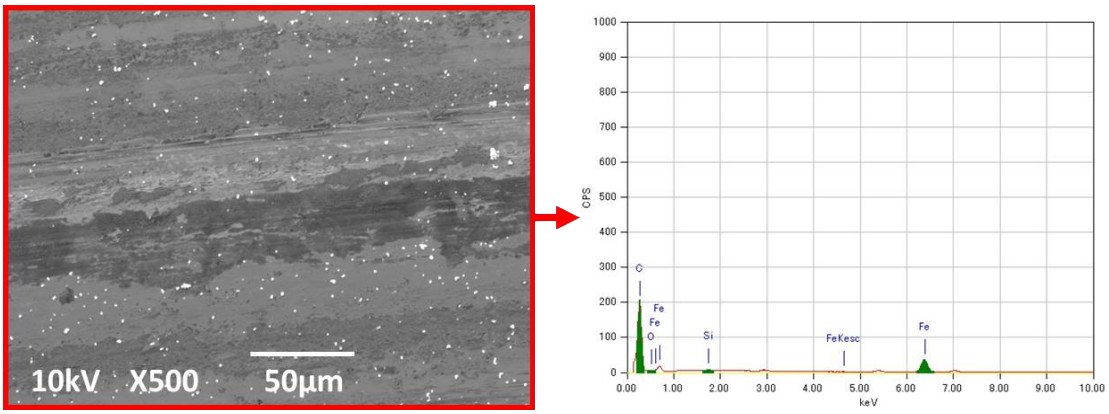

Figure 4.7 SEM micrographs of wear scar on disk lubricated by CeO_2 nanoparticles-containing oil. Panels (b) show element composition of surface (a) by EDS analysis.

Figure 4.8 shows the surface roughness and morphology results of the wear scar on ta-C coated roller and disk specimens lubricated by each type of lubricant oil by the means of three-dimensional scanning white light interferometry. It should be pointed out that, as shown in Fig. 4.8 (b), the morphology of tribofilms is visualized by three-dimensional images and the surface profile of the tribofilm is also measured, which is very smooth with a roughness (Ra) of 5 nm. Meanwhile, the counterpart ta-C coating

is also fine polished to reach a rather smooth surface with a roughness (Ra) of 11 nm. Figure 4.9 presents the roughness of wear scar on the ta-C coated roller and disk when lubricated by CeO_2 nanoparticles-containing oil, no additive oil and ZrO_2 nanoparticles-containing oil respectively. It indicates that addition of ZrO_2 nanoparticles into the oil can result in ultra-fine polishing of ta-C coating and formation of large-scale island-like tribofilm, which also has a quite smooth surface. However, after the friction test lubricated with CeO_2 nanoparticles-containing oil, the roughness of wear scar on ta-C coating does not change significantly but an increase in roughness of disk compared to as-received. Based on the roughness of both mating surfaces, the corresponding lambda values are calculated by Eq. (4.1) and Eq. (4.2). It indicated that for CeO_2 nanoparticles-containing oil lubrication, the lambda Λ value is 0.63, which represent boundary lubrication condition ($\Lambda < 1$). For no additive oil lubrication, the lambda (Λ) value is 1.2, which represent mixed lubrication condition ($1 < \Lambda < 3$). In the case of ZrO_2 nanoparticle-containing oil lubrication, the lambda Λ value is 2.7, which also represent mixed lubrication condition but close to hydrodynamic lubrication condition ($\Lambda > 3$). Figure 4.10 presents the relationship between friction coefficient and calculated lumda value, it indicates that friction coefficient decreases when lumda value increases. In order to investigate the effect of ZrO_2 tribofilm on the friction behavior of ta-C coating under oil boundary lubrication, disk with the adhesion of ZrO_2 tribofilm (followed by the friction test in ZrO_2 nanoparticles-containing oil as shown in Fig. 4.3) was used as counterpart to rub against as-received ta-C under pure PAO oil boundary lubrication condition. As shown in Fig. 4.11, when the tribofilm-adhered disk

rubbing against as-received ta-C, the initial friction coefficient is around 0.062, which is less than that of pristine ta-C/steel contact (0.082). Subsequently, the stable friction coefficient of ta-C/ tribofilm-adhered disk contact is maintained to be 0.058, which is similar to the above-mentioned ta-C/steel in Fig. 4.3.

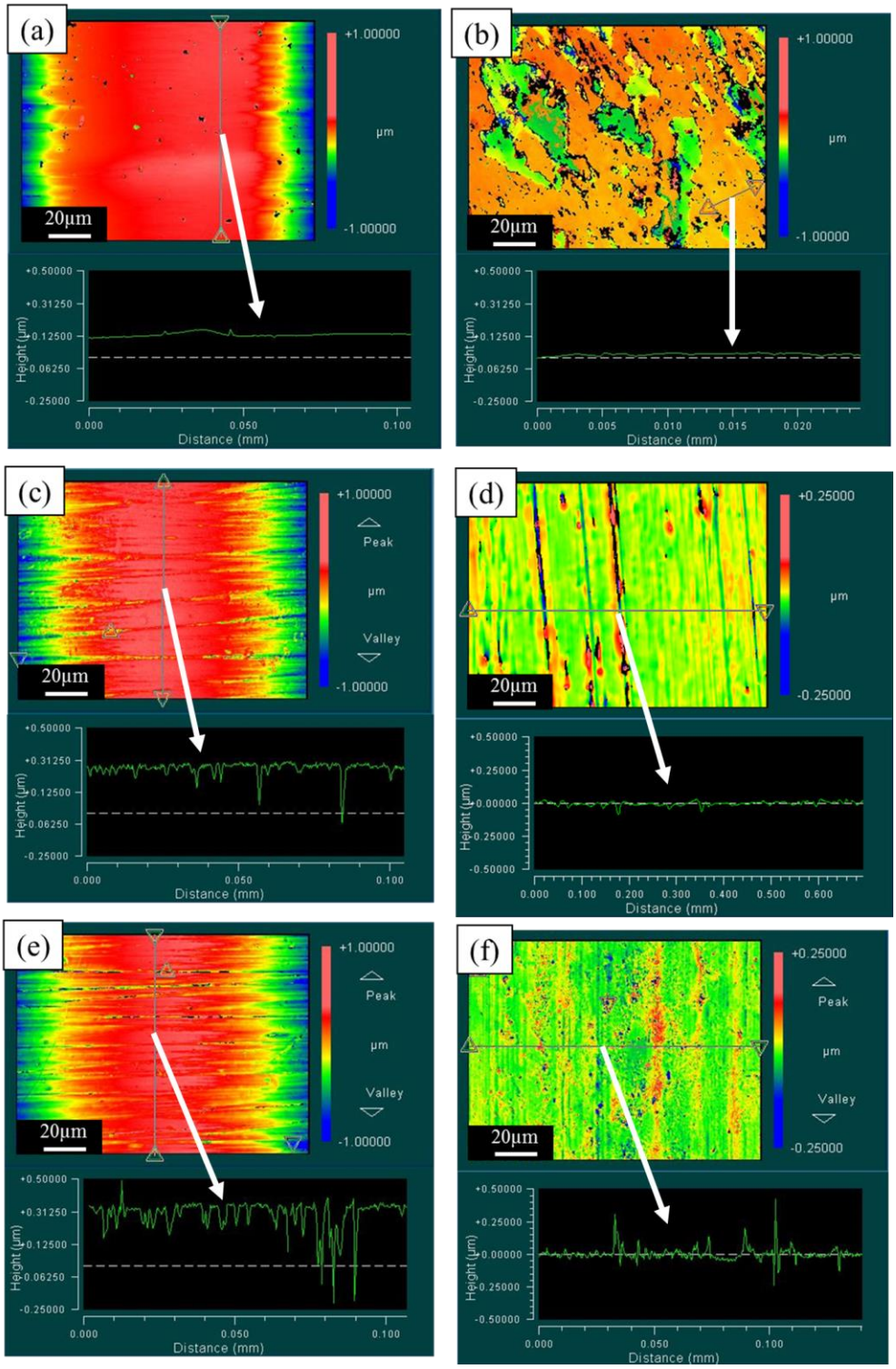

Figure 4.8 Measurement of the roughness and morphology of the wear scar on roller and disk specimens using Zygo Newview. Panels (a) (b) are surface morphology results of wear scar on ta-C coated roller and disk respectively when lubricated by ZrO_2 nanoparticles-containing oil; Panels (c) (d) are surface morphology results of wear scar on ta-C coated roller and disk respectively when lubricated by non-containing oil; Panels (e) (f) are surface morphology results of wear scar on ta-C coated roller and disk respectively when lubricated by CeO_2 nanoparticles-containing oil. The corresponding surface profiles are shown below each surface morphology results.

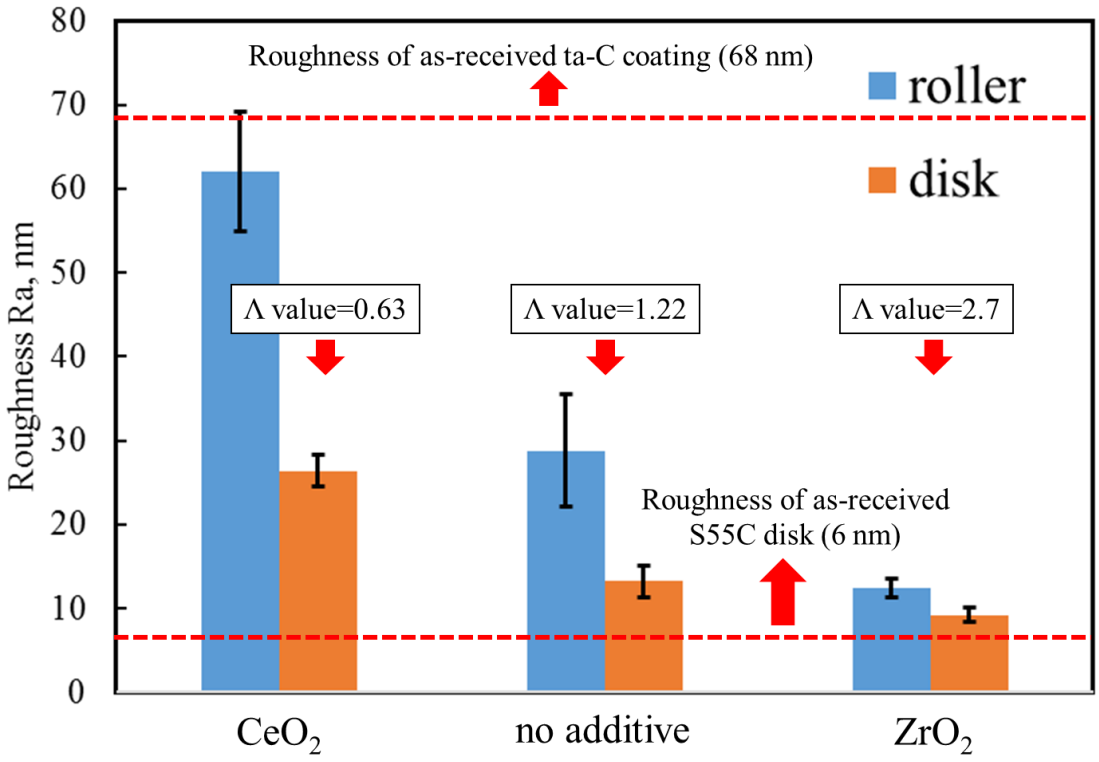

Figure 4.9 Roughness of wear scar on the ta-C coated roller and disk when lubricated by CeO_2 nanoparticles-containing oil, no additive oil and ZrO_2 nanoparticles-containing oil respectively.

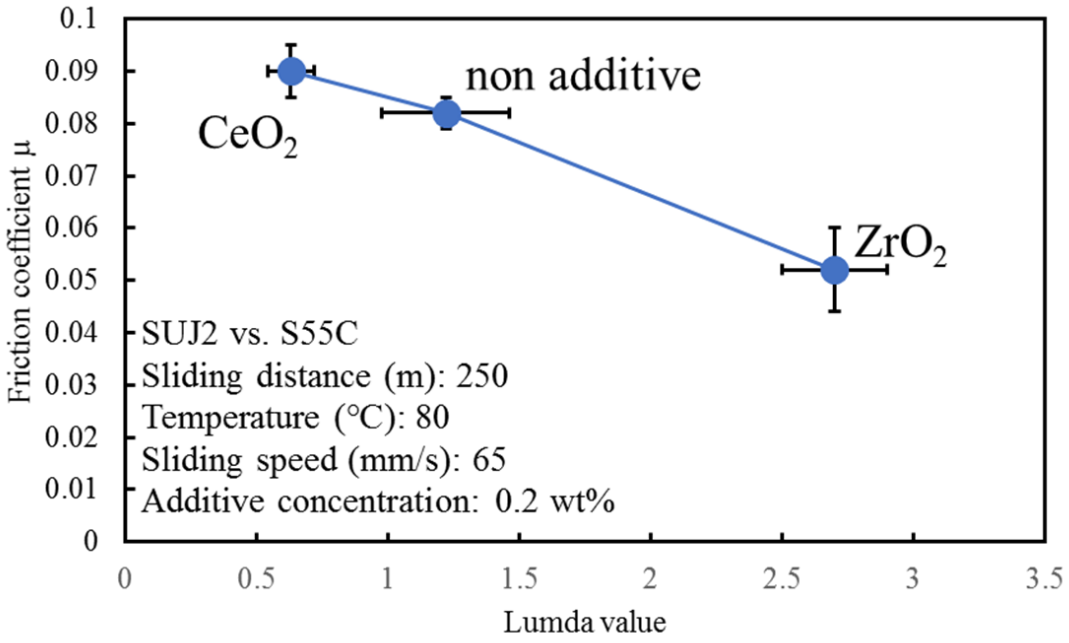

Figure 4.10 Variation of friction coefficient as a function of lambda value when lubricated by CeO_2 nanoparticles-containing oil, no additive oil and ZrO_2 nanoparticles-containing oil respectively.

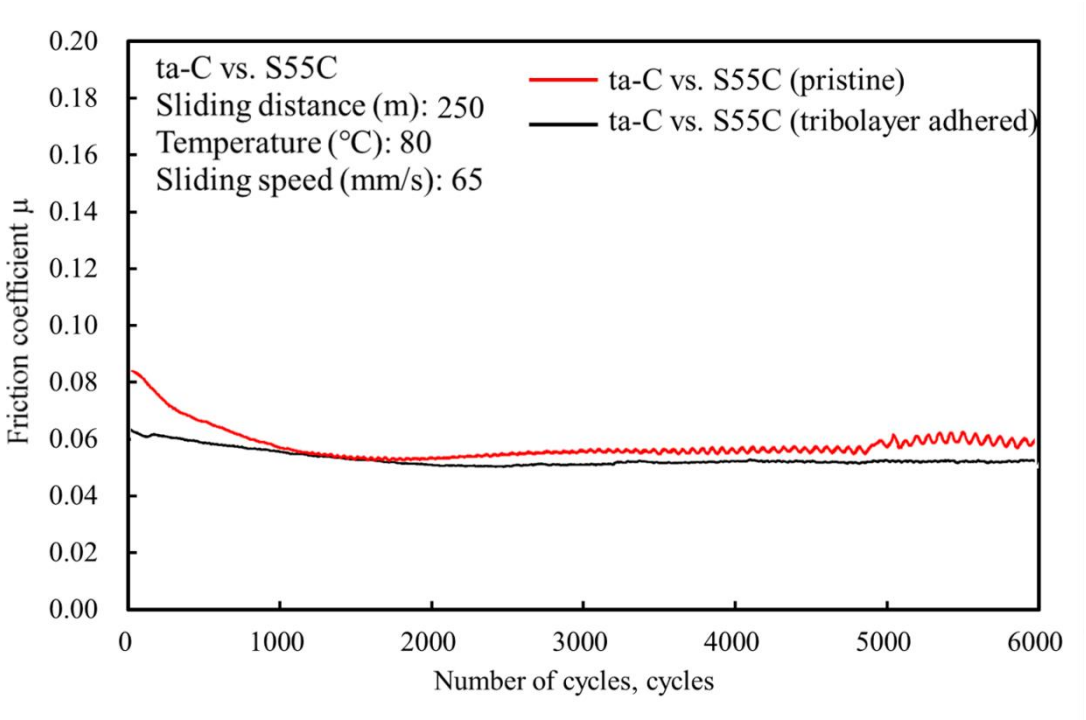

Figure 4.11 Friction coefficient versus sliding cycles for ta-C when rubbing against pristine S55C and ZrO_2 tribolayer-adhered S55C disk.

4.4 Discussion

The results show that, in boundary lubrication condition, the ZrO_2 nanoparticles reduce the friction coefficient of ta-C/steel contact but result in relative higher wear loss. While CeO_2 nanoparticles reduce the wear of ta-C coating significantly but cause relative higher friction coefficient. Namely, low friction and low wear loss cannot be achieved simultaneously by using each nanoparticle individually.

Figure 4.3 clearly shows that ZrO_2 nanoparticles can reduce the friction of ta-C/steel contact by 40% to reach low friction coefficient of 0.05 although accompany by relative higher wear loss (Fig. 4.4). Meanwhile, it is observed that discontinuous tribofilms are formed during friction process only in the case when ZrO_2 nano-additives are used (Fig. 4.5(b)). Up to now, it has been revealed that most studies on the effect of nanoparticles

on tribological properties under oil lubrication condition [111-115] can be generally summarized into two categories: ball bearing effect of nanoparticles and generation of low-shear-strength tribofilm. However, in our research, the average size of nanoparticles is approximately 300 nm - 500 nm, which is larger than the roughness of both mating surfaces before or after friction test. Therefore, it is reasonable to deduce that such nanoparticles are unlikely to enter into the sliding interface to serve as role of ball bearing. Our results show that low friction only occurs in the case of ZrO_2 nano-additives and it is accompanied by the formation of ZrO_2-condensed tribofilm. Hence, the initial ta-C/steel contact is gradually replaced by ta-C/ ZrO_2-tribofilm contact during the friction process, and it is schematically shown in Fig. 4.12(a). Thus, we believe that that tribofilm is very essential to lead in low friction phenomenon.

Based on the above observations, we present the low friction mechanism of ta-C/steel: In the initial running-in period, with the formation of condensed ZrO_2 tribofilm on the steel surface, such tribofilm serves as polishing pad to drastically reduce the roughness of ta-C coating, it is not surprising that relative high wear loss is also inevitable in this process. Meanwhile, rather smooth tribofilms are also formed in the steel surface. EDS analysis confirms that tribofilm is mainly condensed ZrO_2 flake, which is probably caused by tribo-sintering effect [116]. The roughness of those tribofilm and worn ta-C coating surface are measured by three-dimensional scanning white light interferometry to be around 10 nm. The lambda Λ value calculated in Fig. 4.9 clearly shows that for ZrO_2-containing oil lubrication, the lambda value of 2.7 indicates that the lubrication regime between ta-C worn surface and tribofilm is nearly

hydrodynamic lubrication even where some asperity contacts still exist. Consequently, it is reasonable to deduce that when two contacting surfaces become smoother, the lubrication regime would transition from boundary lubrication to mixed or hydrodynamic lubrication. Since there is less direct contact between two sliding surfaces, friction coefficient can achieve a low value eventually. As shown in Fig. 4.10, increased lambda value leads to the drop of friction coefficient.

Some researchers have already shown that the beforehand polishing process of DLC coating is beneficial to provide low friction under lubricated condition [117]. Furthermore, it's worth noting in our study that the ZrO_2-condensed tribofilm is essential to account for the low friction of ta-C/steel contact. Figure 4.11 shows that when ZrO_2 tribofilm-adhered steel disk is rubbed against pristine ta-C coating, the initial friction coefficient is lower than the other two cases where pristine steel disk is used as counter material. After the running-in period, the friction coefficient reaches the similar low value with that has been shown in Fig. 4.3. It indicates that such adhered ZrO_2 tribofilm can continually cause the low friction even the mating ta-C was changed to be rougher.

The results of this study also clearly show CeO_2 nanoparticles additives dramatically improve the wear resistance of ta-C coating under boundary lubrication regime. But unfavorably increase of the friction coefficient of ta-C coating is observed. Since the lubrication regime for CeO_2 nanoparticles-containing condition is boundary lubrication condition, ta-C absolutely contacts directly with disk. Therefore, the friction is dominated by contact area [1]. Under boundary lubrication, aggregations of wear debris

and/or externally introduced particles in the junction of disk and cylinder's curve surface can significantly increase the contact area and therefore cause a rise in friction, as schematically shown in Figures 4.12(b)-(c). For the non-additive condition (Fig. 4.12(b)), even there are no external particles introduced into the oil, a spot of iron oxides is generated as wear debris, which is derived from the steel disk, to aggregate in the junction of disk and cylinder's curve surface. When it comes to anti-wear effect of CeO_2 nanoparticles as oil additives, some research reported that CeO_2 nanoparticles and muscovite/CeO_2 composite particles could improve the antiwear properties of lubricant grease by formation of a chemical reaction film on the worn steel surfaces [118]. However, in our research, there is no visible tribofilm observed on disk or ta-C coating worn surface when CeO_2 nanoparticles are used as oil additives (Figures 4.5(c) and 4.7). Here, we propose that increased contact area results in lowered contact pressure on the ta-C coating, and then the reduction in contact pressure can probably inhibit the wear of ta-C.

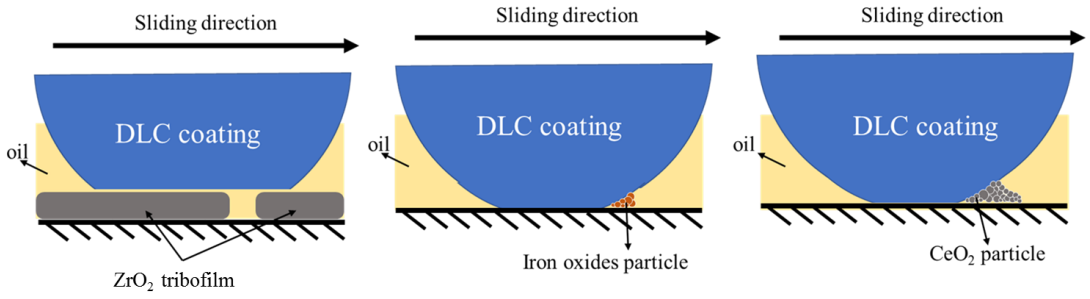

Figure 4.12 Schematic of contact condition of ta-C/steel when (a) ZrO_2 nanoparticles, (b) non-additives and (c) CeO_2 nanoparticles are used as oil additives

4.5 Conclusion

The purpose of this chapter is to clarify the effect of ZrO_2 and CeO_2 nano-particles on the tribological properties of ta-C coating. It is found that when ZrO_2 nanoparticles are introduced into the base oil, the friction coefficient of ta-C/steel fall to 0.05, which is reduced by 40% when it compares with the non-additives lubrication condition. However, ta-C coating shows highest specific wear rate in this case. On the other hand, when it is lubricated by CeO_2 nanoparticles-containing oil, the friction coefficient increases by 22% compared with that in non-additives condition, however wear decreases significantly by nearly 77%. And in the case of ZrO_2 nanoparticles-containing oil, the polishing effect of ZrO_2 nanoparticles on ta-C coating and formation of smooth tribofilm are assumed to jointly cause the lubrication regime transition from boundary lubrication to mixed or hydrodynamic lubrication and therefore it leads to low friction of ta-C/steel contact.

Chapter 5

Conclusion

In this thesis, the tribological performance of ta-C and a-C:H coatings in high contact pressure application was clarified to provide a design guideline for applying DLC coating to engine bearing. Therefore, the effect of applied load, sliding distance, counter materials and nano-particle additives on ta-C and a-C:H coatings under high contact pressure boundary lubrication condition were investigated. From the tribological tests and the surface analysis, the main findings of this thesis can be summarized as follows:

(1) Seizure does not occur in the case of a-C:H/steel tribopair during the whole step-loading process. However, for ta-C/S55C tribopair, seizure does not occur until partial spalling of ta-C coatings is triggered by high load of 50 N (corresponding to a maximum initial Hertzian contact pressure of 380 MPa) and it results in mild seizure. The wear of the ta-C/steel strongly depends on the applied load and sliding distance, whereas the effects of the applied load on the wear of the a-C:H/steel are negligible. The wear mechanism of the ta-C coating is considered to initiate with a brittle microfracture in the protruding parts, followed by partial spalling with the evolution of the microfracture. The spalled ta-C fragments serve as abrasive particles in significantly increasing the wear of the ta-C coating. In comparison, the wear mechanism of the a-C:H coating is strongly due to the graphitization on the topmost surface along with persistent removal of the weakened graphitized layers. Based on the above findings, we propose that ta-C is a promising tribological

coating materials in low applied load and relative short life-span. When it comes to the higher applied load and longer sliding distance, a-C:H is more suitable than ta-C.

(2) The ta-C coating provides high wear resistance when rubbing against steel and Cu. While for a-C:H coating, high wear resistance is provided by rubbing against TiC and steel. Except the case of TiC, a-C:H coating generally shows higher specific wear rate than ta-C. Wear performance of ta-C coating shows a strong dependence on the hardness and roughness of mating material. The specific wear rate of ta-C increases as the increase of hardness and roughness of mating material. While in the low wear condition (less than 9.5×10^{-9} mm^3 /Nm), the main wear mechanism is assumed to be graphitization on the topmost of ta-C. However, in the high wear condition (more than 30×10^{-9} mm^3 /Nm), the microfracture on the contact areas of ta-C coating gives birth to the formation of hard abrasive particles which result in high abrasive wear of ta-C coating. Wear performance of a-C:H coating shows a strong dependency on the increasing rate of I_D/I_G ratio inside the wear track of a-C:H coating. Specific wear rate of a-C:H coating increases as the increasing rate of I_D/I_G ratio increase. It apparently indicates that the main wear mechanism of a-C:H coating is graphitization. On the basis of the above findings, we propose that when mating material is soft and smooth, ta-C coating, which shows higher wear resistance, is more suitable than a-C:H coating. However as mating material becomes harder and rougher, a-C:H could be a promising anti-wear coating material only when the mating material is capable of causing graphitization of a-C:H coating

during work conditions.

(3) When it was lubricated by ZrO_2 nanoparticles-containing oil, the friction coefficient of ta-C/steel contact reaches lowest among for all three cases and ta-C coating shows highest specific wear rate. In addition, when it was lubricated by CeO_2 nanoparticles-containing oil, ta-C coating exhibits lowest specific wear rate but highest friction coefficient. And in the case of ZrO_2 nanoparticles-containing oil, the polishing effect of ZrO_2 nanoparticles on ta-C coating and formation of smooth tribofilm are assumed to jointly cause the lubrication regime transition from boundary lubrication to mixed or hydrodynamic lubrication and therefore it leads to low friction of ta-C/steel contact. According to the above findings, in the tribosystem which including ta-C coating under oil boundary lubrication condition, ZrO_2 and CeO_2 nanoparticles could be a promising replacement of traditional oil additives because not only these nanoparticles-containing oil shows better tribological performance but also they are environmentally friendly.

In the future work, the possibility of applying these green nanoparticles as oil additives to improve the DLC coating-included tribosystems is worth being exploring deeply. In specific, the effect of the shape and size of these green nanoparticles on the tribological behavior of ta-C and other types of DLC coating should be clarified. On the other hand, the search for other new types of nanoparticles as green oil additives is worth being conducted to improve the tribological properties of DLC coatings effectively. Moreover, an advanced in situ observation technologies is required to unveil how do these nanoparticles change the DLC top surface in microscales, since it is

expected such observations will help us to further understand the mechanism of the low friction and/or low wear phenomenon caused by those nanoparticles.

Reference

[1] B. Bhushan, Introduction to tribology. John Wiley & Sons, 2013.

[2] K. Holmberg and A. Erdemir, Global impact of friction on energy consumption, economy and environment, FME Trans 43 (2015) 181-185.

[3] H. P. Jost, Tribology micro & macro economics: A road to economic savings, Tribology and Lubrication Technology 61.10 (2005) 18-23.

[4] Transport Statistics Great Britain (2016) 18-19

[5] C. M. Taylor, Automobile engine tribology—design considerations for efficiency and durability, Wear 221.1 (1998) 1-8.

[6] M. Nakasa, Engine friction overview, Proceedings of International Tribology Conference, Yokohama (1995).

[7] K. Holmberg, P. Anderson and A. Erdemir, Global energy consumption due to friction in passenger cars, Tribol. Int. 47 (2012) 221-234.

[8] K. Holmberg, P. Andersson, N. O. Nylund, K. Mäkelä and A. Erdemir, Global energy consumption due to friction in trucks and buses, Tribol. Int. 78 (2014) 94-114.

[9] S. C. Tung and M. L. Michael, Automotive tribology overview of current advances and challenges for the future, Tribol. Int. 37.7 (2004) 517-536.

[10] G. Straffelini, Surface Engineering for Tribology, Friction and Wear, Springer International Publishing, (2015) 201-235.

[11] K. H. Zum Gahr and J. Schneider, Surface modification of ceramics for improved tribological properties, Ceram. Int. 26.4 (2000) 363-370.

[12] P. Gyftou, M. Stroumbouli, E. A. Pavlatou, P. Asimidis and N. Spyrellis,

Tribological study of Ni matrix composite coatings containing nano and micro SiC particles, Electrochimica Acta 50.23 (2005) 4544-4550.

[13] S. H. Aldajah, O. O. Ajayi, G. R. Fenske and S. David, Effect of friction stir processing on the tribological performance of high carbon steel, Wear 267.1 (2009) 350-355.

[14] G. Cassar, S. Banfield, J. C. Avelar-Batista Wilson, J. Housden, A. Matthews and A. Leyland, Tribological properties of duplex plasma oxidised, nitrided and PVD coated Ti–6Al–4V, Surf. Coat. Tech. 206.2 (2011) 395-404.

[15] G. Cassar, A. Matthews, and A. Leyland, Triode plasma diffusion treatment of titanium alloys, Surf. Coat. Tech. 212 (2012) 20-31.

[16] T. Bonello, J. C. Avelar-Batista Wilson, J. Housden, E. Y. Gutmanas, I. Gotman, A. Matthews, A. Leyland and G. Cassar, Evaluating the effects of PIRAC nitrogen-diffusion treatments on the mechanical performance of Ti–6Al–4V alloy, Mat. Sci. Eng. A-Struct. 619 (2014) 300-311.

[17] M. Priest and C. M. Taylor, Automobile engine tribology—approaching the surface, Wear 241.2 (2000) 193-203.

[18] F. Sahlin, R. Larsson, P. Marklund, A. Almqvist and P. M. Lugt, A mixed lubrication model incorporating measured surface topography. Part 2: roughness treatment, model validation, and simulation, P. I. Mech. Eng. J-J. Eng. 224.4 (2010) 353-365.

[19] P. Liu, T. Huang, R. Lu and T. Li, Tribological properties of modified carbon fabric/polytetrafluoroethylene composites, Wear 289 (2012) 17-25.

[20] H. A. Ching, D. Choudhury, M. J. Nine and N. A. A. Osman, Effects of surface coating on reducing friction and wear of orthopaedic implants, Sci. Technol. Adv. Mat. 15.1 (2014) 014402.

[21] R. J. K. Wood, Tribology of thermal sprayed WC–Co coatings, Int. J. Rrefract. Met. H. 28.1 (2010) 82-94.

[22] P. J. Kelly, H. Li, P. S. Benson, K. A. Whitehead, J. Verran, R. D. Arnell and I. Iordanova, Comparison of the tribological and antimicrobial properties of CrN/Ag, ZrN/Ag, TiN/Ag, and TiN/Cu nanocomposite coatings, Surf. Coat. Tech. 205.5 (2010) 1606-1610.

[23] H. A. Tasdemir, M. Wakayama, T. Tokoroyama, H. Kousaka, N. Umehara, Y. Mabuchi and T. Higuchi, Ultra-low friction of tetrahedral amorphous diamond-like carbon (ta-C DLC) under boundary lubrication in poly alpha-olefin (PAO) with additives, Tribol. Int. 65 (2013) 286-294.

[24] P. Mutafov, J. Lanigan, A. Neville, A. Cavaleiro and T. Polcar, DLC-W coatings tested in combustion engine—Frictional and wear analysis, Surf. Coat. Tech. 260 (2014) 284-289.

[25] M. Kano, DLC coating technology applied to sliding parts of automotive engine, New. Diam. Front. C. Tec. 16.4 (2006) 201-210.

[26] M. Kano, Super low friction of DLC applied to engine cam follower lubricated with ester-containing oil, Tribol. Int. 39.12 (2006) 1682-1685.

[27] S. C. Lim, M. F. Ashby, Overview no.55 wear-mechanism maps, Acta metallurgica 35.1 (1987) 1-24.

[28] H. A. Tasdemir, M. Wakayama, T. Tokoroyama, H. Kousaka, N. Umehara, Y. Mabuchi and T. Higuchi, Wear behaviour of tetrahedral amorphous diamond-like carbon (ta-C DLC) in additive containing lubricants, Wear 307.1 (2013) 1-9.

[29] K. Topolovec-Miklozic, F. Lockwood and H. Spikes, Behaviour of boundary lubricating additives on DLC coatings, Wear 265.11 (2008) 1893-1901.

[30] P. Leduc, B. Dubar, A. Ranini and G. Monnier, Downsizing of gasoline engine: an efficient way to reduce CO2 emissions, Oil. Gas. Sci. Technol. 58.1 (2003) 115-127.

[31] J. W. G. Turner, A. Popplewell, R. Patel, T. R. Johnson, N. J. Darnton, S. Richardson, S. W. Bredda, R. J. Tudor, R. Bithell, R. Jackson, S. M. Remmert, R. F. Cracknell, J. X. Fernandes, A. G. J. Lewis, S. Akehurst, C. J. Brace, C. Copeland, R. Martinez-Botas, A. Romagnoli and A.A. Burluka, Ultra boost for economy: extending the limits of extreme engine downsizing, SAE International Journal of Engines 7.1 (2014) 387-417.

[32] M. Kalin, J. Kogovšek and M. Remškar, Nanoparticles as novel lubricating additives in a green, physically based lubrication technology for DLC coatings, Wear 303.1 (2013) 480-485.

[33] J. Padgurskas, R. Rukuiza, I. Prosyčevas and R. Kreivaitis, Tribological properties of lubricant additives of Fe, Cu and Co nanoparticles, Tribol. Int. 60 (2013) 224-232.

[34] G.W. Stachowiak, A.W. Batchelor, Engineering Tribology, Third edition, Elsevier/Butterworth-Heinemann/Oxford, UK, 2005.

[35] F. P. Bowden and D. Tabor, The friction and lubrication of solids, Vol. 1, Oxford university press, 2001.

[36] G. W. Stachowiak, Wear: materials, mechanisms and practice, John Wiley & Sons, 2006.

[37] B. Bhushan, Modern tribology handbook, two volume set, CRC press, 2000.

[35] L. R. Rudnick (Ed.). Lubricant additives: Chemistry and applications, CRS Press, 2009.

[39] P. Studt, Boundary lubrication: adsorption of oil additives on steel and ceramic surfaces and its influence on friction and wear, Tribol. Int. 22.2 (1989) 111-119.

[40] A. Grill, Diamond-like carbon: state of the art, Diam. Relat. Mater. 8.2 (1999) 428-434.

[41] S. Aisenberg and R. Chabot, Ion−beam deposition of thin films of diamondlike carbon, J. Appl. Phys. 42.7 (1971) 2953-2958.

[42] E. G. Spencer, P. H. Schmidt, D. C. Joy and F. J. Sansalone, Ion−beam−deposited polycrystalline diamondlike films, Appl. Phys. Lett. 29.2 (1976) 118-120.

[43] P. J. Fallon, V. S. Veerasamy, C. A. Davis, J Robertson, G. A. J. Amaratunga, W. I. Milne and J. Koskinen, Properties of filtered-ion-beam-deposited diamondlike carbon as a function of ion energy, Phys. Rev. B 48.7 (1993) 4777.

[44] A. Grill and V. Patel, Low dielectric constant films prepared by plasma-enhanced chemical vapor deposition from tetramethylsilane, J. Appl. Phys. 85.6 (1999) 3314-3318.

[45] P. J. Kelly and R. D. Arnell, Magnetron sputtering: a review of recent

developments and applications, Vacuum 56.3 (2000) 159-172.

[46] Y. Taki, T. Kitagawa and O. Takai, Shielded arc ion plating and structural characterization of amorphous carbon nitride thin films, Thin Solid Films 304.1-2 (1997) 183-190.

[47] J. Xu, H. Fan, H. Kousaka, N. Umehara, D Diao and W. Liu, Growth and properties of hydrogen-free DLC films deposited by surface-wave-sustained plasma, Diam. Relat. Mater. 16.1 (2007) 161-166.

[48] D. L. Pappas, K. L. Saenger, J. Bruley, W. Krakow and J. J. Cuomo, Pulsed laser deposition of diamond−like carbon films, J. Appl. Phys. 71.11 (1992) 5675-5684.

[49] K. Kato, N. Umehara and K. Adachi, Friction, wear and N_2-lubrication of carbon nitride coatings: a review, Wear 254.11 (2003) 1062-1069.

[50] J. Wang, J. Pu, G. Zhang and L. Wang, Tailoring the structure and property of silicon-doped diamond-like carbon films by controlling the silicon content, Surf. Coat. Tech. 235 (2013) 326-332.

[51] D. Y. Wang, K. W. Weng and S. Y. Hwang, Study on metal-doped diamond-like carbon films synthesized by cathodic arc evaporation, Diam. Relat. Mater. 9.9 (2000) 1762-1766.

[52] A. Erdemir and C. Donnet, Tribology of diamond-like carbon films: recent progress and future prospects, J. Phys. D: Appl. Phys. 39 (2006) 311–327.

[53] A. P. Semenov and M. M. Khrushchov, Influence of environment and temperature on tribological behavior of diamond and diamond-like coatings, J. Frict. Wear. 31.2 (2010) 142-158

[54] R. Waesche, M. Hartelt and V. Weihnacht, Influence of counterbody material on the wear of ta-c coatings under fretting conditions at elevated temperature, Wear 267 (2009) 2208-2215.

[55] M. Kalin and J. Vižintin, Differences in the tribological mechanisms when using non-doped, metal-doped (Ti, WC), and non-metal-doped (Si) diamond-like carbon against steel under boundary lubrication, with and without oil additives, Thin solid films 515.4 (2006) 2734-2747.

[56] A. A. Gharam, M. J. Lukitsch, M. P. Balogh, N. Irish and A. T. Alpas, High temperature tribological behavior of W-DLC against aluminum, Surf. Coat. Tech. 206.7 (2011) 1905-1912.

[57] A. A. Gharam, M. J. Lukitsch, Y. Qi and A. T. Alpas, Role of oxygen and humidity on the tribo-chemical behaviour of non-hydrogenated diamond-like carbon coatings, Wear 271.9 (2011) 2157-2163.

[58] H. Ronkainen, S. Varjus, J. Koskinen and K. Holmberg, Differentiating the tribological performance of hydrogenated and hydrogen-free DLC coatings, Wear 249.3 (2001) 260-266.

[59] H. Li, T. Xu, C. Wang, J. Chen, H. Zhou and H. Liu, Tribochemical effects on the friction and wear behaviors of a-C:H and a-C films in different environment, Tribol. Int. 40.1 (2007) 132-138.

[60] M. Nosonovsky and B. Bhushan, Green tribology: biomimetics, energy conservation and sustainability, Springer Science & Business Media, 2012.

[61] A. M. Merlo, The contribution of surface engineering to the product performance in the automotive industry, Surf. Coat. Tech. 174 (2003) 21-26.

[62] A. Vencl and A. Rac, Diesel engine crankshaft journal bearings failures: Case study, Eng. Fail. Anal. 44 (2014) 217-228.

[63] G. C. Pratt, The seizure resistance of aluminium-based materials for engine bearings, Tribology 1.2 (1968) 109-114.

[64] J. Andersson, R. A. Erck and A. Erdemir, Friction of diamond-like carbon films in different atmospheres, Wear 254.11 (2003) 1070-1075.

[65] J. Robertson, Diamond-like amorphous carbon, Mat. Sci. Eng. R. 37.4 (2002) 129-281.

[66] Q. Wang, Seizure failure of journal-bearing conformal contacts, Wear 210.1 (1997) 8-16.

[67] K. Topolovec-Miklozic, F. Lockwood, H. Spikes, Behavior of boundary lubricating additives on DLC coatings, Wear 265.11 (2008) 1893-1901.

[68] B. Podgornik, D. Hren, J. Vižintin, S. Jacobson, N. Stavlid and S. Hogmark, Combination of DLC coatings and EP additives for improved tribological behaviour of boundary lubricated surfaces, Wear 261.1 (2006) 32-40.

[69] T. Haque, A. Morina, A. Neville, R. Kapadia and S. Arrowsmith, Effect of oil additives on the durability of hydrogenated DLC coating under boundary lubrication conditions, Wear 266.1 (2009) 147-157.

[70] J. M. Herdan, Lubricating oil additives and the environment—an overview, Lubr. Sci. 9.2 (1997) 161-172.

[71] K. Vercammen, K. Van Acker, A. Vanhulsel, J. Barriga, A. Arnsek, M. Kalin and J. Meneve, Tribological behaviour of DLC coatings in combination with biodegradable lubricants, Tribol. Int. 37.11 (2004) 983-989.

[72] B. J. Hamrock, S. R. Schmid and B. O. Jacobson, Fundamentals of fluid film lubrication, CRC press, 2004.

[73] A. C. Ferrari, J. Robertson, Interpretation of Raman spectra of disordered and amorphous carbon, Phys. Rev. B. 61.20 (2000) 14095.

[74] D. L. A. De Faria, S. Venâncio Silva and M. T. De Oliveira, Raman microspectroscopy of some iron oxides and oxyhydroxides, J. Raman. Spectrosc. 28.11 (1997) 873-878.

[75] Y. Liu, A. Erdemir and E. I. Meletis, A study of the wear mechanism of diamond-like carbon films, Surf. Coat. Tech. 82.1 (1996) 48-56.

[76] Y. Liu, A. Erdemir and E. I. Meletis, An investigation of the relationship between graphitization and frictional behavior of DLC coatings, Surf. Coat. Tech. 86 (1996) 564-568.

[77] L. Cui, Z. Lu and L. Wang, Probing the low-friction mechanism of diamond-like carbon by varying of sliding velocity and vacuum pressure, Carbon 66 (2014) 259-266.

[78] T. Xin, L. H. Li, L. Hou, X. Hu, S. Zhou, R. Peter, M. Petravic and Y. Chen, Disorder in ball-milled graphite revealed by Raman spectroscopy, Carbon 57 (2013) 515–9.

[79] J. C. Sanchez-Lopez, A. Erdemir, C. Donnet and T. C. Rojas, Friction-induced structural transformations of diamondlike carbon coatings under various atmospheres, Surf. Coat. Tech. 163 (2003) 444-450.

[80] H. Li, T. Xu, C. Wang, J. Chen, H. Zhou and H. Liu, Tribochemical effects on the friction and wear behaviors of a-C: H and a-C films in different environment, Tribol. Int. 40.1 (2007) 132-138.

[81] S. Bhowmick, A. Banerji, A. T. Alpas, Tribological behavior and machining performance of non-hydrogenated diamond-like carbon coating tested against Ti–6Al–4V: Effect of surface passivation by ethanol, Surf. Coat. Tech. 260 (2014) 290-302.

[82] A. Erdemir, The role of hydrogen in tribological properties of diamond-like carbon films, Surf. Coat. Tech. 146 (2001) 292-297.

[83] M. A. Moore and F. S. King, Abrasive wear of brittle solids, Wear 60.1 (1980) 123-140

[84] S. J. Bull, Tribology of carbon coatings: DLC, diamond and beyond, Diam. Relat. Mater. 4.5-6 (1995) 827-836.

[85] K. A. M. Aboua, N. Umehara, H. Kousaka X. Deng, H. A. Tasdemir, Y. Mabuchi, T. Higuchi and M. Kawaguchi, Effect of carbon diffusion on friction and wear properties of diamond-like carbon in boundary base oil lubrication, Tribol. Int. 113 (2017) 389-398.

[86] M. Kalin, I. Velkavrh, J. Vižintin and L. Ožbolt, Review of boundary lubrication mechanisms of DLC coatings used in mechanical applications, Meccanica 43 (2008) 623-637.

[87] A. Erdemir, Review of engineered tribological interfaces for improved boundary lubrication, Tribol. Int. 38 (2005) 249-256.

[88] B. Podgornik and J. Vižintin, Tribological reactions between oil additives and DLC coatings for automotive applications, Surf. Coat. Tech. 200.5 (2005) 1982-1989.

[89] H. A. Tasdemir, T. Tokoroyama, H. Kousaka, N. Umehara and Y. Mabuchi, Influence of zinc dialkyldithiophosphate tribofilm formation on the tribological performance of self-mated diamond-like carbon contacts under boundary lubrication, Thin Solid Films 562 (2014) 389-397.

[90] T. Jimbo and S. Hironaka, Sliding velocity dependence of friction and wear properties of oil-retaining porous silicon carbide, J. Ceram. Soc. Jpn. 105 (1997) 492-495.

[91] J. K. Lancaster, A review of the influence of environmental humidity and water on friction, lubrication and wear, Tribol. Int. 23 (1990) 371-389.

[92] B. Podgornik, S. Jacobson and S. Hogmark, Influence of EP and AW additives on the tribological behaviour of hard low friction coatings, Surf. Coat. Tech. 165 (2003) 168-175.

[93] I. M. Hutchings, Tribology: friction and wear of engineering materials, Mater. Des. 13.3 (1992) 187.

[94] W. Ni, Y. T. Cheng, M. J. Lukitsch, A. M. Weiner, L. C. Lev and D. S. Grummon, Effects of the ratio of hardness to Young's modulus on the friction and wear behavior of bilayer coatings, Appl. Phys. Lett. 85 (2004) 4028-4030.

[95] H. Liu, A. Tanaka and T. Kumagai, Influence of sliding mating materials on the tribological behavior of diamond-like carbon films, Thin Solid Films 352 (1999) 145-150.

[96] K. Kato, Wear in relation to friction—a review. Wear 241 (2000) 151-157.

[97] B. Podgornik and J. Vižintin, Tribological reactions between oil additives and DLC coatings for automotive applications, Surf. Coat. Tech. 200 (2005) 1982-1989.

[98] I. Sugimoto, F. Honda and K. Inoue, Analysis of wear behavior and graphitization of hydrogenated DLC under boundary lubricant with MoDTC, Wear 305 (2013) 124-128.

[99] K. L. Rutherford and I. M. Hutchings, Theory and application of a micro-scale abrasive wear test, J. Test. Eval. 25 (1997) 250-260.

[100] K. L. Rutherford and I. M. Hutchings, A micro-abrasive wear test, with particular application to coated systems, Surf. Coat. Tech. 79 (1996)231–239.

[101] R. I. Trezona and I. M. Hutchings, Three-body abrasive wear testing of soft materials, Wear 233 (1999) 209-221.

[102] Z. Hong and Y. Chengye, Laser shock processing of 2024-T62 aluminum alloy, Mat. Sci. Eng. A-Struc. 257 (1998) 322-327.

[103] R. Gåhlin, M. Larsson and P. Hedenqvist, ME-C: H coatings in motor vehicles, Wear 249 (2001) 302-309.

[104] P. L. Wong, F. He and X. Zhou, Interpretation of the hardness of worn DLC particles using micro-Raman spectroscopy, Tribol. Int. 43 (2010) 1806-1810.

[105] A. G. Thornton and J. Wilks, Clean surface reactions between diamond and steel, Nature 274 (1978) 792-793.

[106] R. Narulkar, S. Bukkapatnam, L. M. Raff and R. Komanduri, Graphitization as a precursor to wear of diamond in machining pure iron: a molecular dynamics investigation, Comp. Mater. Sci. 45 (2009) 358-366.

[107] S. Shimada, H. Tanaka, M. Higuchi, T. Yamaguchi, S. Honda and K. Obata, Thermo-chemical wear mechanism of diamond tool in machining of ferrous metals, CIRP. Ann-Manuf. Tec. 53 (2004) 57-60.

[108] T. Sato, Y. Hirai, T. Fukui, K. Akiyama and H. Usami, Effects of dispersed sulfides in bronze under line contact conditions, Jurnal Tribologi 8 (2016) 1-11.

[109] M. Kalin, J. Vižintin, J. Barriga, K. Vercammen, K. Van Acker and A. Arnšek, The effect of doping elements and oil additives on the tribological performance of boundary-lubricated DLC/DLC contacts, Tribol. Lett. 17.4 (2004) 679-688.

[110] H. A. Tasdemir, M. Wakayama, T. Tokoroyama, H. Kousaka, N. Umehara, Y. Mabuchi and T. Higuchi, Ultra-low friction of tetrahedral amorphous diamond-like carbon (ta-C DLC) under boundary lubrication in poly alpha-olefin (PAO) with additives, Tribol. Int. 65 (2013) 286-294.

[111] V. S. Jatt and T. P. Singh, Copper oxide nano-particles as friction-reduction and anti-wear additives in lubricating oil. J. Mech. Sci. Technol. 29.2 (2015) 793.

[112] W. Y. Ye, T. F. Cheng, Q. Ye., X. Y. Guo, Z. J. Zhang and H. X. Dang, Preparation and tribological properties of tetrafluorobenzoic acid-modified TiO 2 nanoparticles as lubricant additives, Mat. Sci. Eng. A-Struc. 359.1 (2003) 82-85.

[113] M. I. H. C. Abdullah, M. F. B. Abdollah, H. Amiruddin, N. Tamaldin and N. R. M. Nuri, Optimization of Tribological Performance of hBN/AL2O3 Nanoparticles as Engine Oil Additives, Procedia Engineering 68 (2013) 313-319.

[114] W. Dai, B. Kheireddin, H. Gao and H. Liang, Roles of nanoparticles in oil lubrication, Tribol. Int. 102 (2016) 88-98.

[115] Gulzar, M., Masjuki, H.H., Kalam, M.A., Varman, M., Zulkifli, N.W.M., Mufti, R.A. and Zahid, R., 2016. Tribological performance of nanoparticles as lubricating oil additives. Journal of Nanoparticle Research, 18(8): 223.

[116] H. Kato and K. Komai, Tribofilm formation and mild wear by tribo-sintering of nanometer-sized oxide particles on rubbing steel surfaces, Wear 262.1 (2007) 36-41.

[117] M. Tokoro, Y. Aiyama, M. Masuko, A. Suzuki, H. Ito and K. Yamamoto, Improvement of tribological characteristics under water lubrication of DLC-coatings by surface polishing, Wear 267.12 (2009) 2167-2172.

[118] P. F. Du, G. X. Chen, S. Y. Song, H. L. Chen, J. Li and Y. Shao, Tribological properties of muscovite, CeO2 and their composite particles as lubricant additives, Tribol. Lett. 2.62 (2016) 1-9.

Acknowledgements

First of all, I would like to express my sincere gratitude and respect to my supervisor, Prof. Dr. Noritsugu Umehara, for all I have learned from him and for his excellent guidance, continuous help, patience, motivation and support in all stages of this thesis. I would also like to thank him for being an open person to ideas, and for encouraging and helping me to shape my interest and ideas. Without his guidance and persistent help this dissertation would not have been possible.

I would like to thank my committee members, Prof. Dr Yang Ju, Assoc. Prof. Dr. Hedong Zhang and Assoc. Prof. Dr. Takayuki Tokoroyama for sharing their ideas on the improvement of the thesis, and for their encouragement, insightful comments, and suggestions.

The success of this thesis is attributed to the extensive support and assistance from all members of Advanced Material and Manufacturing Laboratory. Especially, I would like to express my grateful gratitude and sincere appreciation to the previous Assoc. Prof. Dr. Hiroyuki Kousaka, Assoc. Prof. Dr. Takayuki Tokoroyama and Mr. Shinkoh Senda for their kindness in examining the research work and providing technical suggestions for improvement and encouragement during my time here.

My special thanks are given to my labmate Mr. Toshiya Sawaki for his cheerful cooperation, encouragement, help and support and enjoyment during the course of my study, Dr.Deng, Dr. Nishimura, Dr.Inoue and Mrs. Liu and all others who I can't write their name in here. I hope our friendship will remain same in coming years.

I would also like to express my special thanks to my family, especially my wife and my parents for always believing in me, for their continuous love and their supports in my decisions. I am particularly grateful for the support, love and good times given by all my relatives and friend. They were always there cheering me up, praying for my health and stood by me through the good times and bad. Without whom I could not have made it here.

Publication list

International Journal:

- **Xiang Li**, Noritsugu Umehara and Motoyuki Murashima. “Effect of nanoparticles as lubricant additives on friction and wear behavior of tetrahedral amorphous carbon (ta-C) coating”. Jurnal Tribologi. (Accepted for publication)
- **Xiang Li**, Toshiya Sawaki, Noritsugu Umehara and Motoyuki Murashima. “Effect of mating materials on wear properties of amorphous hydrogenated carbon (a-C:H) coating and tetrahedral amorphous carbon (ta-C) coatings in base oil boundary lubrication condition”. Jurnal Tribologi 15 (2017) 1-20
- **Xiang Li**, Noritsugu Umehara, Hiroyuki Kousaka and Xingrui Deng. “Comparative study on effects of load and sliding distance on amorphous hydrogenated carbon (a-C:H) coating and tetrahedral amorphous carbon (ta-C) coating under base-oil lubrication condition”. Wear 392 (2017) 84-92.

International Conference:

- **Xiang LI**, Seizure resistance and tribological characteristics of various DLC coatings under the boundary lubrication. 7th International Tribology Conference, Tokyo(Japan), September 2015.
- **Xiang LI**, Effect of applied load on wear property of tetrahedral amorphous carbon and hydrogenated amorphous carbon under the oil boundary lubrication regime, 5th International Conference on INTEGRITY-RELIABILITY-FAILURE, Porto(Portugal), July 2016.
- **Xiang LI**, Different wear behavior of ta-C and a-C:H coatings when rubbing

against various mating materials under base oil boundary lubrication, 7th International Conference on Manufacturing, Machine Design and Tribology. Jeju (Republic of Korea), April 2017.

- **Xiang LI**, Comparative study on effects of load and sliding distance on amorphous hydrogenated carbon (a-C:H) coating and tetrahedral amorphous carbon (ta-C) coating under base-oil lubrication condition, 6th World Tribology Conference, Beijing (China), September 2017.